ORIGINAL ARCHIVAL COPY

POWER GRID OPERATION RISK MANAGEMENT: V2G DEPLOYMENT FOR SUSTAINABLE DEVELOPMENT

BY

GHAZALE J. HADDADIAN

STUART SCHOOL OF BUSINESS

Submitted in partial fulfillment of the
requirements for the degree of
Doctor of Philosophy in Management Science
in the Graduate College of the
Illinois Institute of Technology

Approved ______________________
Co-adviser

Approved ______________________
Co-adviser

Chicago, Illinois
May 2014

ACKNOWLEDGEMENT

I dedicate this dissertation to my amazing parents, Zahra Toussi and Ali Haddadian, who have been my source of inspiration all my life, nurtured my learning, instilled a sense of curiosity in me, and supported my dreams! This work is also dedicated to my husband, Ayden Noohi, whose support, encouragement, quiet patience, and unwavering love are urging me forward; traveling through life with him by my side brings me the greatest happiness. Finally, I dedicate this dissertation to my unique sister, Afsan Haddadian, who has been my cheerleader, and kept me afloat when times were hard or crazy.

I would first like to thank my respected advisor, Professor Nasrin Khalili for her invaluable guidance, support, kindness, and patience throughout my graduate school experience. I am thankful for not only the innumerable academic lessons, but also more life lessons she thought me. I truly appreciated her professional advice, time she took to speak with me, and her lasting friendship. I thank her for introducing me to other researchers and distinguished faculty members at Illinois Institute of Technology (IIT). I also thank her for her incredible and continuous encouragement so that I can reach this milestone in my studies!

I would like to express my profound gratitude to Dean Harvey Kahalas, who believed in me, enabled this whole PhD journey, and has been a constant source of support and insightful advice. This thesis would never have been started without his guidance.

Special thanks to Professor Priyanka Sharma for her contribution to this work. I am most grateful for the time she spent on my work by providing insightful critique and valuable comments that helped hone the content of this dissertation.

I would also like to express my appreciation to the individuals at the Galvin Center for Electricity Innovation who selflessly helped me learn and use the electric power engineering vocabulary, which has been so instrumental in my research work at IIT. Professor Mohammad Shahidehpour, Director of Galvin Center, provided me with financial support, insightful advice, and unfailing geniality. I remain to be very thankful to him. Special thanks go to my former colleague at the Galvin Center, Professor Mohammad Khodayar for providing constant help and active advice while I was conducting my research. His quick response to my technical questions was so reassuring during stressful times of my work. His dedication allowed me to remain focused and disciplined.

Last, but not least, I would like to thank my friend Susanna Duecker, with whom I started this journey, for always laughing with me in numerous difficult junctures of my studies and for being such a true friend throughout these years.

TABLE OF CONTENTS

LIST OF TABLES

LIST OF FIGURES

LIST OF SYMBOLS

Symbol	Definition
i	Index of thermal units
t	Hour index (t=0 to 24)
w	Represents a wind turbine
v	Represents an EV fleet
l	Index of transmission line (l=1 to 7)
b, j, o	Index of bus
s	a scenario
NG	Number of units
NL	Number of lines
NB	Number of buses
NT	Number of periods under study (24 hours)
I_{it}	Commitment state of unit i at time t
$SD_{(.)}^{(.)}$	Shutdown cost of a unit
$SU_{(.)}^{(.)}$	Startup cost of a unit
$F_{c,(.)}$	Production cost function of a thermal unit
$P_{(.)}^{(.)}$	Generation of a unit
$P_{d,w,t}^{(.)}$	Power generation curtailed of wind turbine w at t
$P_{L,t}$	System losses at time t
$P_{i,min}$	Lower limit of real power generation of unit i
$P_{i,max}$	Upper limit of real power generation of unit i
$P_{D,(.)}^{(.)}$	Total system demand
X_{it}^{off}	OFF time of unit i at time t
X_{it}^{on}	ON time of unit i at time t
T_i^{off}	Min down time of unit i
T_i^{on}	Min up time of unit i

Symbol	Definition
UR_i	Ramp-up rate of unit i
DR_i	Ramp-down rate of unit i
$P_{D,t}$	System demand at time t
$\theta_{(.)}^{(.)}$	Bus angle
X_{jo}	Inductance of a line between buses j and o
$PL_{l,t}^{(.)}$	Real power flow on line L at hour t
PL_l^{max}	Maximum capacity of line L
$F_{ei}(.)$	Emission function of unit i
$SD_{e,it}$	Shutdown emission of unit i at time t
$SU_{e,it}$	Startup emission of unit i at time t
$C_{(.)}$	Operation cost of the EV fleet
$E_{v,t}^{(.)}$	Available energy in batteries of fleet v at time t
$E_{v,t}^{net}$	Net discharged energy of EV fleet V at time t
$I_{c,(.)}^{(.)}$	EV fleet in charging mode
$I_{dc,(.)}^{(.)}$	EV fleet in discharging mode
$I_{i,(.)}^{(.)}$	EV fleet in idle mode
$P_{c,(.)}^{(.)}, P_{dc,(.)}^{(.)}$	Charge/discharge power of EV fleet
$P_{m,(.)}^{(.)}$	Charge/discharge power rate at segment m
$F_{c,(.)}^{r}$	Availability cost function of a thermal unit
$\Delta_{(.)}^{max}$	Maximum acceptable power adjustment of a unit
$B_{b,t}^{(.)}$	Set of units that are connected to bus b at time t
$b_{m,(.)}$	Slope of segment m in linearized charge/discharge curve
D_b	Set of loads that are connected to bus b
E_v^{min}	Min energy stored in batteries of EV fleet v
E_v^{max}	Max energy stored in batteries of EV fleet v

Symbol	Definition
$L_{f,b}, L_{t,b}$	Set of lines starting from/ending at bus b
$N_{v,t}$	Status of grid connection of fleet v at time t
$P_{c,v}^{min}$	Min charging capacity of EV fleet v
$P_{c,v}^{max}$	Max charging capacity of EV fleet v
$P_{dc,v}^{min}$	Min discharging capacity of EV fleet v
$P_{dc,v}^{max}$	Max discharging capacity of EV fleet v
$P_{m,v}^{max}$	Maximum power output at segment m in charging/ discharging cost curve of EV fleet v
η_v	Cycle charging efficiency of EV fleet
$DR_{v,t}^{s}$	Energy for EV v to drive at time t in scenario s
P^b	Probability of base case
P^s	Probability of scenario s
$UX_{(.)}^{(.)}, UY_{(.)}^{(.)}$	Outage status, if available 1, and 0 otherwise
EI_{v}, ET_{v}	Initial and terminal stored energy in EV fleet v
NE_{v}^{s}	Ratio of the number of EVs in fleet in scenario s to the number of base case EVs
$\hat{T}$	Time in which the charging state is set to a value

ABSTRACT

The production, transmission, and delivery of cost–efficient energy to supply ever-increasing peak loads/demands along with a quest for developing a low-carbon economy require significant evolutions in the power grid operations. Lower prices of vast natural gas resources in the United States, Fukushima nuclear disaster, higher and more intense energy consumptions in China and India, issues related to energy security, and recent Middle East conflicts, have urged decisions makers throughout the world to look into other means of generating electricity locally.

As the world look to combat climate changes, a shift from carbon-based fuels to non-carbon based fuels is inevitable. It is possible to knock a lot of carbon out of the electric power system through large-scale integrations of renewable sources. However, the variability of distributed generation assets (such as wind and solar) in the electricity grid has introduced major reliability challenges/risks for power grid operators.

While spearheading sustainable and reliable power grid operations, this dissertation develops a multi-stakeholder approach to power grid operation design; aiming to address economic, security, and environmental challenges of the constrained electricity generation. It investigates the role of Electric Vehicle (EV) fleets integration, as distributed and mobile storage assets to support high penetrations of variable and renewable energy sources, in the power grid. The vehicle-to-grid (V2G) concept is considered to demonstrate the bidirectional role of EV fleets both as a provider and consumer of energy in securing a sustainable power grid operation. The V2G concept is regarded as a novel, low-cost, low-emission and sustainable strategy that can address

challenges involve with using renewable energy sources, which require means of storing large quantities of energy.

The proposed optimization modeling is the application of Mixed-Integer Linear Programing (MILP) to large-scale systems to solve the hourly security-constrained unit commitment (SCUC) – an optimal scheduling concept in the economic operation of electric power systems. The Monte Carlo scenario-based approach is utilized to evaluate different scenarios concerning the uncertainties in the operation of power grid system.

Further, in order to expedite the real-time solution of the proposed approach for large-scale power systems, this dissertation considers a two-stage model using the Benders Decomposition (BD) and applies the BD method to the hourly SCUC solution of electric power systems with significant uncertainties.

The numerical simulation demonstrate that the utilization of smart EV fleets in power grid systems would ensure a sustainable grid operation with lower carbon footprints, smoother integration of renewable sources, higher security, and lower power grid operation costs. Further, simulation results indicate that intelligent-controlled mode, in which electric power system operators control the EV fleets charge/discharge decisions based on the system operation requirements, is more effective compare to the rule-based mode, in which consumers control charging/discharging decisions. The numerical simulations, additionally, illustrate the effectiveness of the proposed MILP approach and its potentials as an optimization tool for sustainable operation of large scale electric power systems.

CHAPTER 1

INTRODUCTION

This dissertation focuses on the optimization of operation planning of electric power systems in support of sustainable development in a low carbon economy.

1.1 Sustainability of Power System Operation

The sustainability of a developing economy is extensively influenced by recent evolutions in the energy industry. Industrialized nations are increasingly in search for cheaper, cleaner, and more reliable sources of energy to strengthen their economies and developing countries would require the same for accelerating their progress in a competitive arena. As Peter Voser [Yer12] stated, "Energy is the oxygen of the economy and the life-blood of growth". Furthermore, energy, as cornerstone of every developing economy, is an imperative input to nearly all of the goods and services of the modern world. As such, steady and affordable energy supplies are the key to reigniting, sustaining, and boosting the economic growth in every nation.

Energy development which supports the needs of the present generation without jeopardizing the ability of future generations to meet their own energy needs is referred to as sustainable energy development [1]. The development of a sustainable energy infrastructure is driven by climate policies, energy security, and economics. Accordingly, addressing resource scarcity for an unbiased sustainable economic development is one of the greatest priorities of our time.

---

[1] This definition is inferred from the most frequently quoted general definition of sustainability which is from the World Commission on Environment and Development (WCED), also known as the "Brundtland Commission".

The planning philosophy for the existing electricity grid is a transformation from an era when energy was inexpensive and abundant while addressing the rising demand was the primary concern. We are at evolution to a period when clean energy is at premium, power systems require an adaption to low greenhouse gas (GHG) emission technologies for electricity supply, and customers request greater awareness and participation in energy utilization. Moreover, operating at absolute minimum cost is no longer the only condition for electric power generation due to the pressing public demand for cleaner air [Yer13]. According to the June 2013 report published by the International Energy Agency [Bir13], the world is not on track to address the target agreed upon by governments to limit the long-term escalation in the average global temperature to 2 degrees Celsius (2DC) per the Copenhagen Accord. Yet, many of the environmental problems countries facing today result from fossil fuel dependence. These impacts include global warming, air quality deterioration, oil spills, and acid rain[2] [EPA13]. The energy sector is accountable for about two-thirds of greenhouse-gas emissions, as fossil fuels are facilitating more than 80% of global energy consumption [Bir13].

Energy supply is facilitated through a multifaceted network that initiates with extraction from an array of sources, to transformation, storage, distribution and ultimately utilization. Significant demand growth coupled with global megatrends including climate change, and resource scarcity demand reshuffling of this vital network. Intuitively difficult tradeoffs will need to be balanced as the electric utility industry progresses

---

[2] Global warming - refers to a gradual increase in the overall temperature near Earth's surface. It is generally attributed to the greenhouse effect caused by increased levels of carbon dioxide, chlorofluorocarbons, and other pollutants.

Oil Spill- refers to the release of a liquid petroleum hydrocarbon into the environment, especially marine areas, due to human activity.

Acid rain – refers to a rain or any other form of precipitation that is unusually acidic. It can have damaging effects on plants, aquatic animals and infrastructure. it is caused by emissions of sulfur dioxide and nitrogen oxide, which react with the water molecules in the atmosphere to produce acids toward sustainability and transition to a more modern grid; while still meeting its principal obligation of facilitating affordable, reliable, and safe electricity.

As such, electric power companies are facing a formidable challenge of meeting the imperatives of energy triangle in improving their economic, environmental, and social sustainability performance. State-of-the-art solutions must be found to guarantee that the world's economy is powered in a socially and environmentally manner that is also economic while preventing a potentially disastrous global warming. Furthermore, electric power companies face certain challenges for updating their operations to include pioneering technologies and addressing incipient national security issues[3]. In other words, sustainability is gone from a nice-to-do to a must-to-do in the electric utility industry.

1.2 Electric Power Systems

1.2.1 Background. The electric power industry around the globe has experienced an era of rapid and critical changes concerning the way electricity is generated, transmitted, and distributed, since the mid-1980s. The necessity for more efficiency in power production and delivery, traditionally under the control of federal and state governments, has resulted in privatization, restructuring, and, ultimately, deregulation of power sectors in several countries including the United States.

An electric power system is divided into four major parts including: generation, transmission, distribution, and loads. Commonly several generators are operated in parallel in the electric power system to generate the required power and connected at a common point called a bus. The generated power is transmitted at high voltage,

[3] Fossil fuel dependence means that, to ensure our supply, we may be forced to protect foreign sources of oil. Further, reliance on foreign sources also creates a danger of fuel price shocks or shortages if supply is disrupted.

distributed at medium level voltage, and delivered to load points at low voltage level. Conventionally, electric power networks consist of large centrally-controlled generators connected to the high voltage side of the network and loads at the low voltage side. As such, the power flows from the high voltage side, where generators are connected, to the low voltage side of the network, where medium and small size loads are connected. Figure 1.1 illustrates simplified layout of the conventional electrical grid before alternative energy sources were added in recent years [Li05].

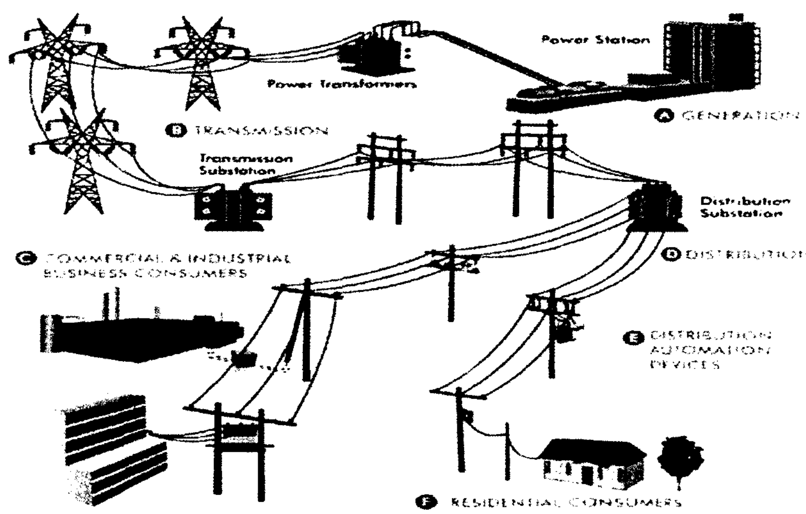

Figure 1.1. Conventional Electrical Grid[4]

1.2.2 Electric Power System Operation. In the electric power system operation, generating units are classified based on the number of hours they are in operation as follows:

- **Base-load units** - are the ones that run at 100% of their capacity on a 24-hour basis. Large fossil fired units and nuclear units fall into this category. The

[4] Source - oncor.com

megawatt generation of these units must remain constant throughout the scheduling horizon to keep the system in thermal balance.

- **Intermediate units** - are the manageable units that run most of the time but not essentially fully loaded. These units are used for power regulation. The hydropower units and small thermal units are regarded as intermediate units.
- **Peaking units** - are committed for a few hours in a day. Gas turbine generators, cascaded and pumped storage hydro units, and compressed gas units are considered as peaking units.

Natural gas units are considered as peaking units since, in contrast to coal or nuclear units, they can start quickly and ramp up to the capacity in a very short period of time. In comparison, natural gas units are cleaner and more expensive. If adequate generation to address off peak hour loads is kept on line during the day, the expensive generating units would be turned on for supplying peak hour loads in the generation scheduling horizon and would be shut down at off-peak periods in order to minimize the ED of generating units [Sha02]

In order to promote energy efficiency, alleviate the dependence on fossil fuel, and boost the security of transmission-constrained electric power systems, distributed generating units are employed progressively at load centers. Furthermore, embraced as a key solution to the trilateral challenges of economic supply, security, and climate change, renewable energy continues to play a pivotal role in today's energy stock; providing a sustainable basis for greening and growing the economy. For example, in the US, the installed wind base has spiraled nearly five-fold since 2006, from 11.6 GW to over 50 GW at the end of 2012. Before 2006, the highest annual rate of deployment in the United

States had been around 2 GW, but since then the industry has revealed it is capable of adding ten or more GW per year. Consequently, the abundant renewable energy resources which are independent of fuel price variations play a major role in modern electric power system operations [Yer13].

The emergence of Smart Grid (SG) has initiated a new revolution in the power sector. A SG is an electricity transmission and distribution network that has the capability to quickly integrate, simplify and understand large amounts of information and utilize it properly by making intensive use of both automation and information and communication technologies (ICTs). Smart grids have profoundly changed the way electricity is produced, consumed and distributed. Smart grid novel network structure allows for efficient use of distributed energy resources (DERs) (including distributed generation, renewable energy sources and distributed energy storage). Smart grid applies a cluster of loads using energy demand response (DR)[5] for offering significant control capacities in electric power system operations [Bal11].

1.2.3 Economics of Electric Power System Operation. The extreme variations in power delivery between peak and off peak hours in the generation scheduling horizon would require expensive generating units which are generally scheduled for supplying peak loads to be shut down at off-peak hours to minimize the fuel cost for SCUC and SCED of generating units.

Unit Commitment (UC) and Economic Dispatch (ED) are two basic concepts in the economic operation of electric power systems. SCUC refers to the economic

[5] Demand-Response is defined as fluctuations in electric consumption by end-use customers from their regular usage patterns in response to variations in the price of electricity over time, or to incentive payments designed to encourage lower electricity use at times of high wholesale market prices or when system reliability is threatened.

scheduling of generating units for supplying the hourly load while satisfying all operation constraints for generating units and transmission power systems. Short-term UC will outline the hourly On/Off status of thermal units over a day while contemplating the cost and addressing physical constraints for starting-up and shutting down of thermal units. ED would determine the least cost operation of an electric power system by dispatching the available electricity generation resources to supply the hourly system load, while satisfying the operation constraints of available generation resources [Li05].

1.2.4 Electric Power System Operation Risk Management. Although fossil fuels are still the leading energy source for the world's economic engine, provision of renewable sources will have to globally overshadow the future energy architecture, to enhance and ultimately replace the more-polluting conventional energy sources. As the world looks to combat climate changes, a shift from carbon-based fuels to non-carbon based fuels is inevitable. It is possible to knock a lot of carbon out of the electric power system through large-scale integrations of renewable sources. Given proper scales, clean energy has the potential to support the balance of the energy triangle in improving their economic, environmental, and social sustainability performance. According to International Energy Agency [Bir13], escalated share of power generation from renewables, as well as natural gas in tandem with limited use of the least efficient coal-fired plants would curb emissions by 640 gigatonnes (Gt) in 2020 and help efforts to restrain local air pollutions. According to World Wind Energy Association [WWE13], the total installed global wind power capacity has increased almost ten-fold between 2000 and 2010, and jumped from 18 gigawatts (GW) to 175 GW.

The main shortcoming of renewables such as solar and wind power is that they must be tailored to a specific area to make best usage of local conditions (i.e. high radiation or major winds). Further, intermittency is the major challenge for renewables. While traditionally large thermal power plants can be operated as base power supply, and many can ramp up and down to address electricity demand fluctuations, renewable generation assets can fluctuate fairly rapidly and dramatically at random hours of a day.

When large-scale renewables are employed, the periodic availability of supply will have a significant impact on energy security. Basically, renewable sources are at the mercy of nature, in that if the sun doesn't shine or the wind doesn't blow then solar panels and wind farms will be ineffective. In the case of wind turbines, the supply could be negatively interrelated with the hourly load since the wind generation is frequently higher at night when the hourly demand is lower.

Producing and maintaining enough power to deal with peak loads on top of the urge for developing a low-carbon economy require significant evolutions in the electricity grid infrastructure. One way to accelerate this transformation is to store energy when demand is less and put that energy back on the grid when demand spikes back up.

As variable renewable generating resources contribute a growing share of power production in the grid, it becomes more challenging to match supply and demand and to smooth out the variability of renewable sources. As such, the higher the penetration level of renewable generation, the higher will be the need for costly and rather fast backup generation so that the electric power system security is not jeopardized when renewable energy resources introduce a significant level of uncertainty into generation portfolios and electric power system operations [Mas04].

Smart grids could immensely support the integration of intermittent renewable technologies into the conventional electricity grids, which will be of paramount importance. Number of key technologies must be developed to transform current, outdated grids to smart ones. Additionally, new business models, capital, political will and, most importantly a collaborative innovation approach are needed to ease this transformation.

One promising methodology for resolving the variability of renewables is the coordination of renewable energy resources with distributed energy storage systems. The coordinated system is viewed as an attractive multi-mode generating unit example which may be used for mitigating transmission flow congestions, lowering operating costs by shutting down peaking units, and reducing system emissions. Batteries play a significant role among the storage alternatives which is because of the possibility of swift charging and discharging. Thus, a battery storage system can improve the reliability of energy supply during peak demand hours and captivate wind energy surplus during the off peak periods when demand is lower than output [Adi01].

The problem is that the battery technology is not where we need it to be in terms of energy density and cost. The total operating cost of wind turbines escalates by adding storage or spinning reserve expenses. Further, an efficient control system is required to shrink the associated cost by extending the battery life [Kha10]. As such utilities cannot afford to buy large and central batteries in order to implement the battery storage scenario.

That is where the distributed storage in EVs can come in and play a constructive role. EV batteries are often considered as a potential source of distributed storage which can be charged at night by wind turbines. Furthermore, replacing internal combustion engine cars with more EVs on the road can significantly lower CO_2 levels. According to IEA [Bir11], For every $1 of investment avoided in the power sector before 2020, an additional $4.30 would need to be spent after 2020 to compensate for increased GHG emissions.

Although behavioral aspects of providing storage while maintaining flexibility and mobility to EV owners could pose complex tradeoffs. Moreover, the battery of an individual vehicle is a trivial resource with a minute influence on the grid. Individual batteries in today's EVs have approximately 25 Kilowatt hour (kWh) of capacity as compared to multi-megawatt-hour batteries that would be required for utility-scale power storage. As such, an individual battery only appears as a noise in the system. However, large aggregations of EV batteries could represent a potential storage unit for electric power system applications. For the purpose of the study in this chapter, EVs are aggregated both on supply side (to provide power for demand balancing) and on demand side (to consume at proper times). Aggregated EVs consider several EV fleets.

Although at present the market for EVs is very limited, but it is anticipated to flourish with advances in new technologies, predominantly in the area of high energy and power density batteries. The introduction of EVs as distributed storage would pave the way towards a sustainable growth with a significant impact on electric power supply systems.

The integration of aggregated fleets of EVs into the electricity grid as distributed resources (V2G). In V2G strategy, EV storage is charged at low price hours and provides the stored charges back to the grid when electricity prices are high. V2G has the potential to extensively reduce renewable energy variability, shrink the carbon footprint of both transportation and utility sectors, and minimize power shortages in a cost-effective and secure manner. To sustain an economic growth, V2G provides a migration path towards energy independence. By merging the smart grid technology with aggregated EV fleets as distributed battery storage, we will have an opportunity to provide ample resources for peak load reductions. EV fleets as distributed battery storage device can facilitate the balance of supply and demand which could otherwise make it difficult to stabilize the system frequency [Zah12].

1.3 Dissertation Goal and Objectives

This study is the application of MILP and BD to large-scale systems. It uses power systems as an example and focuses on the optimization modeling of electric power system operations in support of sustainable developments.

The main goal and objectives of the study in this dissertation is to develop a multi-stakeholder approach to power grid operation design; aiming to address economic, social, and environmental challenges of the constrained electricity generation.

This dissertation investigates the modeling of large-scale Electric Vehicle (EV) integration in electric power systems for compensation the high penetration of wind energy. The study introduces optimization methods for minimizing the operation cost and limiting fossil fuel emissions, as it considers power transmission constraints for supplying the least cost supply options to load centers. A scenario-based MCS approach is developed to evaluate uncertainties involved in the operation of electric power systems; including the forecast error in the hourly wind forecast, hourly load forecast errors, and random outages of generation and transmission components. Further, this dissertation investigate role of storage mobility of EVs in firming the variability of renewable energy sources.

The rest of this dissertation is organized into 6 chapters as described below:

1.4 Employed Mathematical Modeling Approaches

Chapter 2 provides a general view of the mathematical modeling employed in this dissertation. SCUC is discussed and MILP and Lagrangian Relaxation (LR) methods are compared. Further, BD and scenario-Based MCS applied to stochastic simulation models are explained.

1.5 Deterministic Coordination Of Thermal Generating Units With Distributed Battery Storage to Enhance the Security and the Economics Of Power Grid Operation Considering Emission Constraints

Chapter 3 presents steps involve to develop an environmentally benign optimization model that facilitates the reduction in GHG emissions while optimizing the daily operation cost of electric power systems. Stationary EV fleets are deployed as distributed load and storage facilities; namely as virtual power plants. The hourly EV fleet dis/charge decisions are imposed by power system operators. The battery in EV fleets will function as controllable load in order to levelize the hourly system load during off-peak hours and generation resource during peak hours to provide the additional capacity to the grid in order to minimize the daily operation cost while alleviating GHG emissions[6].

Several studies have explored both the potential promise and the possible pitfalls of EV integrations into the power grid, and examined its impact on the power system

[6] Numerous substances act as GHG when emitted into the air. The primary concern, due to the volume of its emissions in energy production, is carbon dioxide (CO_2) and carbon dioxide equivalent (CO_{2e}).

operation. The 2012 report by Downing et al. [Dow11] evaluates the potential for plug-in vehicle as a new source of balancing services to smooth the daily demand profile. Their findings indicate that the UK plug-in vehicle park of 2020 would be capable of delivering an average of 6% of the country's projected daily grid balancing requirement for that year. According to International energy Agency [Bir11] in Organization for Economic Co-operation and Development (OECD) North America, OECD Europe, OECD Pacific and China, the deployment of smart grid technologies alone would restrain the escalation in peak load between 2010 and 2050 to 19% with intelligent EV-load scheduling and 12% when combined with extensive use of V2G, compared with 29% in a baseline case in which no smart grid technologies are utilized.

The integration of EVs may bring potential challenges to electric utility particularly at the distribution level. Shao, et al. study [Sha09] implies that the load created by plug-in-hybrid-vehicles (PHEVs) in some cases may surpass the distribution transformer capacity. A comprehensive approach for assessing the effect of different levels of PHEV penetration on distribution network investments and incremental energy losses is presented by Fernández, et al. [Fer11a].

Wang et al., [Wan12] analyzed the impact of three different EV load models on the grid load curve and on the load rate and peak-valley difference of the grid, and the impact of different scales of EVs on the grid. Their findings indicate that the regional EV load should be estimated beforehand in order to relieve the adverse effects of EVs on power grid operations. Considering discharging process of EVs, Mets, et al. [Met11], Stroehle, et al., [Str11] explored EV charging tactics and their effects on local power distribution networks of a residential zone. Authors investigated the optimal EV battery dis/charging scheduling to attain peak shaving, alleviate load intermittencies, and reduce electric mobility costs.

In this chapter, EV fleets are considered as stationary and distributed energy storage devices for enhancing power system operations. While most of the previous studies only look at the dispatch size without considering the transmission constraints, we are offering a more comprehensive solution. A deterministic SCUC algorithm is developed to coordinate the optimal hourly commitment and dispatch of thermal units and aggregated EV fleets considering transmission constraints. The proposed model's emphasis is on presenting a framework to effectively integrate stationary fleets of EV as distributed energy sources in power grids. The proposed formulation represents a multi-stakeholder model aiming to address economic, social, and environmental challenges of the constrained electricity generation.

The optimization of day-ahead hourly SCUC is facilitated through MILP. Considering the large-scale nature of the coordination problem, BD is considered as a practical solution for the real-time implementation of the proposed method. The BD deployment would simplify the complexity of the optimization problem by decomposing the original large-scale MILP problem into one integer program master (MIP) problem and linear programing (LP) sub-problems. An iterative process between the master problem and sub-problems delivers a minimized cost solution for generation scheduling while addressing network and emission constraints.

1.6 Deterministic Coordination Of Thermal Generating Units, Variable Renewable Sources and Aggregated EV fleets for Sustainable Operation of Power Grid Systems

Chapter 4 depicts a sustainable model that has the potential to accelerate greengrowth. The proposed methodology in this chapter discusses the modeling of aggregated EV fleets as stationary distributed load and energy storage facilities for wind energy, while addressing emission constraints. It examines the coordination between the storage and the renewable energy sources on the optimal operation cost of security-constrained power systems and their carbon footprint. The model is designed to establish a sustainable, low-carbon energy complex beyond fossil fuels and nuclear energy in an efficient, cost-effective manner.

Previous studies have illustrated that EVs could produce substantial profits while offering grid ancillary services. Andersson, et al. [And10] investigated the regulating power markets of PHEVs in both Sweden, and Germany. The simulation results implies that the German regulating power markets contribute significantly higher profit for PHEV than the Swedish markets; maximum average profits generated on the German markets are in the range 30–80 € per vehicle and month. Fernandes, et al. [Fer11b] study demonstrated that, adaptation of V2G strategy, improves system operation by flattening the demand curve and reducing operational reserves requirements causing a sharp cut in total and average system operation costs.

Valentine, et al., [Val13] considered the integration of wind energy and smart charging of EVs into the wholesale electricity market of the New York Control Area. Their results illustrate that grid integration of wind power and V2G can significantly benefit the NYCA as independent system-level resources via substantial cutbacks in wholesale energy market costs.

Pillai, et al. [Pil12] conducted a study on typical wind dominated distribution and transmission networks in Denmark. Their analysis shows that EVs based aggregated battery storage systems provide superior performance than the thermal generation sources to facilitate smooth and robust grid regulation services in electric power systems with high penetration levels of wind power. Their results indicate "EV integration of around 10% is capable of providing sufficient grid regulation services in Danish electric power systems to support wind power penetration of around 50% in Denmark." Tomic, et al. [Tom07] investigated the economic potentials of EVs for participating in regulation services. Raghavan et al. [Rag10] and Lukic et al. [Luk08] focused on storage technologies and power electronic grid-connection interfaces for facilitating large-scale adoptions of PEVs.

Saber, et al. [Sab11] addresses the role of PEV in the integration of renewable energy resources. They employed Particle Swarm Optimization (PSO)[7] to minimize operation cost and emission, in order to make a successful bridge between the electricity and transportation infrastructures.

Most of the previous studies only look at the dispatch size without considering the transmission constraints. This study is considering a bigger picture of the power system's operation, and offering a more comprehensive solution which is more appropriate for large-scale systems such as power grid. In this study, MILP is applied for the optimization of the day-ahead hourly deterministic SCUC considering the transmission constraints. Further, considering the large-scale nature of the coordination problem, BD is considered as a feasible solution for the real-time implementation. The employment of BD would ease the complexity of the optimization problem by decomposing the original large-scale MILP problem into one integer program master (MIP) problem and linear

[7] PSO is a bioinspired algorithm based on the behavior of flock of birds and school of fishes, and it has similarities to other population-based evolutionary algorithms.

programing (LP) sub-problems. An iterative process between the master problem and sub-problems conveys a minimized cost solution for generation scheduling while taking into account the network and emission constraints. This is a multi-stakeholder model pinpointing the challenges of energy supply, security, and climate change.

1.7 V2G for Sustainable Development in an Uncertain Environment – Stochastic Coordination of Thermal Units, Renewable Energy Sources, and Stationary EV fleets

Chapter 5 identifies strategies for a larger integration of variable generation resources without compromising the electric power system security in a scenario based approach. Hourly load and wind energy uncertainties and random outages of generation and transmission components are also taken into consideration. This chapter evaluates the potential for utilizing stationary fleets of electric vehicles (EVs) as distributed storage, in an uncertain environment. The proposed model mitigates energy imbalances caused by the integration of variable renewable sources in electric power systems. For the purpose of the study in this chapter, EVs are considered stationary as various studies indicate that most vehicles are parked an average of 90% of the time [Jen08], [Wir08].

The assimilation of high integration levels of wind power (greater than 30% of energy) into interconnected electric power systems necessitates the redesign of conventional electric power systems and operating practices [Ack05]. Although an increase in the geographic distribution and number of wind turbines alleviates the temporal variability of wind generation, and shrinks the wind forecasting errors, however, the seasonal wind patterns and electricity demand profile may not be correlated. Hence, demand and generation disparities can happen [Har10]. Furthermore, according to [Lun08], the wind energy surplus is more challenging to manage than wind energy shortages, since the wind energy surplus corresponds to the best economic return on wind energy investments that has not been attained properly for mitigating emissions. Numerous methods can be adopted to address this challenge including the integration of wind energy with flexible thermal power plants (e.g. gas turbines), enlargement of transmission system for better grid assimilation, and the utilization of energy storage, ranging from batteries, ultra capacitors, compressed-air storage, flywheels, fuel cell systems or hydroelectric power plants with storage reservoirs [Den11], [Str07].

Several studies have investigated the economic analysis of V2G technology in the literature. For instance, [Zho09] evaluate V2G feasibility in the context of the UK electricity market. De Los Ríos, et al. [Del12] examines the opportunities for V2G-enabled EVs to recognize revenues from the regulation market that offset operating costs, making them more cost competitive with conventional vehicles. [Ric13] explores the feasibility of a premium tariff rate for V2G power, using Ontario, Canada as a case study, similar to existing feed-in-tariff (FIT) programs for intermittent sources.

Previous studies have demonstrated that EVs could produce substantial profits while offering grid ancillary services. [Bor12] evaluates the possibility of integrating a fleet of EVs mingled with large penetration of wind generation into the grid system in northeastern Brazil to regularize possible energy imbalances. [Bat12] examines the role of V2G systems as a support to energy management within realistic configurations of small electric energy systems (SEESs) including intermittent sources, such as Microgrid. Clement et al., [Cle11] investigated the coordinated charging and discharging of EVS, where the objective function is to minimize the power losses; their findings indicate that combination of renewable sources and PHEVs, as distributed storage, can more efficiently match the consumption and generation.

The Hedegaard, et al. [Hed12] study assessed how a large-scale implementation of EVs towards 2030 would impact the electric power systems of five Northern European countries, Denmark, Finland, Germany, Norway, and Sweden; simulation results implies that when smartly charged/discharged , EVs can enable significantly higher wind power penetration.

Mullan, et al. [Mul12] investigated the viability of V2G concept in Western Australia, the smallest wholesale electricity market in the world, from technical, economic and commercial point of view. [Ekm11] examined the impacts of multiple EVs' charging strategies on the balance between wind power production and consumption in the future Danish electric power system scenario. Further, another big chunk of pollutants is coming from transportation sector which currently faces challenges to mitigate climate change, and alleviate reliance on oil products. EVs have the benefit of increasing security of supply by shrinking the transport sector's dependency on oil.

While most of the previous studies addressed the economic aspects of the integration of EVs into electric power systems, they overlook the transmission system security consideration offered by the EV interconnection and its daily profile in electric power systems. This chapter focuses on a practical methodology that has the potential to advance energy sector strategies regarding sustainability, keep the sector on track to address the 2DC climate goals by 2050 while addressing natural security issues. MILP is applied to the optimization of the day-ahead hourly stochastic SCUC while taking into account the network and emission constraints as well as uncertainties. Further, considering the large-scale nature of the coordination problem, BD is applied as a feasible solution for the real-time implementation.

1.8 Spearheading the push to fulfill large energy demand requirements in a sustainable manner: Stochastic Coordination of Thermal Units, Renewable Energy Sources, and EV fleets – considering EV Mobility

Chapter 6 spearheads the push to fulfill today's large energy demand requirements in a sustainable manner. This chapter investigates operational strategies for reliable and efficient integration of renewables at the distribution level. The proposed large-scale stochastic optimization modeling examines the bi-directional role of aggregated EV fleets on the power systems operation with a scenario based approach.

Electric vehicles represent hourly distributed and mobile demands in power systems which could also provide distributed storage to power grids (V2G) . Unlike conventional storage capabilities, the grid-connection storage topography of EVs may vary during the daily operation of power systems. EVs consume energy according to their driving requirements.

Several studies have been conducted regarding the bi-directional role of EVs and their influence on the electric grid. However, they often neglected topological grid operation constraints [Tom07],[Kem05a],[Kem05b].

[Rag12],[Glo08],[Lu09] studies unanimously came into conclusion that V2G concept's bi-directional power flow would moderate uncertainties imposed on power grids by the high penetration of renewable energy resources. The EV mobility would also affect potential costs/revenues in regional electricity markets. The electricity market issues of PEV integration were presented in [Kem05b]. Storage technologies and power electronic grid-connection interfaces for enabling large-scale adoptions of EVs are discussed in references [Lee09] and [Luk08].

An investigation by Public Utilities Fortnightly examined the annual potential revenue of a PHEV owner selling energy to the power grid for regulatory and spinning reserve purposes [Let06]. [Met12] presented an approach to simulate large vehicle fleets on the basis of individual driving profiles; investigating the conflicting relationship between user mobility and grid.

[Hed12] analyzed the influence of the intelligent EVs' charge/discharge on the power systems of five Northern European countries, including: Denmark, Finland, Germany, Norway, and Sweden. Their results indicate that EVs facilitate significantly increased wind power investments in all of the countries analyzed, and can reduce the need for new coal/natural gas power capacities if charge/discharge intelligently. The significant potential for financial return when the V2G service is used for frequency regulation is investigated in [Whi11].

Coordinated charging and discharging is investigated in [Cle11]; their result indicates that uncoordinated charging of EVs in distribution grid can lead to local grid problems. In order to make a more accurate forecast of the technical potential of electric vehicles as dispersed energy storages or controllable loads, [Rol13] introduced a simplified stochastic model based on nonhomogeneous semi-Markov processes for modeling the load behavior of electric vehicles.

Most of the previous studies overlooked the transmission constraints. We are offering a more comprehensive solution which is more appropriate for large-scale systems such as power system grid. The contribution of this study include the modeling of large-scale EV integration as a mobile distributed load and storage facilities and their impacts on the optimal operation of network-constrained power systems, and their carbon footprint. Further, hourly load and wind energy forecast errors, random outages of generation and transmission components, random driving patterns of EVs are taken into consideration in the proposed modeling approach. In this study mixed integer linear programing (MILP) is applied for the optimization of the day-ahead hourly stochastic security-constrained unit commitment considering the transmission, and EV mobility constraints. Further, considering the large scale nature of the coordination problem, Benders decomposition (BD) is considered as a feasible solution for the real-time implementation. As proof of validation, practicality, and reliability of the proposed modeling approach, comparison among three scenarios/case studies is presented.

1.9 Conclusion & Summary

Chapter 7 provides a brief summary, and draws a comprehensive conclusion from all the above studies. The results indicate that the applications of renewable energy sources and the intelligent assimilation of EV fleets (both as a provider and a consumer of energy) offer potentials for alleviating peak demands, mitigating variability and intermittency of wind generation, minimizing power grid operation costs and hourly wind curtailments, removing transmission flow congestions, and limiting the environmental impacts of fossil fuel-based thermal generating units in the operation of electric electric power systems.

CHAPTER 2

EMPLOYED MATHEMATICAL MODELING APPROACHES

This chapter provides an overview of the mathematical modeling approaches employed in this dissertation.

2.1 Security Constrained Unit Commitment (SCUC)

People utilize less electricity on Saturdays than on weekdays, less on Sundays than on Saturdays, and at a lesser rate between midnight and early mornings than during the day, therefore, utilities' daily load patterns exhibit extreme variability between peak and off peak hours. It is possible that some of the units will be operating close to their minimum generating limit during the off-peak period if adequate generation to meet the peak is kept on line throughout the day. A system operator's challenge is to decide which units should be taken offline and for how long. It is preferable to use an optimum or suboptimum operating strategy based on economic criteria. In other words, meeting the power demand at minimum fuel cost utilizing an optimal mix of different power plants is a vital condition in electric power system operation.

UC and ED are two basic optimal scheduling concepts in the economic operation of electric power systems. The optimal UC of thermal systems, results in a great saving for electric utilities. The UC problem is to optimally run (turn ON/OFF and dispatch) a set of generating units over a given time horizon while addressing projected load demands, spinning and operating reserve requirements, minimum ON/OFF time and ramping limits of generating units, generating capacity limits, emission constraints, and so on with the least system production cost. ED would determine the least cost operation of an electric power system by dispatching the available electricity generation resources to supply the hourly system load, while satisfying the operation constraints of available generation resources [Sha02]. ED controls the electric power system's status in real time as system conditions evolves; since majority of thermal generating units are not able to reverse their On/Off status within a short period of time (e.g., 5-10 minutes).

Mathematically, SCUC is a non-convex, nonlinear, large-scale, mixed-integer optimization problem with a large number of binary variables, continuous and discrete control variables, and a series of prevailing equality and inequality constraints. [Li05]. Addressing which units should be on/off is the integer part, and how much power should be dispatched on transmission lines is the continuous part; as such we are dealing with a MILP problem.

Several optimization techniques, including enumeration, priority listing, dynamic programming (DP), Lagrangian relaxation (LR), mixed-integer programming (MIP), and heuristic based methods (e.g., genetic algorithms, artificial neural networks, expert and fuzzy systems) have been deployed for achieving a near optimal solution and minimizing the operating cost, while fulfilling the physical operation constraints. Nevertheless, perceived bottlenecks such as the enumeration calculation, DP's high dimensionality, and heuristic solution's fine-tuning are obstacles to practical applications of UC. With the development of improved optimization techniques, Lagrangian relaxation (LR), and Mixed Integer Programming (MIP) optimization techniques are most widely applied to UC for unraveling day-ahead and real-time generation scheduling problems.

2.2 LR and MILP Methods

The LR method focuses on finding a proper co-ordination approach to generate feasible primal solutions, while minimizing the duality gap. The technique consists of relaxing system constraints, linearizing the augmented item and decomposing the relaxed Lagrangian objective function into subproblems for each unit. The LR method applies the dual optimization technique to a non-convex UC problem with discrete variables for calculating the generating unit status. The basic idea for applying LR is to adjoin coupling constraints (e.g., power balance, reserve requirements) to the objective function by using Lagrangian multipliers. The relaxed UC problem is further decomposed into subproblems for individual generating units. So, the solution of UC is obtained by solving smaller sub-problems. The main difficulty with the LR methods is that, because of the non-convexities of the UC problem, heuristic procedures are required to find feasible solutions, which may be suboptimal. [Yan12].

A MIP solution is the optimization of a linear function with integer and continuous variables. For example:

$$
\begin{aligned}
Min\, C^T x \qquad st.\ & A_1 x = b_1 \\
& A_2 x = b_1 \\
& 1 \le x \le u \\
& x_j \text{ integer for some } j
\end{aligned}
$$

where : C, b_1, b_2, 1, u are vectors and A_1 and A_2 are matrices.

The MIP method could obtain a solution that is more optimal than that of LR in a finite number of steps. This feature facilitates broader applications of the MIP method in power markets. Moreover, it provides a flexible and accurate modeling framework; so that it is easier to add constraints to the MIP model and achieve an optimal solution, without involving heuristics, which could dramatically accelerate the development of UC and facilitate its applications to large-scale electric power systems [Sha05]. In addition, during the search of the problem tree, information on the proximity to the optimal solution is available. Efficient MILP software packages such as the branch-and-cut algorithm have been developed, and optimized commercial solvers with large-scale capabilities are currently available. The main drawback of MIP is still its computational complexity when applied to large-scale UC problems. However, powerful MILP methods, such as the branch-and-cut algorithm with large-scale potentials, could lower the computation burdens of MILP.

The UC problem is formulated as:

$$\min \sum_{t} \sum_{i} \left(F_{c,i}\left(P_{i,t}\right) + SU_{i,t} + SD_{i,t} \right) \qquad \text{(i)}$$

s.t.

$$\sum_{i=1}^{NG} P_{it} = P_{D,t} + P_{L,t} \qquad \left[t = 1,\ldots,NT\right] \qquad \text{(ii)}$$

$$P_{i,t} \in \pi_{j,t} \quad \forall i, \forall t \qquad \text{(iii)}$$

where $\pi_{j,t}$ represents the region of feasible production of generating unit j in time period t. The objective of the UC problem is to minimize the total operation cost, which is defined as the sum of the production cost, the startup cost, and the shutdown cost (i). The production cost often is expressed as a quadratic function of the power output, while the startup cost is usually modeled as a nonlinear (exponential) function of the offline time prior to the startup [Sha02]. Power balances in all periods are represented by the block of constraints which could include electric power system losses (ii). The block of constraints (iii) illustrates, in a compact way, the operating constraints, for every time period, of every unit, e.g., generation limits, ramp rate limits, and minimum up and down times. Binary variables are used to model on/off decisions.

The nonlinear production cost function can be accurately approximated by a set of piecewise linear blocks as shown in Fig. 1. Piecewise linearization is accommodated in LP in which slopes assume different values over ranges of associated variables. Each range of a given variable signifies an upper and lower limit within which the slope is constant.

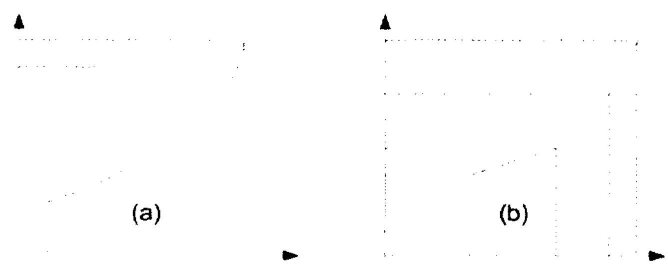

Figure 2.1. Linearization (a) Nonlinear Curve, (b) Piecewise Linear Curve

2.3 Benders Decomposition

The optimization problem in hand is a large mixed-integer programming with two-level hierarchical structure suited for BD applications. BD is widely used for separating large-scale mixed-integer program (MIP), typically used in electric power systems, into several easy-to-solve subproblems. Considering the size of real-world security constraint-UC problems involving hundreds/thousands of generating units and transmission lines, and multiple study hours, security constraint-UC is divided into two problems, one integer program master (MIP) problem - UC - and LP network evaluation sub-problems. The goal of the day ahead resource scheduling is to fulfill load while maintaining transmission flows within their permissible limits at the minimum possible cost. The energy day-ahead resource-scheduling model also includes the network simulation, through dc power flow calculation, which considers the relevant network constraints.

Master problem solves UC and ED with all prevailing constraints. The lower bound solution of the master problem may involve fewer constraints. The sub-problems will examine the dc power flow according to the master problem's UC solution in the base case for minimizing transmission flow violations. If any violations arise, the corresponding feasibility Benders cuts are continuously generated and fed back to the master problem for the solution of the next iteration. Accordingly, a new lower bound solution of the original problem will be achieved by re-calculating the master problem with more constraints. The process continues until all violations are mitigated. The iterative process between the master problem and sub-problem delivers a minimized cost solution for generation scheduling while addressing transmission, voltage, and emission constraints. The optimal solution of the original problem will be achieved when the upper bound and the lower bound are adequately close; which will confine the final solution to be close enough to the global optimal solution of the original problem [Sha05].

Here master problem offers network constraint-UC a chance to improve the original UC solution to satisfy all transmission network constraints (i.e., transmission flows and bus voltages limits). Decomposition is the only feasible option for the solution of the large-scale SCUC problem in real time. Fig. 2.2 illustrates the flowchart of the discussed hourly security constraint-UC formulation.

If the solution to the master problem is infeasible, we have to curtail the load; which is referred to as load shedding. The infeasibility of the master problem is out of the scope of this dissertation.

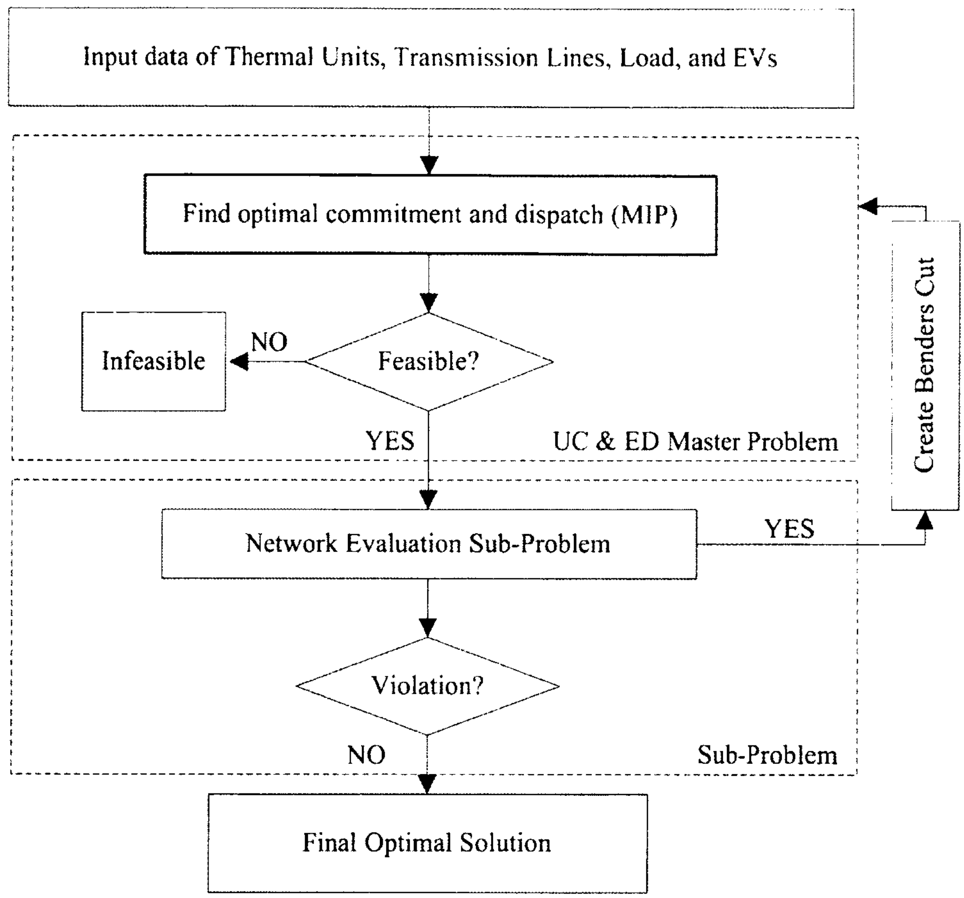

Figure 2.2. Operation and Control of Electric Power Systems

2.4 Monte Carlo Simulation (Scenario-Based Stochastic Simulation)

Scenarios are generated to showcase electric power system uncertainties through the MCS employment. Uncertainties include random outages of generators and transmission lines, and day-ahead forecast errors of hourly demand and wind speed. The MCS parameters consist of forced outage rates of electric power system components and probability distribution functions for load and wind speed forecast errors.

The load forecast error is denoted in (2.1) by a truncated normal distribution in which the mean is the hourly power forecast and the standard deviation is 5% of the mean [Bil96].

$$f(x)=\begin{cases} 0 & x<\mu-3.5\sigma \ or \ x>\mu+3.5\sigma \\ \dfrac{1}{a\sqrt{2\pi\sigma}}.e^{\frac{(x-\mu)^2}{2\sigma^2}} & \mu-3.5\sigma\leq x\leq\mu+3.5\sigma \end{cases} \tag{2.1}$$

Where μ and σ are the mean and standard deviation of the normal distribution respectively.

And $\alpha=\int\limits_{\mu-3.5\sigma}^{\mu+3.5\sigma}\frac{1}{\sqrt{2\pi\sigma}}.e^{\frac{-(x-\mu)^2}{2\sigma^2}}dx$

The wind speed forecast error is characterized by the auto- regressive moving average (ARMA[8]) [Sod04], [Boo05]. As the time lag escalates, the autocorrelation factor (ACF) and partial autocorrelation factor (PACF) of the wind speed time series declines radically. Accordingly, the hourly wind speed forecast error is denoted by a lower order ARMA (1,1) as shown in (2.2).

The ARMA constants are attained by minimizing the root mean square error (RMSE) between the simulated ARMA time series and the measured wind speed data [Boo05]. For the purpose of this study, the ARMA constants are considered as $\alpha=0.98$ and $\beta=0.7$, and it is assumed that *Z*(*t*) follows Gaussian distribution function with the standard deviation of 10% of the wind speed projection.

The projected wind speed time series is obtained by employing the probability transition matrix, which is either characterized by historical data or by probability distribution parameters of wind speed time series [Man06]. The probability transition matrix outlines probabilities of transiting from one wind speed category to others.

[8] In the statistical analysis of time series, autoregressive–moving-average (ARMA) models deliver a parsimonious description of a (weakly) stationary stochastic process in terms of two polynomials, one for the auto-regression and the second for the moving average

The wind speed is categorized into several ranges of wind speeds, which are signified by the mean value at each category, in order to obtain the probability transition matrix from historical data. Alternatively, the probability transition matrix is obtained employing the Weibull distribution function and the autocorrelation factor; by composing an initial probability vector, a weighting matrix, and a normalizing vector [Man06]. Once the probability transition matrix is constructed, the wind speed time series is created using the Markov chain method [Man06],[Man02].

$$X(t) = \alpha.X(t-1) + \beta.Z(t-1) + z(t) \qquad (2.2)$$

The diurnal pattern strength, which has a sinusoidal form, illustrates the daily wind speed pattern. The peak value in this pattern specifies the ratio of the maximum wind speed to the daily average wind speed [Man06],[Man02]. The diurnal pattern strength is then applied to the wind speed time series. Lastly, the hourly wind power generation is acquired using the power curve of wind turbines and the hourly wind speed. Further, a low discrepancy method, Latin Hypercube Sampling (LHS), is developed to generate evenly distributed random samples with a smaller variance in order to improve the efficiency of the scenario-based stochastic simulation [Wu07],[Wu08],[Gla03].

Additionally, scenario reduction techniques offer a goodness-of-fit adjustment between the computation speed and the accuracy, by removing scenarios with very low probabilities and aggregating scenarios that are very close in terms of statistical metrics [Wu07],[Wu08],[Gla03],[Dup03],[Gam02].

CHAPTER 3

DETERMINISTIC COORDINATION OF THERMAL GENERATING UNITS WITH DISTRIBUTED BATTERY STORAGE TO ENHANCE THE SECURITY AND THE ECONOMICS OF POWER GRID OPERATION CONSIDERING EMISSION CONSTRAINTS

This chapter is organized into 4 sections as follows: section 3.1 formulates the proposed deterministic SCUC model with penetration of aggregated EV fleets, as distributed battery storage, considering emission reductions. Section 3.2 depicts the effectiveness of the proposed approach by a case study on a 6-bus system. Challenges of the proposed model are presented in section 3.3. Finally section 3.4 provides concluding remarks on the effectiveness of the proposed formulation for a smarter, cleaner, socially responsible and sustainable generation of electricity.

3.1 Thermal Units – Aggregated EV Fleets Coordination Methodology

The proposed SCUC is formulated as a MILP optimization model that optimizes the coordination between conventional thermal units, with stationary EV fleets as distributed battery storage facilities, while incorporating emission constraints. The proposed model spearheads economic goals with substantial cutback on carbon-footprints, focusing on day-ahead scheduling (short-term operation). The MILP problem is solved using Generic Algebraic Modeling System (GAMS) software with a dc power flow algorithm that considers network constraints utilizing CPLEX optimizer solver.

Number of EVs in a fleet and their energy requirements are considered as variables in the proposed SCUC optimization problem. The physical characteristics and operation constraints of thermal generating units are considered as input. The hourly UC and dispatch of generating units and dis/charge states of EV fleets provide the optimal hourly solution.

The objective of SCUC (3.1) includes minimizing the daily operation cost in which the projected quantities of loads and EV batteries are included, subject to generating unit, system, and emission constraints. The objective function (1) consists of the generation cost of thermal units, startup and shutdown costs of thermal units, and the operation cost of EV fleets. F_C is the production cost function, which is the generating units input/output (I/O) curve. The production cost is typically expressed as a quadratic function of the power output $F_{c,i}(p_{it}) = a_i + b_{ci}p_{it} + c_{ci}p_{it}^2$ where a, b, and c are the cost coefficients.

The second term denotes the startup cost (SU), which is a function of the length of time that the unit has been off. The startup cost is given as

$$SU_{it} = I_{it}\left[1 - I_{i(t-1)}\right]\left[\alpha_i + \beta_i(1 - e^{-x_{it}^{off}/\lambda_i})\right]$$

where □ is the integrated cost of startup and equipment maintenance, β_i is the startup cost of unit when initiating from cold conditions, X^{off} is the number of hours that the unit has been Off, and λ_i is the thermal time constant that characterizes the cooling speed of the unit. Similarly, the shutdown cost (SD), which is formulated as $SD_{it} = kP_{it}$; here k is the incremental shutdown cost. The operation cost of EVs, $C_{v,t}$, depends on the number of vehicles and dis/charging depth and frequency [Kho12].

The system and generating unit constraints are presented in (2)-(20); the unit generation capacity limits given in (3.2) indicate that once committed (I=1), the generation unit must run between its min and max generating capacity. If I=0, the unit is turned off.

The min down/up time constraints are given in (3.3) and (3.4); (3.3) indicates that a unit must be OFF for a certain period before it can be turned on again. By contrast, (3.4) indicates that a unit must be ON for a certain period before it can be turned off again. Equations (3.5) and (3.6) represent the operating ramp up/down limits. The operating ramping up/down bounds limit the movement of a generating unit between adjacent hours. Equation (3.5) denotes that when unit i is starting up at time t its generating output (P_{it}) should be equal to the minimum generating output of unit (p_{min}). Likewise, equation (3.6) implies when unit i is shutting down at time t, its generating output $\left(P_{i(t-1)}\right)$ should also be equal to the minimum generating output of unit (p_{min}) [Sha05].

The emission constraint (3.7) illustrates that the daily emission must be less than or equal to a required limit. Numerous substances act as GHG when emitted into the air. The primary concern, due to the volume of its emissions in energy production, is carbon dioxide (CO_2) and carbon dioxide equivalent (CO_{2e}). The emission function is considered as a convex function of power generation which is modeled as $F_{e,i}\left(p_{it}\right) = a_{ei} + b_{ei}p_{it} + c_{ei}p_{it}^2$ in which a_{ei}, b_{ei}, c_{ei} are emission coefficients[9]. The above nonlinear emission function is piecewise linearized and incorporated into the proposed MILP formulation. The startup and shutdown emission is represented by $SU_{e,it}^{ET}$ & $SD_{e,it}^{ET}$.

Equation (3.8)-(3.9) corresponds to the system load balance and dc power flow constraints, respectively. Power flow for each transmission line is represented by (3.9)

[9] For each thermal units, heat curve (MBTU/MW) and (MBTU/Metric Tons of emissions) are considered; their interactions is computed as emission cure (MW/metric tons).

which is dependent on the voltage angle difference between adjacent buses and the line impendence. Transmission flow limits are represented by (3.10).

The EV fleet constraints are given in (3.11)-(3.18). The net hourly absorbed/injected energy and the dispatched power of EV fleet is given in (3.11) which illustrates that the difference between the energy stored in the aggregated EV battery and the EV energy injected back to the grid is measured by the charging cycle efficiency of the aggregated EV. The hourly charge/discharge/idle modes of EV fleets which are mutually exclusive are given by (3.12). Once an EV fleet is connected to the electric power system ($N_{v,t}$=1), the aggregated battery will be charged, discharged, or stay in the idle mode. Equations (3.13)-(3.14) represent charge/discharge power constraints. The hourly energy balance is given in (3.15). Equations (3.16)-(3.17) show the energy capacity limit of each aggregated unit. Equation (3.18) represents the piecewise linear function of convex charge/discharge cost curve of EV batteries which indicates the operation cost of aggregated EVs has a direct correlation with the depth of charging/discharging batteries; a higher depth in battery charging/ discharging causes the number of cycles to failure decrease which in turn corresponds to an increase in the cost of EV charging/discharging [Tom07]. In the proposed MILP formulation, the nonlinear battery dis/charging cost curves are piecewise linearized. A tighter piecewise linear estimation is presented in [Wu11]. Equation (3.19) illustrates the assumption that the aggregated state of charge (SOC) of batteries is set to be fixed at specific operation periods [Kh012]; It is anticipated that the SOC is at 100% when a PEV fleet is leaving the station.

$$\min \sum_t \sum_i \left(F_{c,i}\left(P_{i,t}\right) + SU_{i,t} + SD_{i,t} \right) + \sum_t \sum_v C_{v,t} \tag{3.1}$$

S.t.

$$P_{i,\min} I_{i,t} \le P_{i,t} \le P_{i,\max} I_{i,t} \quad \forall i, \forall t \tag{3.2}$$

$$\left[X_{i(t-1)}^{off} - T_i^{off}\right] * \left[I{it} - I{i(t-1)}\right] \ge 0 \quad \forall i, \forall \mathrm{t} \tag{3.3}$$

$$\left[X_{i(t-1)}^{on} - T_i^{on}\right] * \left[I{i(t-1)} - I_{it}\right] \ge 0 \quad \forall i, \forall \mathrm{t} \tag{3.4}$$

$$P_{it} - P_{i(t-1)} \le \left[1 - I_{it}(1 - I_{i(t-1)})\right] UR_i + I_{it}\left(1 - I_{i(t-1)}\right) P_{i,\min} \quad \forall i, \forall t \tag{3.5}$$

$$P_{i(t-1)} - P_{it} \le \left[1 - I_{i(t-1)}\left(1 - I_{it}\right)\right] DR_i + I_{i(t-1)}\left(1 - I_{it}\right) P_{i,\min} \quad \forall i, \forall t \tag{3.6}$$

$$\left\{ \begin{array}{l} \sum_i \sum_{t=1}^{24} \left[F_{e,i}^{ET}(p_{it}) + SU_{e,it}^{ET} + SD_{e,it}^{ET} \right] \le EMS_{\max,i}^{ET} \\ \forall i \;, ET = \left\{CO_2 \;\&\, CO_{2e}\right\} \end{array} \right\} \tag{3.7}$$

$$\sum_i P_{i,t} + \sum_v P_{v,t} + \sum_w P_{w,t} = \sum_{d \in D_b} P_{D,t}^d + \sum_{l \in L_{f,b}} PL_{l,t} - \sum_{l \in L_{t,b}} PL_{l,t} \quad \forall i, \forall t \tag{3.8}$$

$$PL_{l,t} = \left(\frac{\theta_{j,t} - \theta_{o,t}}{X_{jo}} \right) \text{ line l is from bus } j \text{ to bus } o \tag{3.9}$$

$$\left|PL_{l,t}\right| \le PL_l^{\max} \tag{3.10}$$

$$\left\{ \begin{array}{l} E_{v,t}^{net} = \eta_v . P_{c,v,t} - P_{dc,v,t} \\ P_{v,t} = P_{c,v,t} - P_{dc,v,t} \end{array} \right\} \tag{3.11}$$

$$I_{dc,v,t} + I_{c,v,t} + I_{i,v,t} = N_{v,t} \tag{3.12}$$

$$I_{c,v,t} . P_{c,v}^{\min} \le P_{c,v,t} \le I_{c,v,t} . P_{c,v}^{\max} \tag{3.13}$$

$$I_{dc,v,t} . P_{dc,v}^{\min} \le P_{dc,v,t} \le I_{dc,v,t} . P_{dc,v}^{\max} \tag{3.14}$$

$$E_{v,t} = E_{v,t-1} + E_{v,t}^{net} \tag{3.15}$$

$$E_v^{\min} \le E_{v,t} \le E_v^{\max} \tag{3.16}$$

$$E_{v,0} = E_{v,NT} \tag{3.17}$$

$$\left\{ \begin{array}{l} C_{v,t} = N_{v,t} \cdot \left[\sum_m b_{m,v} \cdot P_{m,v,t} \right] \\ 0 \le P_{m,v,t} \le P_{m,v}^{\max} \\ N_{v,t} \cdot \left| E_{v,t} - E_{v,t-1} \right| = \sum_m P_{m,v,t} \end{array} \right\} \tag{3.18}$$

$$E_{v,T} = E_v^{\max} \tag{3.19}$$

Fig. 2.2 illustrates the flowchart of the discussed hourly security constraint-UC formulation.

3.2 Numerical Results

In this section, the impact of introducing stationary EVs as distributed battery storage on power grid operations is examined. Following 3 cases are investigated:

Case 1: Hourly SCUC solution without emission constraints

Case 2: Hourly SCUC solution with emission constraints

Case 3: Hourly SCUC solution with emission constraints and stationary EV fleets.

3.2.1 6-Bus System. The 6-bus electric power system, depicted in Figure 3.1, is analyzed to illustrate the effectiveness of the proposed formulation.

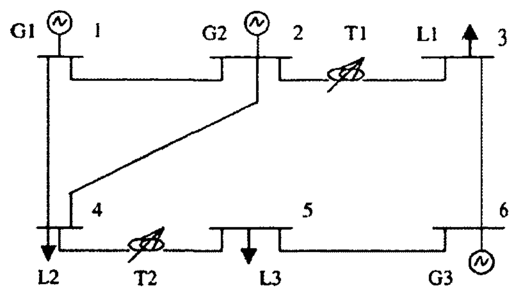

Figure 3.1. 6-Bus Electric power system

The 6-Bus system has three thermal units, and five transmission lines; G1 is the cheapest generating unit with the highest level of emission. The characteristics of generating units, transmission lines, and the forecasted hourly load for 24h are illustrated in Tables 3.1 and 3.2 and Figure 3.2, respectively. Table 3.3 represents the emission function coefficients.

Table 3.1. Thermal Unit Characteristics

Unit	a ($/MW^2)	b ($/MW)	c ($/h)	P_{min} (MW)	P_{max} (MW)	SU ($)	SD ($)	Min. Up(h)	Min Dn.(h)
G1	0.099	6.589	211.4	100	320	100	50	4	3
G2	0.203	7.629	217.4	10	160	200	40	3	2
G3	0.494	10.07	102.8	10	100	80	10	1	1

Table 3.2. Transmission Line Characteristics

Line ID	From Bus	To Bus	Impedance (p.u)	Capacity (MW)
1	1	2	0.17	35.6
2	1	4	0.258	35.6
3	2	4	0.197	78.54
4	5	6	0.14	110.36
5	3	6	0.018	69.42
6	2	3	0.037	26.70
7	4	5	0.037	16.02

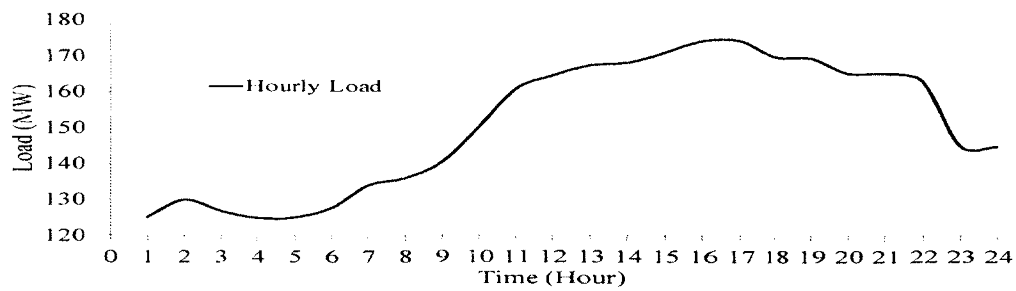

Figure 3.2. Hourly Load

Table 3.3. Emission Function Coefficients

Unit	a ($/lb^2)	b ($/lb)	c ($/h)
G1	0.000304	19.943	0.0
G2	0.000312	18.933	0.0
G3	0.000351	10.032	0.0

3.2.2 Case 1: Hourly SCUC without emission constraint. In this case there are 3 thermal units G1, G2, G3. The hourly UC schedule is depicted in Table 3.4 in which 1 and 0 signify the hourly ON/OFF states of generating units, and hour 0 represents the initial condition. The daily operating cost is $84,743 in which unit G3 is committed mainly at peak hours in order to minimize the operation cost, while the cheaper, more pollutant units G1 and G2 are committed longer. Figure 3.3 illustrates the hourly generation dispatch in which G1 and G2 would supply most of the hourly load.

Table 3.4. UC Solution – Case 1

Daily Cost = $84,743.210																								
Unit	Hour (1-24)																							
G1	1	1	1	1	1	1	1	1	1	1	1	1	1	1	1	1	1	1	1	1	1	1	1	1
G2	1	1	1	1	1	1	1	1	1	1	1	1	1	1	1	1	1	1	1	1	1	1	1	1
G3	0	0	0	0	0	0	0	0	0	1	1	1	1	1	1	1	1	1	1	1	1	1	0	0

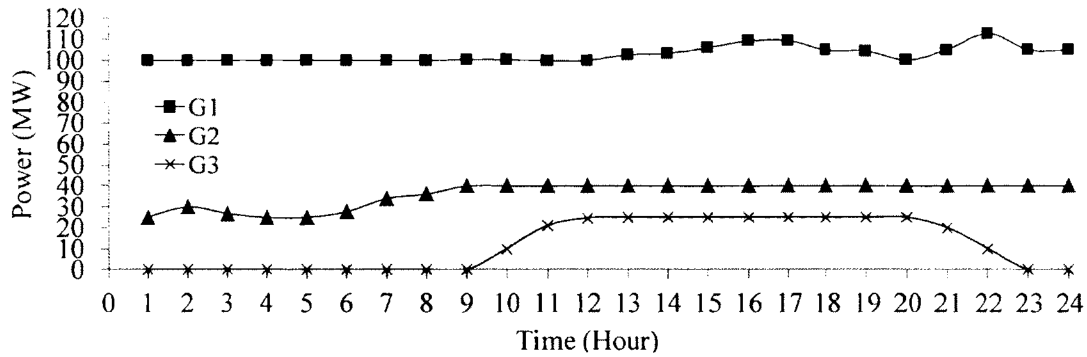

Figure 3.3. Hourly Generation Dispatch - Case 1

Figure 3.4 sketches the hourly emission trend as a function of hourly dispatch. The aggregate daily emission for the two coal units and one gas unit is 64,303.445 metric tons.

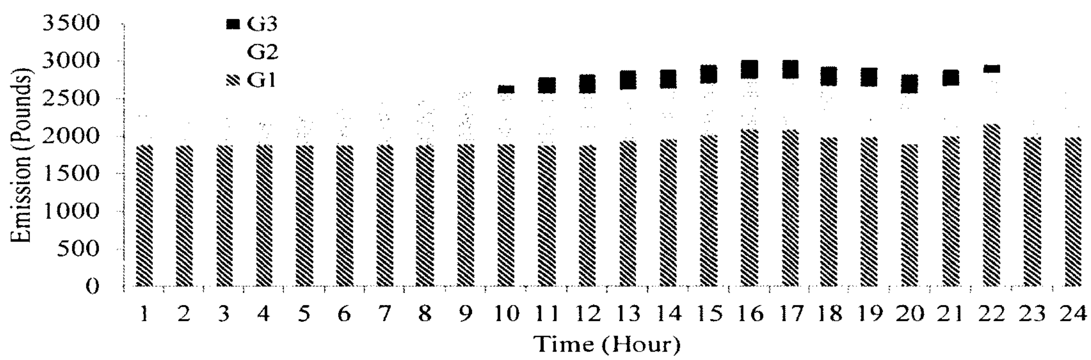

Figure 3.4. Hourly Emission Trend of Thermal Units - Case 1

3.2.3 Case 2: Hourly SCUC solution with emission constraints. In this case, a daily emission cap of 60,100 metric tons is imposed on Case 1. In Table 3.5, G3, which is the most expensive and least pollutant unit, is committed longer to satisfy the emission constraint while G2 is committed for a shorter period. In this case, the operation cost is increased by 12.62% to $95,435.

Table 3.5. UC Solution – Case 2

Daily Cost = $95,435.471																								
Unit	Hour (1-24)																							
G1	1	1	1	1	1	1	1	1	1	1	1	1	1	1	1	1	1	1	1	1	1	1	1	1
G2	0	0	0	0	0	0	0	0	0	0	1	1	1	1	1	1	1	1	1	1	1	1	0	0
G3	1	1	1	1	1	1	1	1	1	1	1	1	1	1	1	1	1	1	1	1	1	1	1	1

Figure 3.5 shows that G2 is mainly dispatched at peak hours while G1 carry less load compared to the previous case.

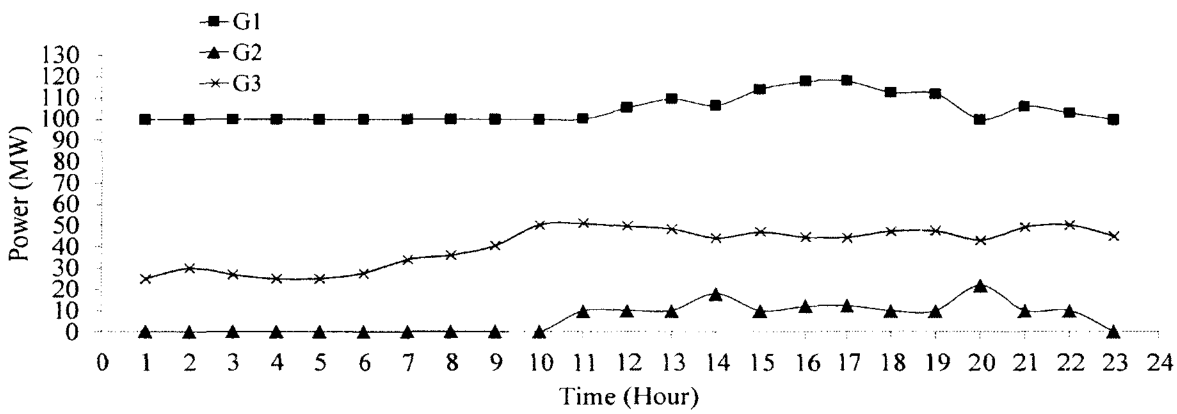

Figure 3.5. Hourly Generation Dispatch - Case 2

In Figure 3.6, the emission level of G2 is reduced considerably in order to address the emission constraint.

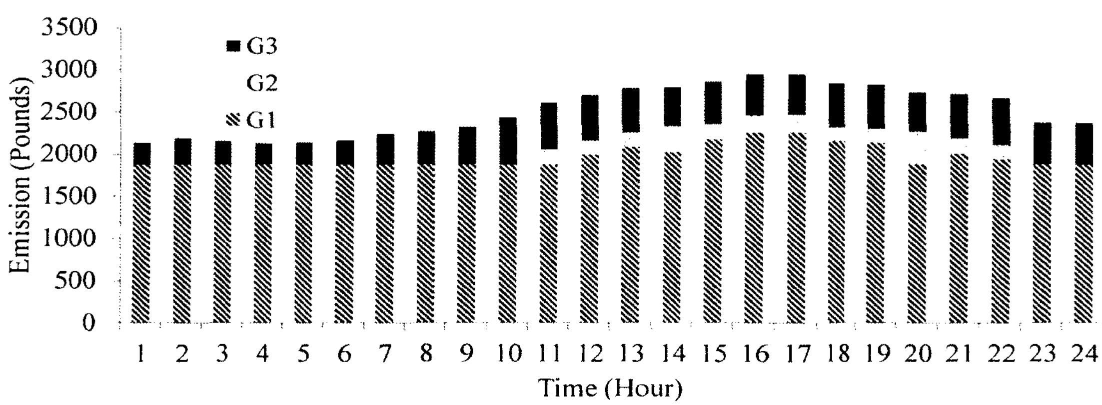

Figure 3.6. Hourly Emission Trend of Thermal Units - Case 2

3.2.4 Case 3: Hourly SCUC solution with emission constraints and stationary EV fleets. For the purpose of this study, EVs in multiple geographical locations are sorted into fleets and considered as virtual stationary power plants. EV fleet characteristics including max/min capacities, SOC, and max/min charging/discharging capacities are aggregated characteristics of the available energy, max/min capacity and charge/discharge power, of individual vehicles. Table 3.6 presents the characteristics of the existing five EV fleets consisting of 3,400, 2000, 1,000, 1,600, 2,000 vehicles respectively. The charging efficiency of a fleet, i.e., ratio of energy stored in the battery to energy drawn from the power grid, is 85%.

Table 3.6. Electric Vehicle Fleet Features

EV Fleet No.	Min Cap. (MWh)	Max Cap. (MWh)	Min Charge/Discharge (kW)	Max Charge/Discharge (kW)	a ($/MW^2)	b ($/MW)	c ($/h)
1	13.152	65.76	7.3/6.2	24.8/21.08	0.17	8.21	0
2	10.96	54.8	7.3/6.2	14.58/12.4	0.20	8.21	0
3	5.48	27.4	7.3/6.2	7.29/6.2	0.41	8.21	0
4	8.768	43.84	7.3/6.2	11.67/9.92	0.25	8.21	0
5	10.96	54.8	7.3/6.2	14.58/12.4	0.20	8.21	0

Table 3.7 depicts the hourly commitment schedule. Once we introduce the 5 EV fleets, the daily operation cost is reduced by 3% to $92,644.492.

Table 3.7. UC Solution – Case 3

Daily Cost = $92,644.492																								
Unit	Hour (1-24)																							
G1	1	1	1	1	1	1	1	1	1	1	1	1	1	1	1	1	1	1	1	1	1	1	1	1
G2	0	0	0	0	0	0	0	0	0	0	0	1	1	1	1	1	1	1	1	1	1	1	0	0
G3	1	1	1	1	1	1	1	1	1	1	1	1	1	1	1	1	1	1	1	1	1	1	1	1

Figure 3.7 shows the hourly generation dispatch of generating units in which G1is committed at its minimum capacity of 100 MW, G2 is committed at peak hours, and G3 is dispatched less compared to the previous case. The total daily operation cost is lower at peak hours, when the electricity price is high and EV fleets inject power back to the grid. The daily emission trend is plotted in Figure 3.8 in which G1 emits constant hourly emission, G2 emits at pick hours, and G3 emits less amount of pollution compare to the previous case.

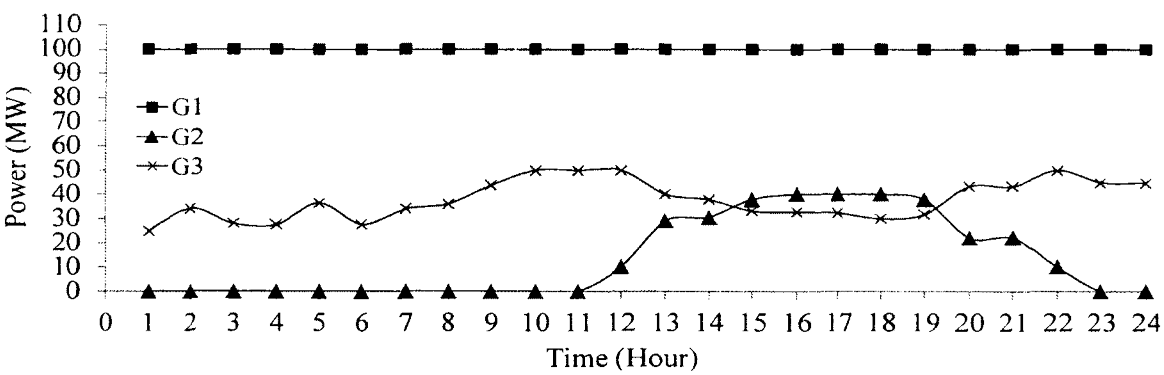

Figure 3.7. Hourly generation dispatch - case 3

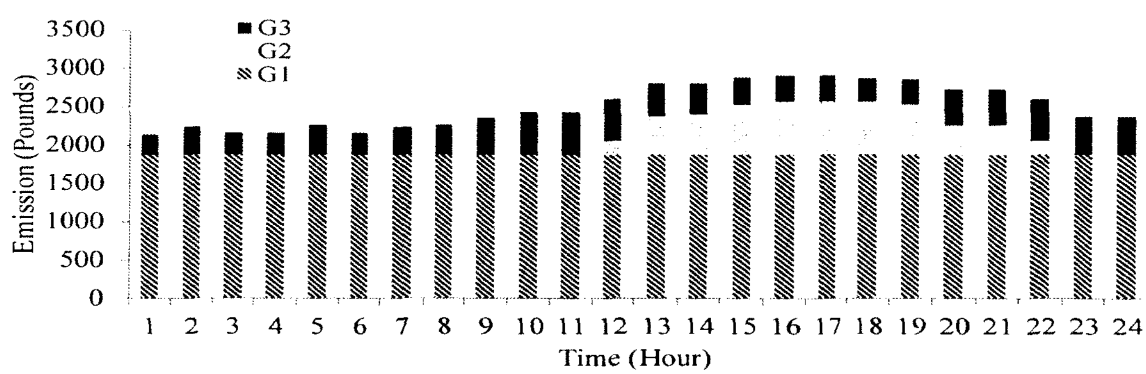

Figure 3.8. Hourly Emission trend of Thermal Units - case 3

Figure 3.9 captures the aggregated dis/charge of EV fleets in which V2G facilitates a cheaper energy delivery at peak hours. Negative numbers indicate EV charging at off-peak hours, while positive numbers denote discharges at peak hours. At hours 12, 16, and 22, when the bus locational marginal price (LMP) is higher, fleets are injecting power back to the grid. That is, V2G implementation reinforces the hourly dispatch at peak hours. As the results indicate the V2G technology holds out the promise of higher energy efficiency with a greener footprint.

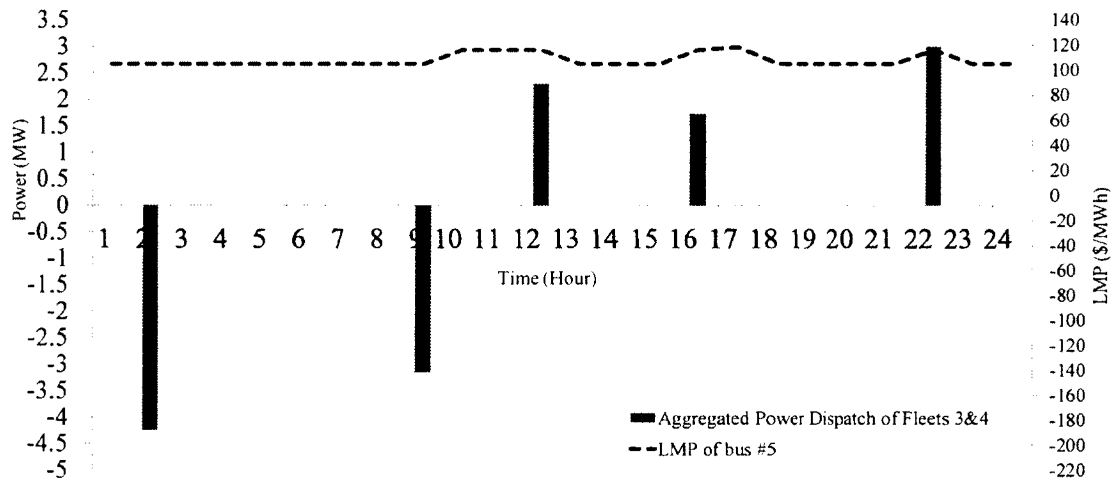

Figure 3.9. Hourly Aggregated Dispatch of Fleets 3&4 with Bus #5 LMP

3.3 Potential Challenges

Several challenges need to be addressed for an effective and viable integration of V2G into the electricity grid. The proposed model would require a large network of EVs to be connected to the smart grid and synchronized properly to smooth out peaks and valleys in a utility's power operation. On the technical side, intelligent charging strategies are needed for a large-scale integration of EVs to coordinate their energy demand with the production of renewable energy and the distribution grid. In addition, the current batteries are not specifically designed and optimized for V2G infrastructure. Also the battery life cycle would need to be improved to support a greater number of charge/discharge cycles. Moreover, the business case for investment in a charging station infrastructure is still an issue with questions over the required level of investment, market response to infrastructure investments, and where the investment should come from to make zero-emissions transport a market reality. Since smooth integrations of V2G into power grids are critical to energy independence, these issues would need to be addressed urgently. The V2G technology has the potential to reduce the dependence on foreign oil, reduce greenhouse gas emissions, and save large sums of money for utility and transportation industries.

3.4 Conclusions

The proposed scheduling algorithm offers a potential model to address the need for a sustainable and long-term solution to power generation in which economic and environmental factors are balanced. This paper proposed a methodology for day-ahead energy resource scheduling and the coordination between distributed battery storage, and thermal generating units considering intensive use of EV fleets and V2G. The contributions of this paper include an efficient methodology for day-ahead energy resource scheduling, which investigates the effect of distributed battery storage, in particular stationary EV fleets, on the hourly generation schedule of thermal units with emission constraints. The proposed model is very generic which can be easily expanded to large-scale systems with additional constraints representing a proper degree of details corresponding to real world cases.

The model has been tested on a 6-bus system, and numerical simulation proves that the proposed model has the potential to considerably improve the efficiency of the electricity generation and utilization, and shrink the grid operation cost while addressing environmental concerns. Our results indicate that V2G implementation could guarantee the optimal supply of electricity with a positive environmental impact.

The following chapters will integrate renewable sources as well as the mobility of EVs to the existing model.

CHAPTER 4

DETERMINISTIC COORDINATION OF THERMAL GENERATING UNITS, VARIABLE RENEWABLE SOURCES, AND AGGREGATED EV FLEETS FOR SUSTAINABLE OPERATION OF POWER GRID SYSTEMS

This content of chapter is outlined as follows. Section 4.1 discusses the proposed Thermal Units – Wind - Aggregated EV Fleets Coordination Methodology. Section 4.2 investigates the effectiveness of the proposed approach utilizing a 6-bus system. Conclusions are drawn in section 4.3.

4.1 Thermal Units – Wind - Aggregated EV Fleets Coordination Methodology

The proposed day-ahead scheduling problem synchronizes variable energy sources, mainly wind, with stationary fleets of EVs, as distributed storage facilities, while incorporating emission constraints to demonstrate how their integration to the electric power system can effectively satisfy electric power system network requirements while achieving economic goals with substantial cutback on carbon-footprints, with the focus on day-ahead scheduling (short-term operation). Further the discussed model optimizing the hourly coordination of wind-EV fleets' power generation with the thermal unit dispatch. The problem is implemented with Generic Algebraic Modeling System (GAMS) software with a dc power flow algorithm that considers network constraints utilizing CPLEX optimizer solver.

In order to determine the wind energy potential of a given site and to approximate the energy output from a wind turbine installed there, statistical analysis can be used. If time series measured data are obtainable at the desired location and height. There may be no need for a data analysis in terms of probability distributions and statistical techniques. In contrast, if prediction of measured data from one location to another is needed, or when only summary data are available, then there are distinct benefits to the use of analytical representations for the probability distribution of wind speed.

Two probability distributions are generally used in wind data analysis: (1) the Rayleigh and (2) the Weibull. The Rayleigh distribution employs one parameter: the mean wind speed. The Weibull distribution is based on two parameters: k, a shape factor, and c, a scale factor (both parameters are functions of $\bar{U}$ and σ_U) and can better represent a broader variety of wind regimes. The Weibull probability density function and the cumulative distribution function are given by [Man09] :

$$p(\mathrm{U}) = \left(\frac{k}{c}\right)\left(\frac{U}{c}\right)^{k-1} \exp\left[-\left(\frac{u}{c}\right)^{k}\right]$$

$$F(U) = 1 - \exp\left[-\left(\frac{u}{c}\right)^{k}\right]$$

4.1.1 Assumptions. In the discussed deterministic optimization model, the wind energy and load forecast errors, number of EVs in a fleet and their energy requirements are considered as variables. The physical characteristics and operation constraints of all generating units are also considered as input. Wind speed variations are simulated by the Weibull distribution function, auto correlation factor and diurnal pattern; wind generation is attained using the power curve of wind turbines and the hourly wind speed as discussed by Manwell, et al. [Man09]. The optimal solution incorporates the hourly UC, dispatch, and emission of generating units, and charge/discharge states of stationary EV fleets for a day.

4.1.2 **Deterministic SCUC.** We formulate the coordination between wind, stationary EV fleets, and thermal units as an MILP problem in SCUC as follows. The objective (4.1) is to minimize the base case operation cost, in which the projected quantities of load, and EV batteries are included, which is subject to system and generating unit constraints. The objective function (1) consists of the generation cost of thermal units, startup and shutdown costs of thermal units, and the operation cost of EV fleets. Since wind farms usually have trivial operation costs, no cost, related to the operation of wind power generation unit is considered in the objective function. The system and generating unit constraints are demonstrated in (4.2)-(4.21).

$$\min \sum_{t}\sum_{i}\left(F_{c,i}\left(P_{i,t}\right)+SU_{i,t}+SD_{i,t}\right)+\sum_{t}\sum_{v}C_{v,t} \tag{4.1}$$

where F_C is the production cost function expressed as a quadratic function of the power dispatch,

$$F_{c,i}\left(p_{it}\right)=a_i+b_{ci}p_{it}+c_{ci}p_{it}^2$$

where a, b, and c are the cost coefficients. The nonlinear production cost function can be approximated by a set of piecewise linear blocks as shown in Figure 4.1 piecewise linearization is accommodated in the LP which would cause the cost or sensitivity to assume different values over different ranges of the associated variable.

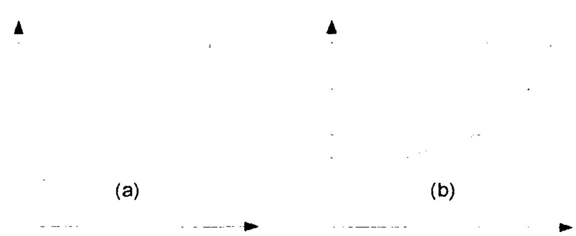

Figure 4.1. Piecewise Linearization (a) Nonlinear Curve, (b) Linear Curve

The second term in (4.1) denotes the startup cost (SU), which is a function of the length of time that the thermal unit has been off. The startup cost is given as:

$$SU_{it} = I_{it}\left[1 - I_{i(t-1)}\right]\left[\alpha_i + \beta_i(1 - e^{-x_{it}^{off}/\lambda_i})\right]$$

where α is the integrated cost of for startup and equipment maintenance, β is the startup cost of unit when initiating from cold conditions, X^{off} is the number of hours that the unit has been Off, and λ_i is the thermal time constant that characterizes the cooling speed of the unit. Similarly, the shutdown cost (SD), which is formulated as $SD_{it} = kP_{it}$, here k is the incremental shutdown cost. The operation cost of EVs, $C_{v,t}$, depends on the number of vehicles and charging/discharging depth and frequency [Kho12]

The wind curtailment happens when there is an inadequate ramping down capability of thermal units or major transmission congestion for utilizing the available wind power in electric power systems. The wind curtailment constraint is given in (4.2) in which the sum of dispatched and curtailed wind power is the same as the wind power forecast.

$$P_{w,t} + P_{d,w,t} = P_{f,w,t} \tag{4.2}$$

The thermal unit generation range (4.3) implies that once committed (I=1), the generation unit must operate between its min and max generating capacity. If I=0, the unit is de-committed.

$$P_{i,\min} I_{i,t} \le P_{i,t} \le P_{i,\max} I_{i,t} \quad \forall i, \forall t \tag{4.3}$$

Equation (4.4) denotes min off time indicating that a unit must be off for a certain period before it can be turned on again. Equation (4.5) denotes that a unit must be on for a certain period before it can be turned off, representing min on time constraint.

$$\left[X^{off}_{i(t-1)} - T^{off}_{i}\right] * \left[I_{it} - I_{i(t-1)}\right] \geq 0 \qquad \forall i, \forall t \tag{4.4}$$

$$\left[X^{on}_{i(t-1)} - T^{on}_{i}\right] * \left[I_{i(t-1)} - I_{it}\right] \geq 0 \qquad \forall i, \forall t \tag{4.5}$$

System ramp up/down limits between adjacent hours are demonstrated by (4.6)-(4.7). Equation (4.6) conveys that when unit i starts up at time t, its generating output (P_{it}) is equal to the minimum generating capacity of unit (p_{min}), while (4.7) conveys when unit i is shutting down at time t, its generating output ($P_{i(t-1)}$) is equal to the minimum generating capacity of unit (p_{min}) [Sha05].

$$P_{it} - P_{i(t-1)} \leq \left[1 - I_{it}(1 - I_{i(t-1)}\right] UR_i + I_{it}\left(1 - I_{i(t-1)}\right) P_{i,\min} \qquad \forall i, \forall t \tag{4.6}$$

$$P_{i(t-1)} - P_{it} \leq \left[1 - I_{i(t-1)}\left(1 - I_{it}\right)\right] DR_i + I_{i(t-1)}\left(1 - I_{it}\right) P_{i,\min} \qquad \forall i, \forall t \tag{4.7}$$

Equation (4.8) indicates that the daily emission is capped. For the purpose of this study, the primary concerns are carbon dioxide CO2 and carbon dioxide equivalent CO^2_e. The emission function, as a convex quadratic function of power generation, is modeled as[10]: $F_{e,i}(p_{it}) = a_{ei} + b_{ei} p_{it} + c_{ei} p_{it}^2$

where a_{ei}, b_{ei}, c_{ei} represent emission coefficients[11] of unit i.

$$\sum_{i}\sum_{t=1}^{24}\left[F^{ET}_{e,i}(p_{it}) + SU^{ET}_{e,it} + SD^{ET}_{e,it}\right] \leq EMS^{ET}_{\max,i} \qquad \forall i, ET = \left\{CO^2 \,\&\, CO^2_e\right\} \tag{4.8}$$

Emission constraints are coupling constraints over a group of generating units and period of study. The startup/shutdown emissions denoted by SU_e and SD_e The nonlinear

---

[10]Emission functions are computed using historical generator data. For each thermal units, heat curve (MBTU/MW) and (MBTU/Metric Tons of emissions) are considered; their interactions is computed as emission curve (MW/metric tons); the curves are piecewise linearized. Slope of segments indicate the incremental emission for each unit.

emission function is piecewise linearized and incorporated into the proposed MILP formulation.

The system power balance and dc power flow constraints are expressed by (4.9)-(4.11), respectively. The power flow equation (4.10) indicates that the flow on transmission line is dependent on the voltage angle difference between the corresponding buses and the line impendence. The power flow is limited by (4.11).

$$\sum_i P_{i,t} + \sum_v P_{v,t} + \sum_w P_{w,t} = \sum_{d \in D_b} P_{D,t}^d + \sum_{l \in L_{f,b}} PL_{l,t} - \sum_{l \in L_{t,b}} PL_{l,t} \quad \forall i, \forall t \tag{4.9}$$

$$PL_{l,t} = \left(\frac{\theta_{j,t} - \theta_{o,t}}{X_{jo}} \right) \quad \text{line l is from bus j to bus o} \tag{4.10}$$

$$\left| PL_{l,t} \right| \leq PL_l^{\max} \tag{4.11}$$

The EV fleet constraints are expressed by (4.12)-(4.19) where (4.12) conveys the net hourly absorbed/injected energy and the dispatched power of EV fleet; showing that the difference between the energy stored in the aggregated EV battery and the EV energy injected back to the grid is measured by the charging cycle efficiency of the aggregated EV.

$$E_{v,t}^{net} = \eta_v . P_{c,v,t} - P_{dc,v,t} \tag{4.12}$$

$$P_{v,t} = P_{c,v,t} - P_{dc,v,t}$$

Once an EV fleet is connected to the electric power system ($N_{v,t}=1$), the aggregated battery will be charged, discharged, or remain in the idle mode (4.13).

$$I_{dc,v,t} + I_{c,v,t} + I_{i,v,t} = N_{v,t} \tag{4.13}$$

Charging and discharging constraints for preserving the battery life are given in (4.14)-(4.15).

$$I_{c,v,t}.P_{c,v}^{\min} \le P_{c,v,t} \le I_{c,v,t}.P_{c,v}^{\max} \tag{4.14}$$

$$I_{dc,v,t}.P_{dc,v}^{\min} \le P_{dc,v,t} \le I_{dc,v,t}.P_{dc,v}^{\max} \tag{4.15}$$

Energy balance per hour is ensured by (4.16).

$$E_{v,t} = E_{v,t-1} + E_{v,t}^{net} \tag{4.16}$$

Energy range of each aggregated unit is addressed in (4.17)-(4.18); showing the capacity limit in each fleet.

$$E_{v}^{\min} \le E_{v,t} \le E_{v}^{\max} \tag{4.17}$$

$$E_{v,0} = E_{v,NT} \tag{4.18}$$

Piecewise linear function of convex charge/discharge cost curve of EV batteries is expressed by (4.19); implying that the operation cost of aggregated batteries has a direct correlation with the depth of charging/discharging batteries. A higher depth in battery charging/discharging causes the number of cycles to failure dramatically decrease which corresponds to an increase in the cost of EV charging/discharging [Tom07]. The nonlinear battery charging/discharging cost curves which are convex quadratic functions are piecewise linearized in the discussed MILP formulation. A tighter piecewise linear estimation is presented in [Kho12].

$$\left\{\begin{array}{l} C_{v,t} = N_{v,t} \cdot \left[\sum\limits_{m} b_{m,v} . P_{m,v,t}\right] \\ 0 \le P_{m,v,t} \le P_{m,v}^{\max} \\ N_{v,t} \cdot \left|E_{v,t} - E_{v,t-1}\right| = \sum\limits_{m} P_{m,v,t} \end{array}\right\} \tag{4.19}$$

The assumption that the aggregated state of charge (SOC) of batteries is set to be fixed at specific operation periods is addressed by (4.20).

$$E_{v,T} = E_v^{\max} \tag{4.20}$$

Figure 2.2 illustrates the flowchart of the proposed hourly SCUC formulation.

4.2 Numerical Results

In this section, a 6-bus electric power system, shown in Figure 4.2, is utilized to demonstrate the effectiveness of the proposed day-ahead solution. The example examines the effect of generating unit coordination strategies on electric power system generation scheduling. Further, it investigates the coordination of wind-EV fleets at bus-level and system-level on the hourly commitment and dispatch of coal and natural gas units. Furthermore, total operation cost, total emission, and expected wind energy curtailment are evaluated in this case study. The following 3 cases are examined:

Case 1: SCUC with three coal units and one wind turbine, considering environmental externalities

Case 2: SCUC with two coal units, one natural gas unit, and one wind turbine, considering environmental externalities

Case 3: Integration of stationary EV fleets and wind generation effect on the hourly SCUC solution considering environmental externalities.

4.2.1 6-Bus System. The 6-bus system incorporates G1, G2, either G3-Coal or G3-Gas (depending on the case study), and a wind turbine. G1-G3 units are least to most expensive units, with most to least pollution levels, respectively. Furthermore, the system includes 7 transmission lines.

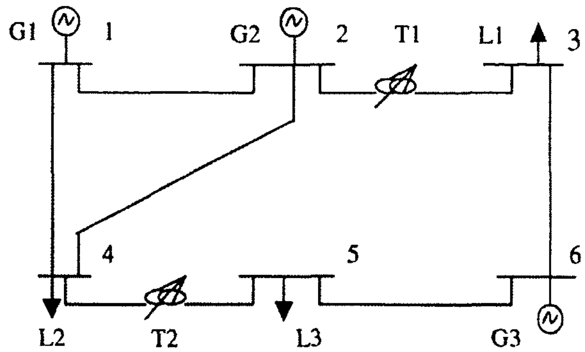

Figure 4.2. 6-Bus Electric power system

The parameters of generating units, transmission lines, and hourly load forecasts for 24 hours are depicted in Tables 4.1 and 4.2 and Figure 4.3, respectively. Table 4.3 shows the emission function coefficients.

Table 4.1. Thermal Unit Characteristics

Unit	a ($/MW^2)	b ($/MW)	c ($/h)	P_{min} (MW)	P_{max} (MW)	SU ($)	SD ($)	Min. Up(h)	Min Dn.(h)
G1	0.099	6.589	211.4	100	320	100	50	4	3
G2	0.203	7.629	217.4	10	160	200	40	3	2
$G3^C$	0.089	6.58	210.4	10	220	10	80	1	1
$G3^G$	0.494	10.07	102.8	10	100	80	10	1	1

Table 4.2. Transmission Line Characteristics

Line ID	From Bus	To Bus	Impedance (p.u)	Capacity (MW)
1	1	2	0.17	35.6
2	1	4	0.258	35.6
3	2	4	0.197	78.54
4	5	6	0.14	110.36
5	3	6	0.018	69.42
6	2	3	0.037	26.70
7	4	5	0.037	16.02

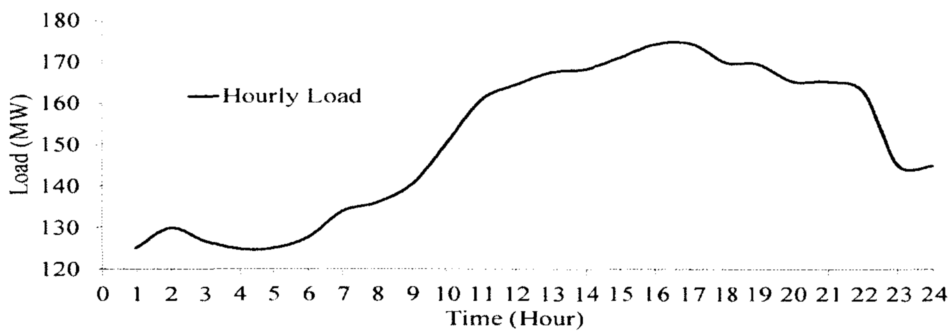

Figure 4.3. Total Hourly Load

Table 4.3. Emission Function Coefficients

Unit	a ($/lb^2)	b ($/lb)	c ($/h)
G1	0.000304	19.943	0.0
G2	0.000312	18.933	0.0
$G3^C$	0.000300	17.934	0.0
$G3^G$	0.000351	10.032	0.0

4.2.2 Case 1: SCUC with three coal units and one wind turbine, considering environmental externalities. In this case the coordination between 3 coal units (G1, G2, $G3^C$), and one variable renewable source (wind) is evaluated. The wind turbine is assumed to have zero operation cost. Table 4.4 illustrates the hourly UC in which diurnal emission cap of 86,300 pounds is imposed.[12] G1 and G2 are committed for 24 hours while $G3^C$ which is the most expensive coal unit is commits for 21 hours to address the cost minimization objective.

[12] Daily emissions are computed using historical generator data. Daily emission cap is also imposed based on the historical data. (Ellerman, et al., 2001) [3]

Table 4.4. UC Solution – Case 1

Daily Cost = $114,596.419																								
Unit	Hour (1-24)																							
G1	1	1	1	1	1	1	1	1	1	1	1	1	1	1	1	1	1	1	1	1	1	1	1	1
G2	1	1	1	1	1	1	1	1	1	1	1	1	1	1	1	1	1	1	1	1	1	1	1	1
G3^C	1	1	1	1	1	1	1	1	1	1	1	1	1	0	0	1	1	1	1	0	1	1	1	1

The daily operation cost is $ 114,596.419 and the wind curtailment is 177.373 MW/h. This is the case in which wind curtailment is high due to insufficient ramping down capability of coal units. Figure 4.4 depicts the diurnal generation dispatch of thermal units in which the standard deviations of generation dispatch for G1, G2, and G3^C are 24.91, 13.78, and 10.62 MW, respectively.

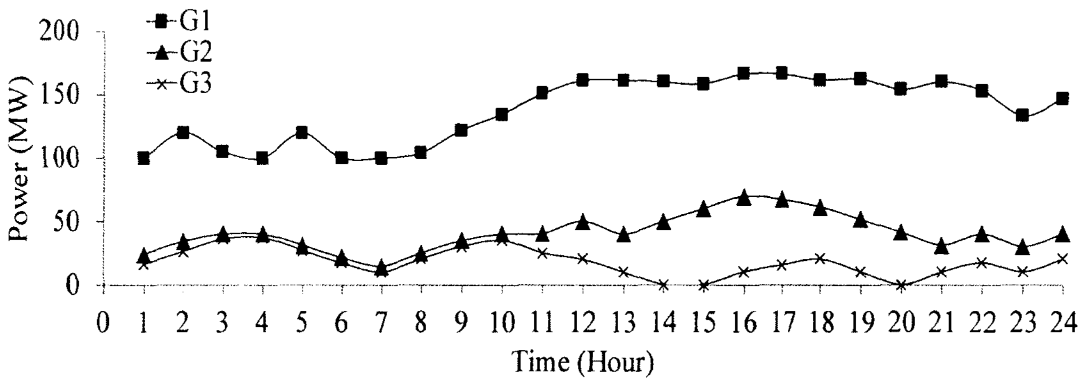

Figure 4.4 Thermal Generation Dispatch of Units - Case 1

Hourly emission of each unit is represented in Figure 4.5 in which G1 emits the most followed by G2, and G3^C, respectively. The cumulative daily emission is capped at 86,300 pounds.

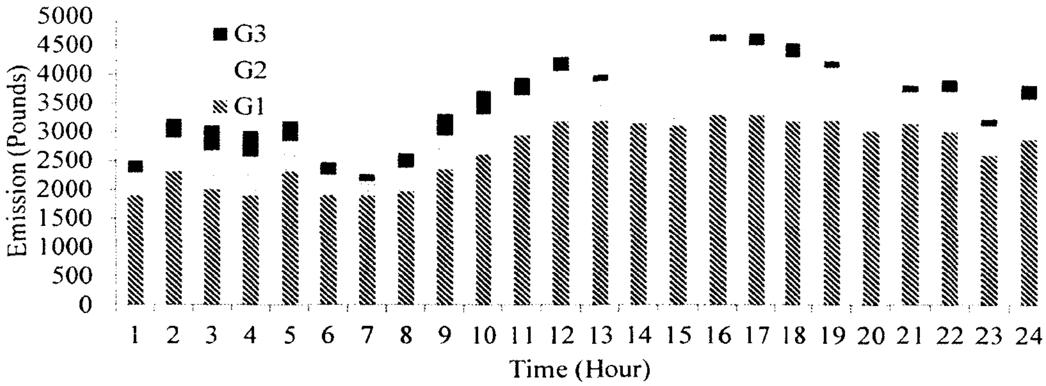

Figure 4.5. Hourly Emission Trend of Thermal Units - Case 1

4.2.3 Case 2: SCUC with two coal units, one natural gas unit, and one wind turbine, considering environmental externalities. In this case we replace $G3^C$ with a more expensive, less pollutant, peaking natural gas $G3^G$ unit. Natural gas capability to regulate power generation within minutes offers a significant potential for the integration with variable energy sources and serving as a reliable peak load supplier. Industry leaders concur that coal to natural gas switching is becoming the standard which will extensively transform the U.S. energy landscape. Natural gas is projected to account for 82% of new capacity while coal plants are anticipated to be just 10% of total new capacity in the U.S. by 2014 [Hea11].

The daily operation cost of the system rises by 2.25% to $117,180.059 while cumulative diurnal emission and wind curtailment is ameliorated to 85,422.239 pounds and 138.696 MW/h respectively. This result implies that the natural gas unit reduces the emission level and follows the wind turbine closely, due to its ramping capability, with a lower wind curtailment in the scheduling horizon. Table 4.5 demonstrates that G2 and $G3^G$ are committed less which is due their ramping flexibility.

Table 4.5. UC Solution – Case 2

Daily Cost = $117,180.059																								
Unit	Hour (1-24)																							
G1	1	1	1	1	1	1	1	1	1	1	1	1	1	1	1	1	1	1	1	1	1	1	1	1
G2	1	1	1	1	1	0	0	0	1	1	1	1	1	1	1	1	1	1	1	1	1	1	1	1
G3^G	1	1	1	1	1	1	0	1	1	1	1	1	0	0	0	1	1	1	1	0	0	1	0	1

Figure 4.6 shows that the standard deviations for the dispatch of G1, G2, and G3^G are reduced to 23.35, 13.68, and 9.6 MW, respectively which indicate a smoother generation profile as compared to that in Case 1. Hence, the replacement of a coal unit with a natural gas unit can alleviate the generation dispatch volatility when integrating renewable energy resources into the grid. Also, G3-G is committed only when the wind turbine generation is low.

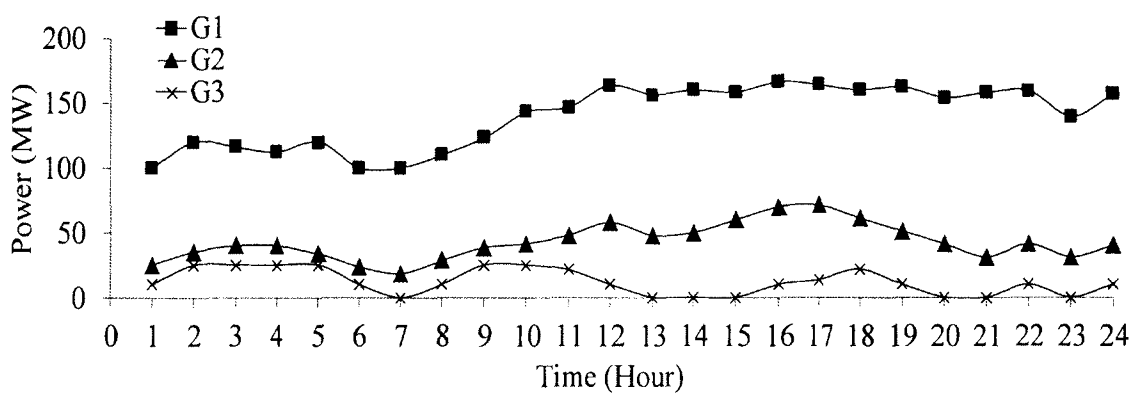

Figure 4.6. Hourly generation dispatch - case 2

Figure 4.7 illustrates the hourly emission trend of the thermal units in which the minute G3^G emission indicates that G3^G is a clean source which reduces the wind energy curtailment.

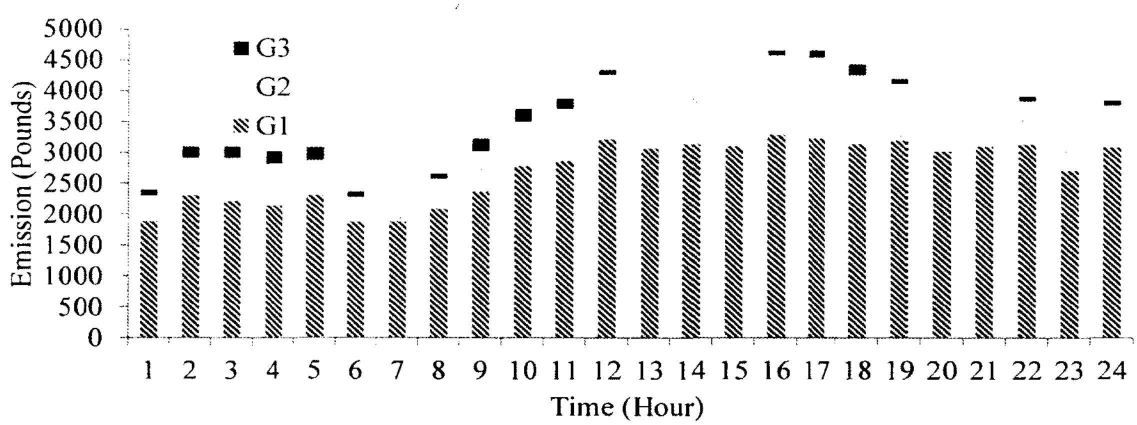

Figure 4.7. Hourly Emission Trend of Thermal Units - Case 2

4.2.4 Case 3: Integration of stationary EV fleets and wind generation impact on the hourly SCUC solution considering environmental externalities. In order to further improve the operation cost, reduce the emission level, and facilitate higher penetration of variable renewable energy resources, we introduce 5 stationary EV fleets, with distributed storage that is always connected to a bus. EV fleet characteristics include max/min capacities, SOC, and charge/discharge capacities of aggregated vehicles. Table 4.6 denotes the characteristics of the five EV fleets consisting of 3,400, 2000, 1,000, 1,600, and 2,000 vehicles, respectively. The charging efficiency of a fleet, i.e., ratio of energy stored in the battery to energy drawn from the power grid, is assumed 85%. The introduction of V2G into the electric power system would reduce the daily operation cost by 4.3% to $112,360.05, abates the daily emission by 4.45% to 81,779.459 pounds, and cut down any wind curtailments to zero.

Table 4.6. Electric Vehicle Fleet Features

EV Fleet No.	Min Cap. (MWh)	Max Cap. (MWh)	Min Charge/Discharge (kW)	Max Charge/Discharge (kW)	a ($/MW^2)	b ($/MW)	c ($/h)
1	13.152	65.76	7.3/6.2	24.8/21.08	0.17	8.21	0
2	10.96	54.8	7.3/6.2	14.58/12.4	0.20	8.21	0
3	5.48	27.4	7.3/6.2	7.29/6.2	0.41	8.21	0
4	8.768	43.84	7.3/6.2	11.67/9.92	0.25	8.21	0
5	10.96	54.8	7.3/6.2	14.58/12.4	0.20	8.21	0

Table 4.7 illustrates the hourly UC of generators in which the hourly commitment of G2 is increased by three hours. Figure 4.8 depicts the hourly generation dispatch in which the standard deviations are reduced to 20.43, 3.4, and 8.55 MW for G1, G2, G3-G respectively, indicating a flatter profile. As such, V2G can further moderate the volatility of thermal unit dispatch when integrating renewable energy resources.

Table 4.7. UC Solution – Case 3

Daily Cost = $112,360.048																								
Unit	Hour (1-24)																							
G1	1	1	1	1	1	1	1	1	1	1	1	1	1	1	1	1	1	1	1	1	1	1	1	1
G2	1	1	1	1	1	1	1	1	1	1	1	1	1	1	1	1	1	1	1	1	1	1	1	1
G3^G	1	1	1	1	1	0	0	1	1	1	1	1	1	1	1	1	1	1	1	0	0	0	0	0

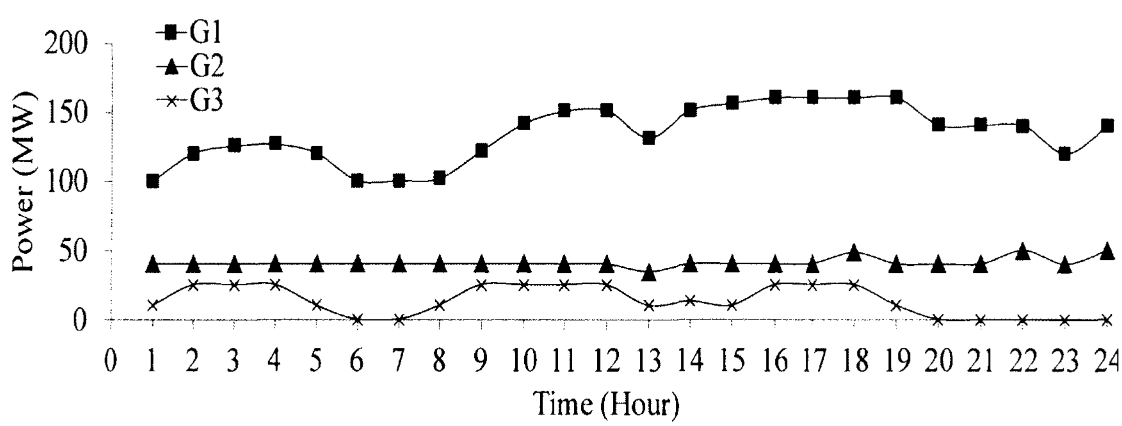

Figure 4.8. Hourly generation dispatch - case 3

Figure 4.9 illustrates the stacked diurnal emission dispatch of generators with sharp aggregated daily declines as compared to previous cases due to a wider usage of wind energy and the EV storage, at peak hours.

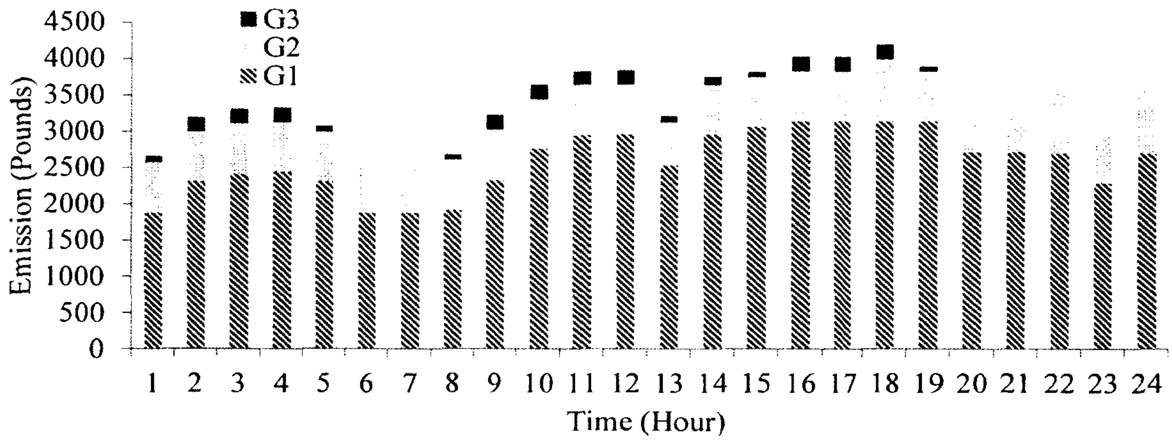

Figure 4.9. Hourly Emission Trend of Thermal Units – case 3

Figure 4.10 shows the aggregated charge/discharge of EV fleets in which the V2G facilitates a cheaper energy delivery at peak hours. Negative numbers indicate that the EVs are charged at off-peak hours, while positive numbers denote period when EVs are discharged at peak hours. At hour 12, when the bus locational marginal price (LMP) is higher, the first fleet discharge for injecting power to the grid.

Further, Figure 4.10 illustrates the diurnal pattern of LMP variation at bus #5; in which LMPs are lower at off-peak hours, and start rising from hour 12 to 22, during peak hours. It also demonstrates hourly aggregated charge/discharge pattern of fleets #3 and #4, which both are located on bus #5. Indicating EV fleets are either idle or charging during off-peak hours, and at hour 12 in which LMP rises from 30.35$/MWh to 36.35$/MWh, fleets are providing power back to the system; helping to alleviate the load during hours 12 to 22/peak hours.

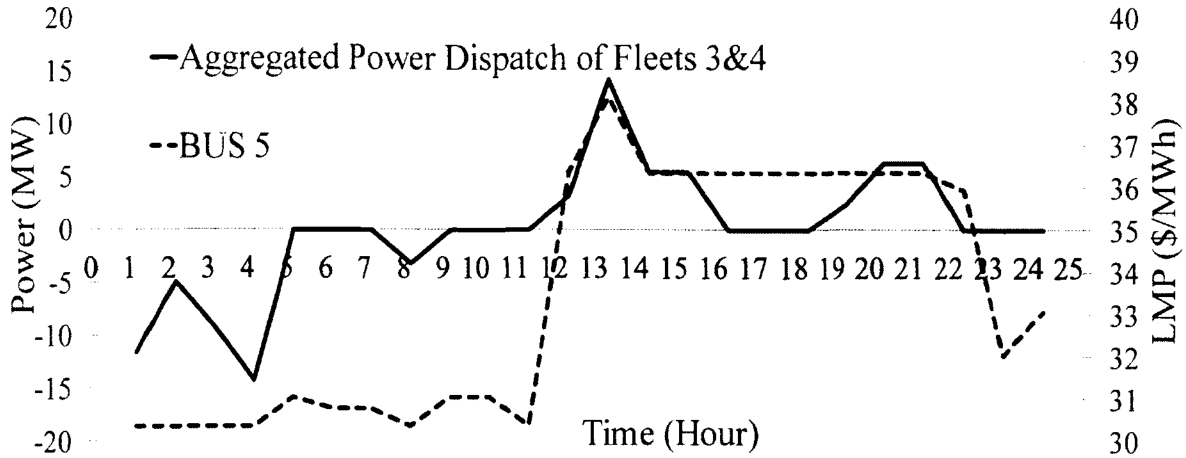

Figure 4.10. Hourly Aggregated Power Dispatch of Fleets 3&4 with BUS #5 LMP's Oscillation

The aggregated hourly load dispatch with and without the V2G deployment, considering no congestion, is sketched in Figure 4.11. Here, at off-peak hours, in which LMPs[13] are lower the EV fleets are either charged or in the idle mode as such demand is higher. At hour 12 when the LMP increases from 185.35 $/MWh to 191.93 $/MWh at peak-hours, EV fleets would supply power back to the system which would lower the aggregated demand. This case implies that providing a distributed storage through V2G could accommodate the variability of renewable energy resources for supplying the hourly demand.

[13] LMP stands for Locational Marginal Price: which expresses the hourly price at each bus.

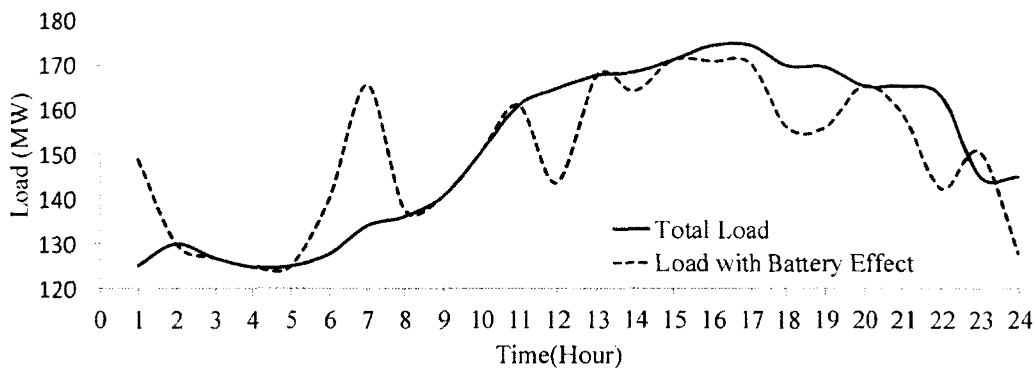

Figure 4.11. Hourly Aggregated Load with and without storage (No Congestion)

Table 4.8 Summrizes the conclusions from the above mentioned case studies.

Table 4.8. Summary – Cases 1,2,3

Case #	**Daily Operation Cost ($)**	**Daily Emission (Pounds)**	**Wind Curtailment Mwh**	**Standard Deviation of Dispatch (Mw)**		
				G1	**G2**	**G3**
1	*114,596.419*	86,300	177.373	24.91	13.78	10.62
2	$117,180.059 (2.25 % ↑)	85,422	138.696	23.35	13.68	9.6
3	$112,360.05 (4.3%↓)	81,779 (4.45%↓)	0.0	20.43	3.4	8.55

4.2 Conclusion

This chapter proposed a methodology for the day-ahead scheduling in electric power systems with coordinated wind, distributed storage, and thermal units. The study in this dissertation examines a sustainable model that has the potential to accelerate the clean and variable energy deployment in large electric power systems. We spearheaded the push to advance electric power system operation and control with accessibility, affordability, and reliability to alleviate environmental externalities. Decoupling electricity and transportation industries, which represent main sources of greenhouse gas emission, from their reliance on oil would enable positive changes for global prosperity. The decoupling would also provide foreseeable and sustainable energy, improve the quality of life, and reduce climate-relevant emissions. Our simulation results back the following conclusions:

First, natural gas is a fundamental partner to the expansion of utility-scale renewables, providing cleaner, reliable backup power when the sun is dimming or the wind dies down. Natural gas is considered as a bridge fuel between coal and variable sources not only because it causes less pollution per unit of electric power generated as compared with coal, but also due to its potential to regulate power generation within minutes which enables superior integration with renewable sources and serves as a reliable supply for meeting peak demands.

Second, the salient feature of the proposed approach is the deployment of EV-fleets as distributed storage and their optimal coordination with wind energy. V2G implementation is an especially promising method for ensuring that the renewable energy supply would match the hourly demand, smoothening out the variability of resources, and providing a long-term, decentralized form of electricity storage in a electric power system. Although distributed storage systems are much smaller than conventional energy sources for providing base firm capacity, they demonstrate advantageous technical and economical features when providing short-term power.

Numerical studies indicate that the integration of EV fleets as stationary distributed storage facilities could cut the diurnal operation cost, abate the emission, and enable thorough consumption of forecasted wind with zero wind curtailment. Our analyses points out that V2G technologies have the potential to make a paradigm shift in a number of fundamental ways including: diminishing the installation of conventional peak generation capacity, encouraging the installation of renewable electricity sources, and accelerating the adaptation of new transport technologies.

The implementation of such models worldwide could reduce the global warming, eliminate energy insecurity, and pave the road towards a greener growth. This plan may serve as a template for more ambitious goals. An expansion of the proposed model in a larger scope with stochastic scenarios would demonstrate a lower emission when conventional vehicles are replaced gradually with EV fleets.

CHAPTER 5

V2G FOR SUSTAINABLE DEVELOPMENT IN AN UNCERTAIN ENVIRONMENT – STOCHASTIC COORDINATION OF THERMAL UNITS, RENEWABLE ENERGY SOURCES, AND STATIONARY EV FLEETS

The content of this chapter is structured as follows. The proposed stochastic SCUC optimization model, in its initial (non-robust) and stochastic (robust) formulations, is described in Section 5.1. The results of the effectiveness of the proposed model are presented and discussed, utilizing a 6-bus system, in Section 5.2. Finally, Section 5.3 sums up the core results and conclusions of the study, and offers some hints about potential future developments.

5.1 Proposed Stochastic SCUC Optimization Model

The proposed stochastic day-ahead scheduling problem harmonizes variable energy sources, mainly wind, with stationary fleets of EVs, as distributed storage facilities, in an uncertain environment. Further, it incorporates emission constraints to exhibit how the renewable energy integration to the electric power system can effectively satisfy electric power system network requirements while achieving economic goals with substantial cutback on carbon-footprints, with a focus on short-term operation. Further the discussed model, optimizing the hourly coordination of wind-EV fleet generation with the thermal unit dispatch. The problem is implemented with Generic Algebraic Modeling System (GAMS) software with a dc power flow algorithm that considers network constraints utilizing CPLEX optimizer solver.

The synchronization between wind, stationary EV fleets, and conventional thermal units is formulated as a MILP problem in stochastic SCUC. The objective (1) is to minimize the operation cost, in which the projected quantities of load, wind, and EV batteries are included, subject to system and generating unit constraints. The objective function (5.1) consists of the base case operation cost, including generation cost of thermal units, startup and shutdown costs of thermal units, and the operation cost of EV fleets; in which outages of generators and transmission lines are not included. Further, the availability costs for facilitating spinning reserve in MCS scenarios are taken into consideration in the objective function.

The payment to the generators that facilitate spinning reserve refers to as the availability cost. One third of the marginal cost of a generating unit is considered as availability cost [Gan03]. In response to the existence of uncertainties, the provision of reserve is exercised as a remedial action by generators. Generators capability to provide remedial actions are bounded by their ramp up/down limitations. The objective function also considers the expected cost of remedial actions in scenarios for accommodating uncertainties. Thermal units are assumed to be non-quick start units; as such their scenario commitment status is the same as that in the base case. So no extra startup/shutdown costs are introduced in scenarios.

Moreover, since wind farms usually have trivial operation costs, we consider a no cost operation for wind energy units in the objective function. The system and generating unit constraints in the base case are demonstrated in (2)-(21).

$$\left\{ \min \begin{bmatrix} \sum_t \sum_i \left(p^b F_{c,i}\left(P_{i,t}\right) + SU_{i,t} + SD_{i,t} \right) + \\ \sum_t \sum_v p^b . C_{v,t} \end{bmatrix} + \left[\sum_t \sum_i (F^r_{c,\mathrm{i}}(\Delta^{\max}_{i,t})) \right] + \sum_s P^s . \left[\sum_t \sum_i F_{c,i}\left(P^s_{i,t}\right) + \sum_t \sum_v C^s_{v,t} \right] \right. \tag{5.1}$$

$$F_{c,i}\left(p_{it}\right) = a_i + b_{ci} p_{it} + c_{ci} p_{it}^2$$

Where a, b, and c are the cost coefficients. The nonlinear production cost function can be approximated by a set of piecewise linear blocks as described in the previous chapters. The second term in (5.1) denotes the startup cost (SU), which is a function of the length of time that the thermal unit has been off. The startup cost is given as:

$$SU_{it} = I_{it}\left[1 - I_{i(t-1)}\right]\left[\alpha_i + \beta_i(1 - e^{-x_{it}^{off}/\lambda_i})\right]$$

Where α is the integrated cost of for startup and equipment maintenance, β is the startup cost of unit when initiating from cold conditions, X^{off} is the number of hours that the unit has been Off, and λ_i is the thermal time constant that characterizes the cooling speed of the unit. Similarly, the shutdown cost (SD), which is formulated as $SD_{it} = kP_{it}$, here k is the incremental shutdown cost. The operation cost of EVs, $C_{v,t}$, depends on the number of vehicles and charging/discharging depth and frequency [Kho12]. Further, $F_{c,i}^{r}(\Delta_{i,t}^{max})$ represents the hourly cost of corrective action.

The wind curtailment happens when there is an inadequate ramping down capability of thermal units or major transmission congestion for utilizing the available wind energy in electric power systems. The wind curtailment constraint is given in (5.2) in which the sum of dispatched and curtailed wind power is the same as the wind power forecast.

$$P_{w,t} + P_{d,w,t} = P_{f,w,t} \tag{5.2}$$

The thermal unit generation range (5.3) implies that once committed (I=1), the generation unit must operate between its min and max generating capacity. If I=0, the unit is de-committed.

$$P_{i,\min} I_{i,t} \leq P_{i,t} \leq P_{i,\max} I_{i,t} \quad \forall i, \forall t \tag{5.3}$$

Equation (5.4) denotes min off time indicating that a unit must be off for a certain period before it can be turned on again. Equation (5.5) denotes that a unit must be on for a certain period before it can be turned off, representing min on time constraint.

$$\left[X_{i(t-1)}^{off} - T_i^{off}\right] * \left[I_{it} - I_{i(t-1)}\right] \geq 0 \quad \forall i, \forall t \tag{5.4}$$

$$\left[X_{i(t-1)}^{on} - T_i^{on}\right] * \left[I_{i(t-1)} - I_{it}\right] \geq 0 \quad \forall i, \forall t \tag{5.5}$$

System ramp up/down limits between adjacent hours are demonstrated by (5.6)-(5.7). Equation (5.6) conveys that when unit i starts up at time t, its generating output (P_{it}) is equal to the minimum generating capacity of unit (p_{min}), while (5.7) conveys when unit i is shutting down at time t, its generating output ($P_{i(t-1)}$) is equal to the minimum generating capacity of unit (p_{min}) [Sha05].

$$P_{it} - P_{i(t-1)} \leq \left[1 - I_{it}(1 - I_{i(t-1)}\right] UR_i + I_{it}\left(1 - I_{i(t-1)}\right) P_{i,\min} \quad \forall i, \forall t \tag{5.6}$$

$$P_{i(t-1)} - P_{it} \leq \left[1 - I_{i(t-1)}\left(1 - I_{it}\right)\right] DR_i + I_{i(t-1)}\left(1 - I_{it}\right) P_{i,\min} \quad \forall i, \forall t \tag{5.7}$$

Equation (5.8) indicates that the daily emission is capped. Carbon dioxide (CO_2) and carbon dioxide equivalent (CO_{2e}) are assumed the primary concerns in this study. The emission function, as a convex quadratic function of power generation, is modeled as[14]: $F_{e,i}\left(p_{it}\right) = a_{ei} + b_{ei} p_{it} + c_{ei} p_{it}^2$

[14] Emission functions are computed using historical generator data. For each thermal units, heat curve (MBTU/MW) and (MBTU/Metric Tons of emissions) are considered with their interactions computed as emission curve (MW/metric tons); the curves are piecewise linearized. Slope of segments indicate the incremental emission for each unit.

Where a_{ei}, b_{ei}, c_{ei} represent emission coefficients[15] of unit i.

$$\sum_{i}\sum_{t=1}^{24}\left[F_{e,i}^{ET}(p_{it})+SU_{e,it}^{ET}+SD_{e,it}^{ET}\right]\leq EMS_{\max,i}^{ET} \qquad \forall i\,, ET=\{CO_2\,\&CO_{2e}\} \tag{5.8}$$

Emission constraints are coupling constraints over a group of generating units and period of study. The startup/shutdown emissions denoted by SU_e and SD_e The nonlinear emission function is piecewise linearized and incorporated into the proposed MILP formulation.

The system power balance and dc power flow constraints are expressed by (5.9)-(5.11), respectively. The power flow (5.10) indicates that the transmission flow is dependent on the voltage angle difference between the corresponding buses and the line impendence. The power flow is limited by (5.11).

$$\sum_{i}P_{i,t}+\sum_{v}P_{v,t}+\sum_{w}P_{w,t}=\sum_{d\in D_b}P_{D,t}^{d}+\sum_{l\in L_{f,b}}PL_{l,t}-\sum_{l\in L_{t,b}}PL_{l,t} \qquad \forall i\,,\forall t \tag{5.9}$$

$$PL_{l,t}=\left(\frac{\theta_{j,t}-\theta_{o,t}}{X_{jo}}\right) \qquad \text{line l is from bus j to bus o} \tag{5.10}$$

$$\left|PL_{l,t}\right|\leq PL_{l}^{\max} \tag{5.11}$$

The EV fleet constraints are expressed by (5.12)-(5.19) where (5.12) conveys the net hourly absorbed/injected energy and the dispatched power of EV fleet. Here, the difference between the energy stored in the aggregated EV battery and the EV energy injected back to the grid is measured by the charging cycle efficiency of the aggregated EV.

$$\begin{cases} E_{v,t}^{net} = \eta_v . P_{c,v,t} - P_{dc,v,t} \\ P_{v,t} = P_{c,v,t} - P_{dc,v,t} \end{cases} \tag{5.12}$$

Once an EV fleet is connected to the electric power system ($N_{v,t}=1$), the aggregated battery will be charged, discharged, or remain in the idle mode (5.13).

$$I_{dc,v,t} + I_{c,v,t} + I_{i,v,t} = N_{v,t} \tag{5.13}$$

Charging and discharging constraints for preserving the battery life are given as (5.14) & (5.15):

$$I_{c,v,t} . P_{c,v}^{\min} \le P_{c,v,t} \le I_{c,v,t} . P_{c,v}^{\max} \tag{5.14}$$

$$I_{dc,v,t} . P_{dc,v}^{\min} \le P_{dc,v,t} \le I_{dc,v,t} . P_{dc,v}^{\max} \tag{5.15}$$

Energy balance per hour is ensured by (5.16).

$$E_{v,t} = E_{v,t-1} + E_{v,t}^{net} \tag{5.16}$$

Energy range of each aggregated unit is addressed in (5.17)-(5.18) representing the capacity limit in each fleet.

$$E_v^{\min} \le E_{v,t} \le E_v^{\max} \tag{5.17}$$

$$E_{v,0} = E_{v,NT} \tag{5.18}$$

The piecewise linear function of convex charge/discharge cost curve of EV batteries is expressed by (5.19) which shows a direct correlation with the number of vehicles and the depth of charging/discharging cycles. A higher depth in battery charging/discharging causes the number of cycles to failure decrease dramatically, which corresponds to an increase in the cost of EV charging/discharging [Tom07].

The nonlinear battery charging/discharging cost curves which are convex quadratic functions are piecewise linearized in the MILP formulation. A tighter piecewise linear estimation is presented in [Kh012]. The assumption that the aggregated state of charge (SOC) of batteries is set to be fixed at specific operation periods is addressed by (5.20).

$$\begin{cases} C_{v,t} = N_{v,t} \cdot \left[\sum_{m} b_{m,v} . P_{m,v,t} \right] & 0 \le P_{m,v,t} \le P_{m,v}^{\max} \\ N_{v,t} \cdot \left| E_{v,t} - E_{v,t-1} \right| = \sum_{m} P_{m,v,t} \end{cases} \tag{5.19}$$

$$E_{v,T} = E_{v}^{\max} \tag{5.20}$$

The system and generating unit constraints in the MCS scenarios comprise those that are similar to base case constraints, except the base case variables are replaced by scenario variables. The scenario constraints for EV fleets are demonstrated in (5.21)-(5.33). We consider an expected emission limit (5.34) for scenario emission constraints.

$$\begin{cases} C_{v,t}^{s} = N_{v,t} \cdot \left[\sum_{m} b_{m,v} . P_{m,v,t}^{s} \right] & 0 \le P_{m,v,t}^{s} \le P_{m,v}^{\max} . NE_{v}^{s} \\ N_{v,t} \cdot \left| E_{v,t}^{s} - E_{v,t-1}^{s} \right| = \sum_{m} P_{m,v,t}^{s} \end{cases} \tag{5.21}$$

$$\begin{cases} E_{v,t}^{net,s} = \eta_{v} . P_{c,v,t}^{s} - P_{dc,v,t}^{s} \\ P_{v,t}^{s} = P_{c,v,t}^{s} - P_{dc,v,t}^{s} \end{cases} \tag{5.22}$$

$$I_{dc,v,t}^{s} + I_{c,v,t}^{s} + I_{i,v,t}^{s} = N_{v,t} \tag{5.23}$$

$$\mathrm{N}_{v,t} . I_{c,v,t}^{s} . P_{c,v}^{\min} . NE_{v}^{s} \le P_{c,v,t}^{s} \le \mathrm{N}_{v,t} . I_{c,v,t}^{s} . P_{c,v}^{\max} . NE_{v}^{s} \tag{5.24}$$

$$\mathrm{N}_{v,t} . I_{dc,v,t}^{s} . P_{dc,v}^{\min} . NE_{v}^{s} \le P_{dc,v,t}^{s} \le \mathrm{N}_{v,t} . I_{dc,v,t}^{s} . P_{dc,v}^{\max} . NE_{v}^{s} \tag{5.25}$$

$$E_{v,t}^{s} = E_{v,t-1}^{s} - E_{v,t}^{net,s} \tag{5.26}$$

$$E_v^{\min}.NE_v^s \le E_{v,t}^s \le E_v^{\max}.NE_v^s \tag{5.27}$$

$$E_{v,0}^s = E_{v,NT}^s = E_{v0}.NE_v^s \tag{5.28}$$

The consumer-controlled scenario scheme is shown in (5.29).

$$P_{v,\widehat{\mathrm{T}}}^s = E_v^{\max}.NE_v^s \tag{5.29}$$

Equation (5.30) addresses the scenario corrective action;

$$\begin{cases} -\Delta_{i,t}^{\max} \le P_{i,t}^s - UX_{i,t}^s.\mathrm{P}_{i,t} \le \Delta_{i,t}^{\max} \\ \mathrm{P}_i^{\min}.UX_{i,t}^s.I_t^i \le P_{i,t}^s \le \mathrm{P}_i^{\max}.UX_{i,t}^s.I_t^i \end{cases} \tag{5.30}$$

The DC power flow constraints for each MCS scenario are denoted by Equations (5.31)–(5.33). The grid connection of PEV fleet at time t is illustrated by $B_{b,t}^v$ in equation (5.32).

$$\sum_{i \in B_b^i} P_{i,t}^s + \sum_{v \in B_{b,t}^v} P_{v,t}^s + \sum_{w \in B_b^w} P_{w,t}^s = \sum_{d \in D_b} P_{D,t}^{d,s} + \sum_{l \in L_{f,b}} PL_{l,t}^s - \sum_{l \in L_{t,b}} PL_{l,t}^s \tag{5.31}$$

$$-M.(1-UY_{l,t}^s) \le PL_{l,t}^s - \left(\frac{\theta_{j,t}^s - \theta_{o,t}^s}{X_{jo}} \right) \le M.(1-UY_{l,t}^s) \tag{5.32}$$

$$-PL_l^{\max} UY_{l,t}^s \le PL_{l,t}^s \le PL_l^{\max} UY_{l,t}^s \tag{5.33}$$

$$\sum_i \sum_{t=1}^{24} p^b.\left[F_{e,i}^{ET}(p_{it}) + SU_{e,it}^{ET} + SD_{e,it}^{ET} \right] + \sum_s P^s.\left[F_{e,i}^{ETS}(p_{it}) + SU_{e,it}^{ETS} + SD_{e,it}^{ETS} \right] \le Expected(EMS_{\max,i}^{ET}) \tag{5.34}$$

The flowchart of the proposed stochastic SCUC formulation is demonstrated in Figure 5.1. The two-level hierarchical structure of the MILP problem makes it a suitable candidate for BD. Indeed, decomposition is the only feasible option for the solution of the large-scale stochastic SCUC problem in real time [Sha05]. Considering the stochastic nature and the practical size of the SCUC problem involving hundreds/thousands of generating units and transmission lines and multiple study hours, BD would decompose the original large-scale MILP problem into one integer program master (MIP) problem and several linear programing (LP) sub-problems.

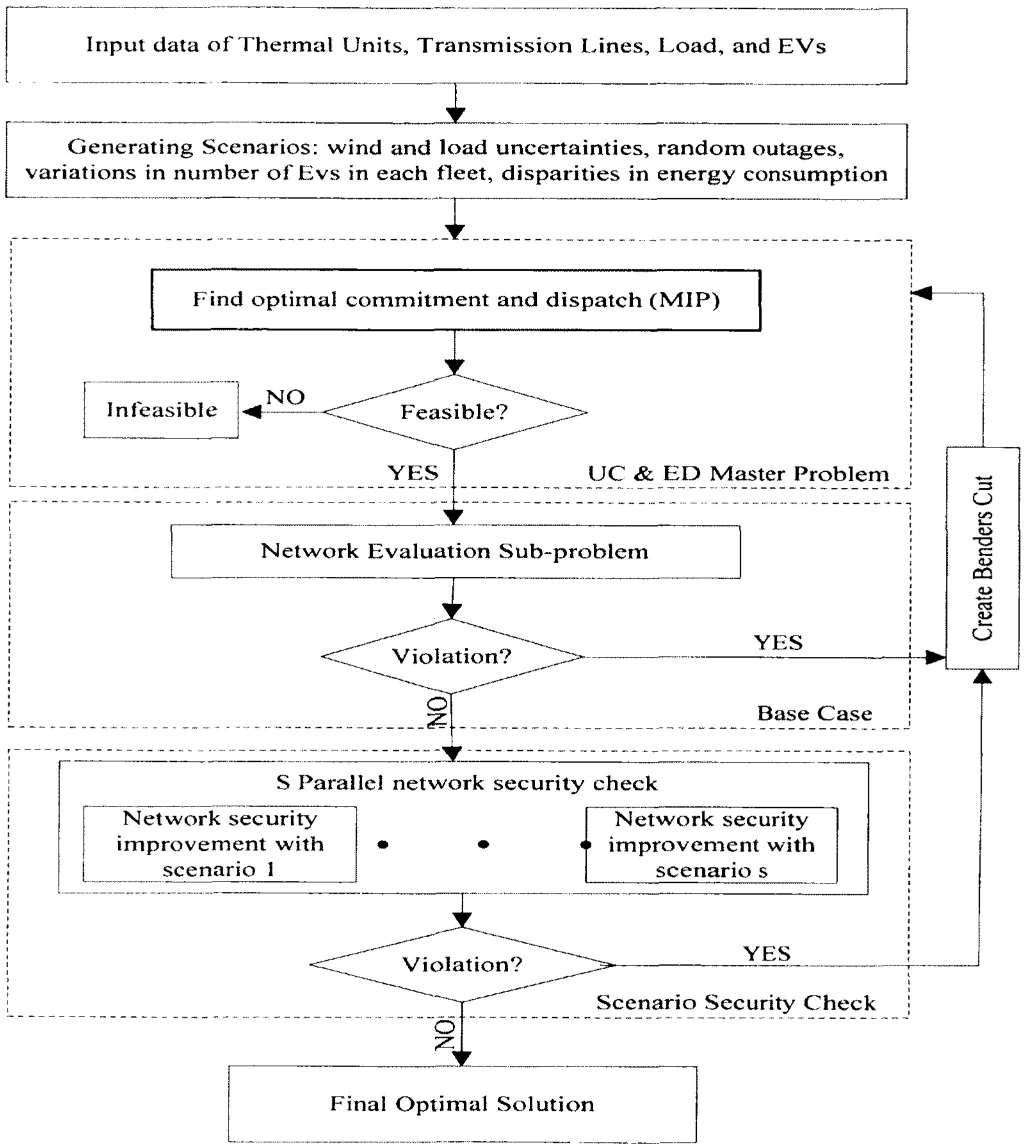

Figure 5.1. Stochastic SCUC for the Coordinated Scheduling of Constrained Thermal, EV, and Renewable Units

The master problem solves the hourly UC with dominant constraints. The lower bound solution of the master problem would involve fewer constraints. The sub-problems will examine the DC power flow according to the master problem's UC solution in the base case and all scenarios for minimizing transmission flow violations. Transmission networks, which are assessed independently for the base case and all scenarios, can be optimized in parallel. If any violations arise, the corresponding feasibility cuts are generated and added to the master problem for the solution of the next iteration.

Accordingly, a new lower bound solution of the original problem will be attained by re-calculating the master problem with more constraints. The process continues until all violations are mitigated. The optimal solution for the original problem will be achieved when upper and lower bounds are adequately close; which will confine the final solution to be close to the global optimal solution of the original problem [Sha05]. The iterative process between the master problem and sub-problem delivers a minimized cost solution for generation scheduling while addressing transmission, voltage, and emission constraints.

5.2 Numerical Results

In this section, a 6-bus electric power system, shown in Figure 5.2, is utilized to demonstrate the effectiveness of the proposed day-ahead solution. The examples investigate the coordination of wind-EV fleets at bus-level and system-level on the hourly commitment and dispatch of coal and natural gas units. Furthermore, total expected operation cost, base cost, capacity cost, total diurnal expected emission, base and expected wind energy curtailment are evaluated.

5.2.1 6-Bus System. The 6-bus system incorporates two coal units (G1,G2), one natural gas unit (G3), and a wind turbine. G1-G3 units are least to most expensive units, with most to least pollutant, respectively. The installed wind capacity is 75 MW, which is about 30% of the system peak load. Furthermore, the system includes 7 transmission lines.

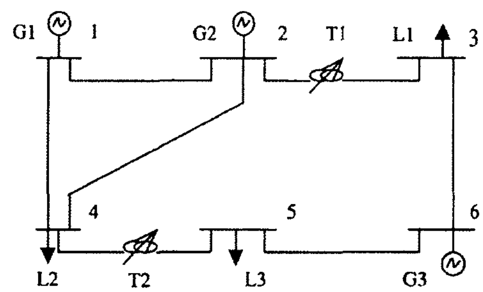

Figure 5.2. 6-Bus Electric power system

The parameters of generating units, transmission lines, and hourly load forecasts for 24-hours are depicted in Tables 5.1 and 5.2 and Figure 5.3, respectively. Table 5.3 shows the emission function coefficients.

Table 5.1. Thermal Unit Characteristics

Unit	a ($/MW^2)	b ($/MW)	c ($/h)	P_{min} (MW)	P_{max} (MW)	SU ($)	SD ($)	Min. Up(h)	Min Dn.(h)
G1	0.099	6.589	211.4	100	320	100	50	4	3
G2	0.203	7.629	217.4	10	160	200	40	3	2
$G3^C$	0.089	6.58	210.4	10	220	10	80	1	1
$G3^G$	0.494	10.07	102.8	10	100	80	10	1	1

Table 5.2. Transmission Line Characteristics

Line ID	From Bus	To Bus	Impedance (p.u)	Capacity (MW)
1	1	2	0.17	35.6
2	1	4	0.258	35.6
3	2	4	0.197	78.54
4	5	6	0.14	110.36
5	3	6	0.018	69.42
6	2	3	0.037	26.70
7	4	5	0.037	16.02

The following 4 cases are examined in which the diurnal emission cap of 86,300 pounds and diurnal expected emission cap of 175,000 pounds is imposed in all cases.[16]

Case 1: Stochastic SCUC with two coal units and one natural gas unit considering environmental externalities

Case 2: Stochastic SCUC with two coal units, one natural gas unit, and one wind turbine considering environmental externalities

Case 3: Intelligent integration of stationary EV fleets and wind generation, and their coordination in the hourly stochastic SCUC solution considering environmental externalities.

Case 4: Rule-based integration of stationary EV fleets and wind generation, and their coordination in the hourly stochastic SCUC solution considering environmental externalities.

[16] Daily emissions are computed using historical generator data. Daily emission cap is also imposed based on the historical data.

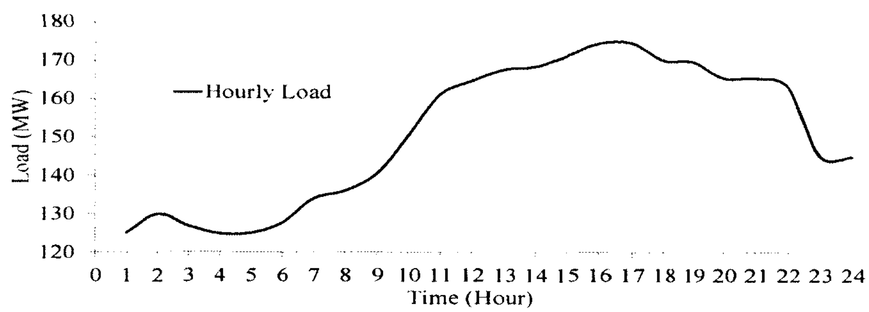

Figure 5.3. Total Hourly Load

Table 5.3. Emission Function Coefficients

Unit	a ($/lb^2)	b ($/lb)	c ($/h)
G1	0.000304	19.943	0.0
G2	0.000312	18.933	0.0
G3^G	0.000351	10.032	0.0

5.2.2 Case 1: Stochastic SCUC with two coal units and one natural gas unit considering environmental externalities. In this case the coordination between 2 coal units (G1, G2) and one gas unit (G3), without considering any variable renewable source is evaluated. Load forecast errors, generation, and transmission outages are considered random. The load projection error follows a normal distribution with a mean value that is equivalent to the predicted load and a standard deviation of 5% of the mean value. Table 5.4 illustrates the hourly UC of generators in which all units are committed for 24 hours. The daily base cost, availability cost, and expected cost are $121,445, $10,762, $121,991.695 respectively.

Table 5.4. UC Solution – Case 1

Diurnal Base Cost = \$ 121,445.015 **Diurnal Availability Cost = \$ 10,762.094** **Diurnal Expected Cost = \$ 121,991.695**																								
Unit	Hour (1-24)																							
G1	1	1	1	1	1	1	1	1	1	1	1	1	1	1	1	1	1	1	1	1	1	1	1	1
G2	1	1	1	1	1	1	1	1	1	1	1	1	1	1	1	1	1	1	1	1	1	1	1	1
G3	1	1	1	1	1	1	1	1	1	1	1	1	1	1	1	1	1	1	1	1	1	1	1	1

Figure 5.4 depicts the diurnal generation dispatch of thermal units, in which G1 dispatches more power to minimize the cost, while the other coal unit (G2) dispatches less as compared to the gas unit (G3) to address the emission constraints. In Figure 5.5, G1 emits the most emission followed by G2, and G3, respectively. The cumulative expected daily emission in scenarios is 73,789.270 pounds.

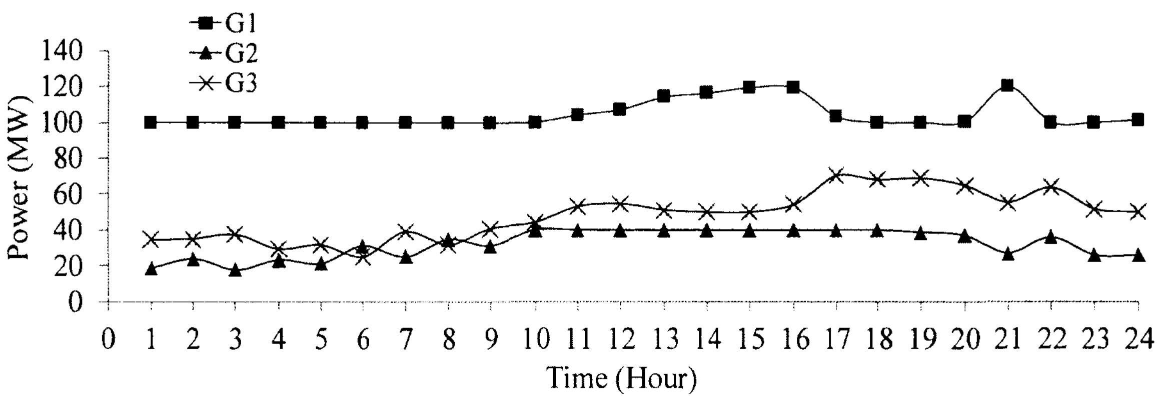

Figure 5.4. Thermal Generation Dispatch of Units - Case 1

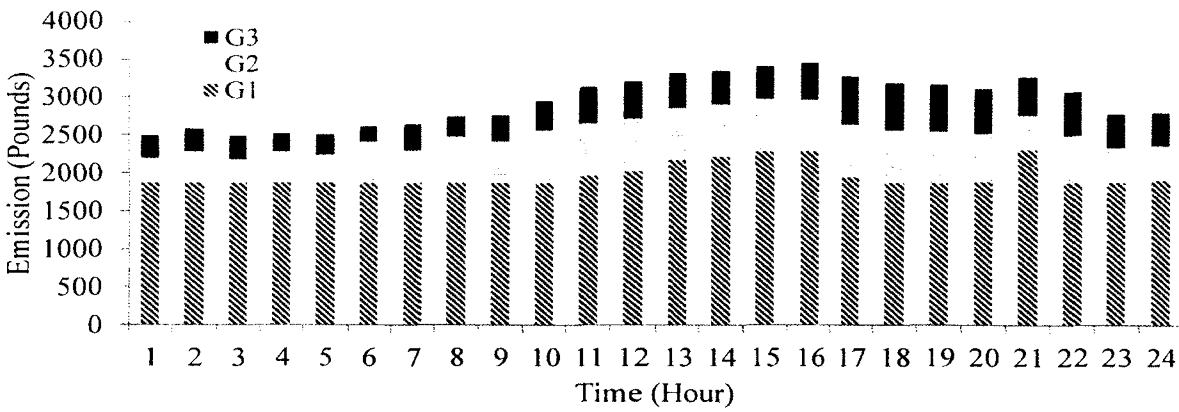

Figure 5.5. Hourly Emission Trend of Thermal Units - Case 1

5.2.3 Case 2: Stochastic SCUC with two coal units, one natural gas unit, and one wind turbine considering environmental externalities. In this case the coordination between 2 coal units (G1, G2), one gas unit (G3), and one renewable source (wind) is examined. Wind forecast errors are considered and the wind unit generation is based on the wind speed data and typical wind power curve. The mean daily wind speed is 10 meter per second (m/s), which follows a Weibull distribution function with Weibull coefficient equal to 2.1. The wind turbine is assumed to have zero operation cost.

In Table 5.5, G1 and G2 are committed for 24 hours while G3, which is the most expensive gas unit, is committed during peak times to minimize the cost. The sufficient ramping down capability of gas unit supports the variable wind source. The daily base cost, availability cost and expected cost drop by 16.91%, 31.92%, and 20.07% to $100,913.29, $7,326.04, and $97,501.83 respectively.

Table 5.5. UC Solution – Case 2

Diurnal Base Cost = \$ 100,913.293 Diurnal Availability Cost = \$ 7,326.035 Diurnal Expected Cost = \$ 97,501.829																								
Unit	Hour (1-24)																							
G1	1	1	1	1	1	1	1	1	1	1	1	1	1	1	1	1	1	1	1	1	1	1	1	1
G2	1	1	1	1	1	1	1	1	1	1	1	1	1	1	1	1	1	1	1	1	1	1	1	1
G3	0	0	0	0	0	1	1	1	1	1	1	1	1	1	1	1	1	1	0	0	0	0	0	0

The natural gas unit which serves as a peak load supplier would adjust its dispatch within minutes, which offers a potential for the integration of variable energy sources. The wind curtailment in the base case and the expected wind curtailment in scenarios are 377.93 MWh and 107.30 MWh respectively. Figure 5.6 portrays the diurnal generation dispatch of thermal units in which the standard deviations of generation dispatch for G1, G2, and G3 are 13.15, 7.15, and 10.15 MW, respectively. Figure 5.7 shows that G2 and G3 discharge less emission as compared to the previous case. The wind turbine is followed closely by natural gas, which reduces the cumulative expected daily emission in scenarios by 8.91% to 67,775.51 pounds.

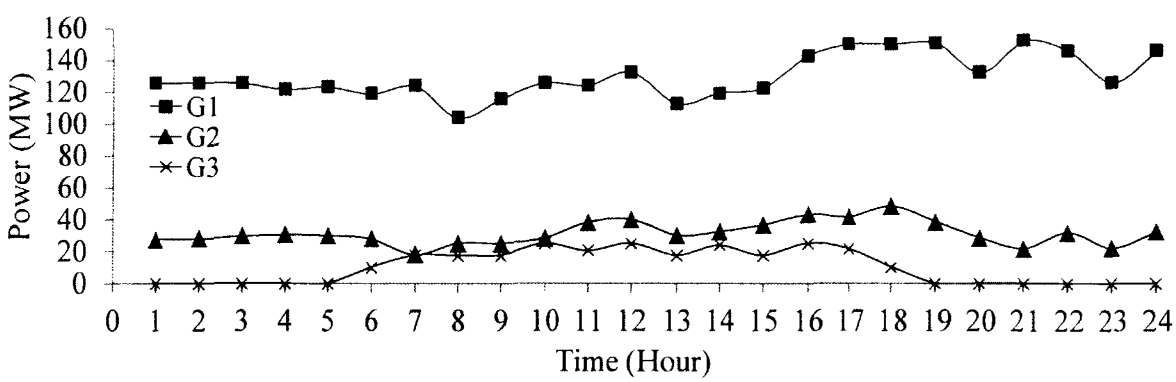

Figure 5.6. Thermal Generation Dispatch of Units - Case 2

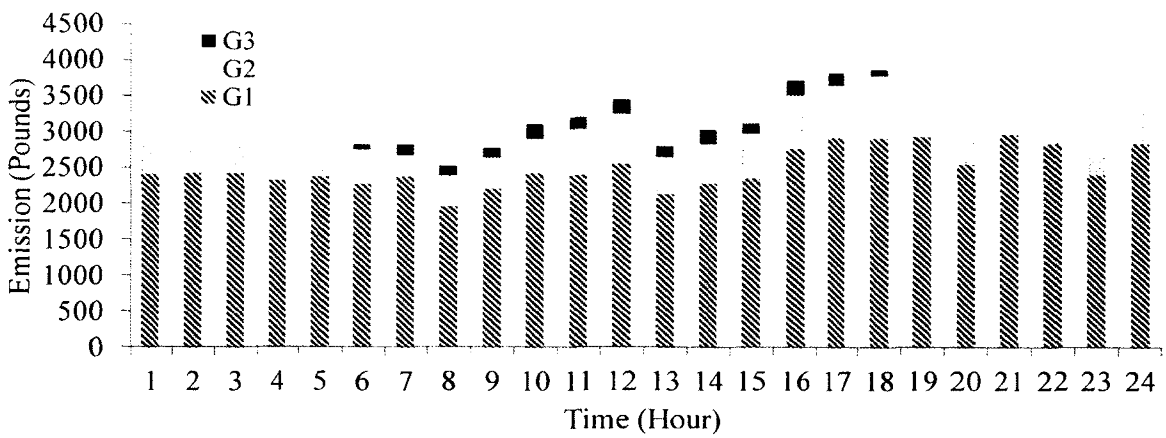

Figure 5.7. Hourly Emission Trend of Thermal Units - Case 2

In cases 3 and 4, two modes of operation are considered for the V2G deployment. In the intelligent-controlled mode, electric power system operators control the EV fleets charge/discharge decisions based on the system operation requirements. While in the rule-based mode, SOCs are tuned at certain hours to showcase consumer charging/discharging adjustments.

5.2.4 Case 3: Intelligent integration of stationary EV fleets and wind generation, and their coordination in the hourly stochastic SCUC solution considering environmental externalities. In order to further optimize the operation cost, abate the emission level, and facilitate higher integrations of variable renewable energy resources, we introduce 5 stationary EV fleets, as distributed storage, that are always connected to a specific bus (stationary EV fleets). EVs' energy requirements are considered random. EV fleet characteristics include max/min capacities, SOC, and charge/discharge capacities of aggregated vehicles. Table 5.6 denotes the characteristics of the five EV fleets consisting of 3,400, 2000, 1,000, 1,600, and 2,000 vehicles respectively. The charging efficiency of a fleet, i.e., ratio of energy stored in the battery to energy drawn from the power grid, is assumed 85%.

Table 5.6. Electric Vehicle Fleet Features

EV Fleet No.	Min Cap. (MWh)	Max Cap. (MWh)	Min Charge/Discharge (kW)	Max Charge/Discharge (kW)	a ($/MW^2)	b ($/MW)	c ($/h)
1	13.152	65.76	7.3/6.2	24.8/21.08	0.17	8.21	0
2	10.96	54.8	7.3/6.2	14.58/12.4	0.20	8.21	0
3	5.48	27.4	7.3/6.2	7.29/6.2	0.41	8.21	0
4	8.768	43.84	7.3/6.2	11.67/9.92	0.25	8.21	0
5	10.96	54.8	7.3/6.2	14.58/12.4	0.20	8.21	0

Table 5.7 illustrates the hourly UC of generators in which the hourly commitment of G3 is reduced by four hours; only committing during peak hours. The introduction of V2G into the electric power system would reduce the diurnal base cost, availability cost and expected cost by 5.41%, 63.48%, and 6.29% to $95,457.61, $ 2,675.73, and $ 91,372.30.

Further, the base case and the expected wind curtailment in scenarios are ameliorated to 210.77 MWh and 90.51 MWh correspondingly.

Table 5.7. UC Solution – Case 3

Diurnal Base Cost = $ 95,457.611
Diurnal Availability Cost = $ 2,675.725
Diurnal Expected Cost = $ 91,372.304

Unit	Hour (1-24)																						
G1	1	1	1	1	1	1	1	1	1	1	1	1	1	1	1	1	1	1	1	1	1	1	1	1
G2	1	1	1	1	1	1	1	1	1	1	1	1	1	1	1	1	1	1	1	1	1	1	1	1
G3	0	0	0	0	0	0	0	0	1	1	1	1	1	1	1	1	1	0	0	0	0	0	0	0

Figure 5.8 shows the generation dispatch profile which indicates that the standard deviations for the dispatch of G1, G2, and G3 are reduced to 7.88, 2.79, and 10.83 MW, respectively; implying a smoother generation profile as compared to that in Case 2. The generation dispatch volatility could escalate the grid operation cost caused by turbine

wear and tear. As such, a flexible EV control can moderate the volatility when integrating renewable resources into the grid. Figure 5.9 demonstrates the stacked daily diurnal emission dispatch of generators is declines to 67,322.37 pounds as compared to previous cases due to a wider usage of wind energy and the EV storage at peak hours.

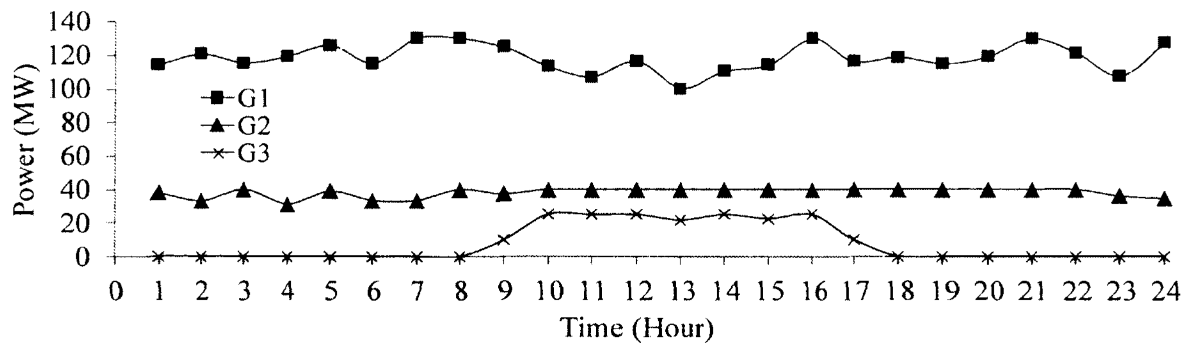

Figure 5.8. Hourly Generation Dispatch - Case 3

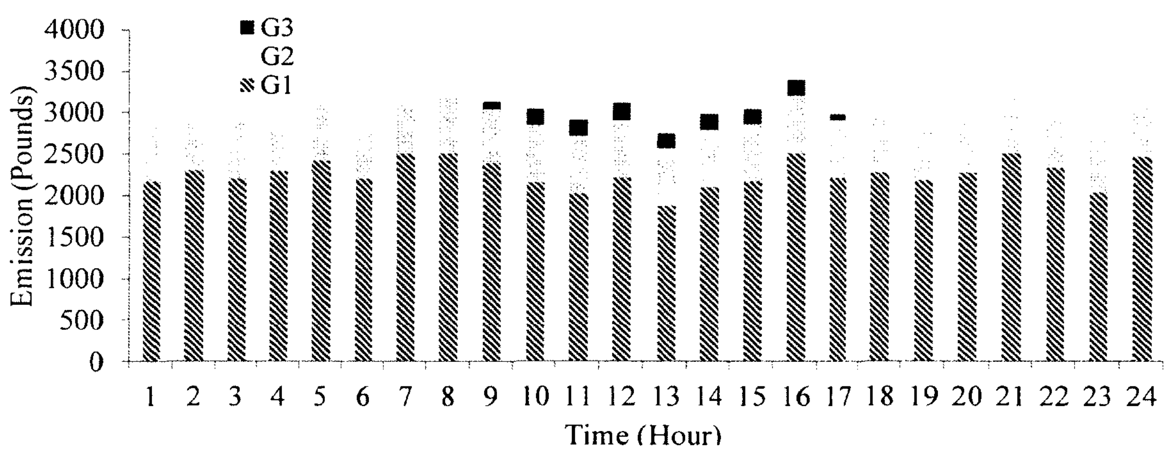

Figure 5.9. Hourly Emission trend of Thermal Units – case 3

5.2.5 Case 4: Rule-based integration of stationary EV fleets and wind generation, and their coordination in the hourly stochastic SCUC solution considering environmental externalities. In this case consumers enforce further constraints on charge/discharge of EVs. As such, the base case operation cost, availability cost, and expected cost are increased, in comparison with Case 3, to $96,097.86, $4,273.43, and $93,084.26. In addition, base case and the expected wind curtailment in scenarios are 222.91 MWh and 90.18 MWh respectively; here, the base case wind curtailment is increased as compared to the previous case. Table 5.8 displays the hourly UC in Case 4 in which the commitment of G3 is decreased by one hour.

Table 5.8. UC Solution – Case 4

Diurnal Base Cost = $ 96,097.805 Diurnal Availability Cost = $ 4,273.427 Diurnal Expected Cost = $ 93,084.255																								
Unit	Hour (1-24)																							
G1	1	1	1	1	1	1	1	1	1	1	1	1	1	1	1	1	1	1	1	1	1	1	1	1
G2	1	1	1	1	1	1	1	1	1	1	1	1	1	1	1	1	1	1	1	1	1	1	1	1
G3	0	0	0	0	0	0	0	0	0	0	1	1	1	1	1	1	1	0	0	0	0	0	0	0

In Figure 5.10, the standard deviations of generation dispatch for G1-G3 is increased to 11.11, 5.71, and 10.10 MW, indicating sharp disparities in the generation profile of G1 and G2 in comparison with those in the previous case. Figure 5.11 shows the aggregated daily emission dispatch of generators in which the diurnal aggregated expected emission is slightly higher than that in the previous case, which is due to less efficient use of EV fleets.

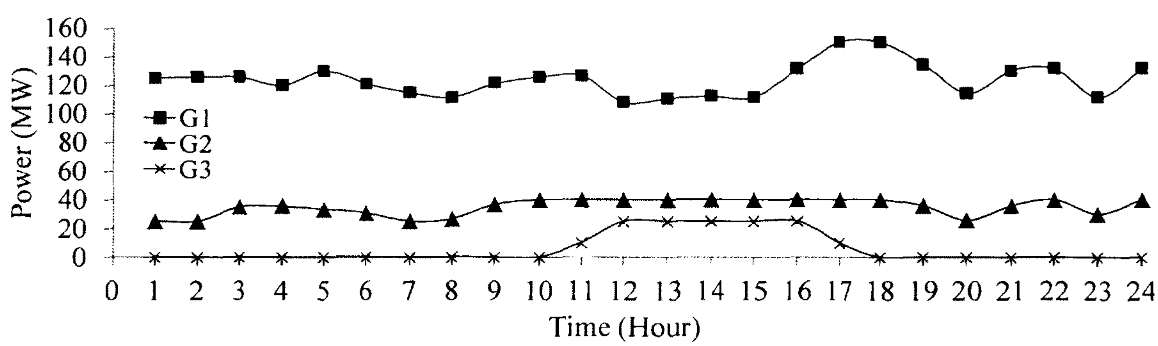

Figure 5.10. Hourly Generation Dispatch - Case 4

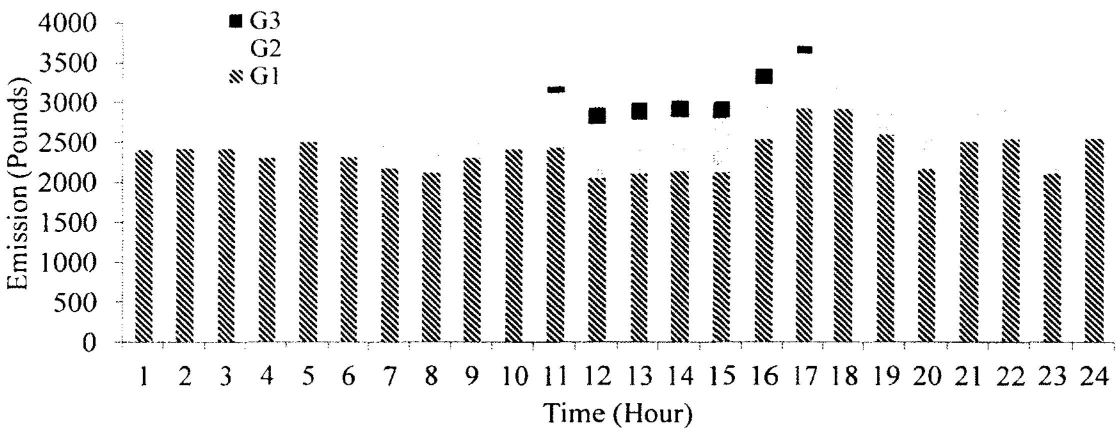

Figure 5.11. Hourly Emission Trend of Thermal Units – Case 4

Table 5.9 summarizes the optimal diurnal base case cost, wind curtailment, and aggregated emission in each case.

Table 5.9. Summary of Results for Four Cases – Base Case

Case	Cost ($)	Wind Curtailment (MWh)	Emission (Pounds)
1	121,445.06	NA	73,789.270
2	100,913.29	377.93	67,775.51
3	95,457.61	210.765	67,322.365
4	96,097.86	222.914	67,767.739

Figure 5.12 shows the aggregated hourly load dispatch in the base case, with and without the intelligent V2G deployment. We do not consider the transmission congestion here in which the V2G facilitates a cheaper energy delivery at peak hours. At off-peak hours when LMPs[17] are lower, the EV fleets are either charged or in the idle mode, and as such the demand is higher. At hour 10 when the LMP increases at peak hours, EV fleets would supply power back to the system which would lower the aggregated demand. So

[17] LMP is the Locational Marginal Price which expresses the hourly price at each bus.

the distributed storage through V2G could accommodate the variability of renewable energy resources for supplying the hourly demand.

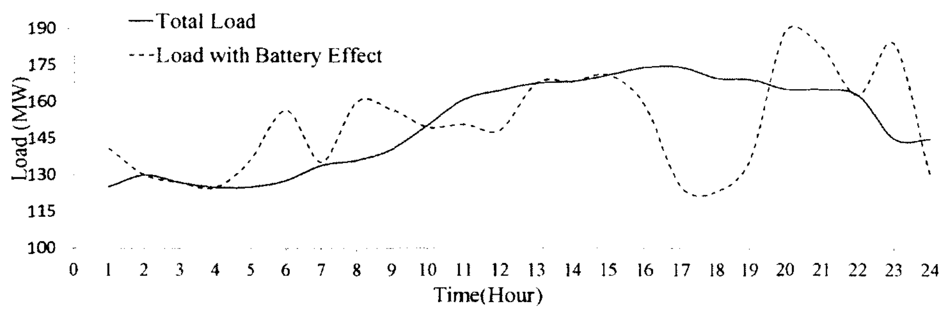

Figure 5.12 Hourly Aggregated Load with and without Storage - Base Case

5.3 Conclusion

This chapter suggested a stochastic programming framework for the day-ahead scheduling in electric power systems with coordinated wind, EV fleets as distributed storage, and thermal units considering system and operation uncertainties. The proposed model is driven by its environmental benefits and operational effectiveness. Further, the flexibility of the proposed model makes it suitable as a support tool for the V2G implementation in practical applications. The coordination between EV fleets and variable renewable sources provides the energy sector with a practical tool to spearhead environmental, social, and economic pillars of sustainability. It also provides potentials for filling out the gap between the energy path the world is on and an energy pathway harmonious with a 2DC climate goal.

Understanding and gauging the impacts associated with the introduction of EV fleets as virtual power plants is essential to guide a society's energy policy; hence, this paper was instigated to support decision-makers to facilitate a more effective transition to new energy architectures. Our simulation results indicate that the intelligent integration of EV fleets as stationary distributed storage facilities could cut the diurnal operation cost, abate the emission from fossil fuels, and enable superior consumption of forecasted wind with minimal wind curtailment.

The intelligent V2G implementation is an especially promising method for ensuring that the renewable energy supply would match the hourly demand, smoothening out the variability of resources, and providing a long-term, decentralized form of electricity storage in electric power systems. Although distributed storage systems are much smaller than conventional energy sources for providing base firm capacity, they demonstrate advantageous technical and economical features when providing short-term power. Further, our analyses points out that intelligent V2G technology have the potential to make a paradigm shift in a number of fundamental ways we operate electric power systems including: delaying the installation of conventional peak generation capacity, encouraging the installation of renewable electricity sources, and accelerating the adaptation of electric transportation technologies. An expansion of the proposed model in a larger scope considering the mobility of EVs would demonstrate a lower emission when conventional vehicles are replaced gradually with EV fleets.

CHAPTER 6

SPEARHEADING THE PUSH TO FULFILL LARGE ENERGY DEMAND REQUIREMENTS IN A SUSTAINABLE MANNER: STOCHASTIC COORDINATION OF THERMAL UNITS, RENEWABLE ENERGY SOURCES, AND EV FLEETS – CONSIDERING EV MOBILITY

This chapter is outlined as follows. Section 6.2 discusses the proposed stochastic security constraint unit commitment optimization model, in its initial (non-robust) and stochastic (robust) formulations, considering the uncertainties involved with the mobility of EVs. Section 6.2 investigates the effectiveness of the proposed approach, utilizing a 30-bus system, through comparison among 3 case studies. Finally, Section 6.3 sums up the core results and conclusions of the study, and offers potential future studies.

6.1 Proposed Stochastic SCUC Optimization Model

The proposed stochastic day-ahead scheduling problem harmonizes variable energy sources, mainly wind, with fleets of EVs, as mobile distributed storage facilities, in an uncertain environment. In this chapter the random behavior of EVs is taken into consideration. Further, it incorporates emission constraints to show how the synchronization between conventional energy sources, renewable energy sources, and fleets of mobile EVs in the power grid system can effectively satisfy power system network requirements while achieving economic goals with substantial cutback on carbon-footprints. The focus is on short-term operation (day ahead scheduling). The discussed model optimizes the hourly coordination of wind-EV fleet generation with the thermal unit dispatch. Generic Algebraic Modeling System (GAMS) software which as a core employs the CPLEX[18] optimizer solver is utilized to implement the problem with a dc power flow algorithm that considers network constraints.

The coordination between wind, mobile EV fleets, and conventional thermal units is formulated as a MILP problem in stochastic SCUC. In the proposed stochastic optimization problem, the wind energy and load forecast errors, power system outages, number of available EVs in a fleet and their energy requirements are considered as variables.

EVs in different locations are classified into different fleets based on their driving characteristics. Departure and arrival locations of EV fleets, departure and arrival times at selected locations and EV charging locations and patterns construct the EV fleets characteristics. Each fleet consists of random number of EVs. Energy utilization, min/max capacity, and state of charge (SOC) of an EV fleet is a function of number of EVs and their operating characteristics. The energy utilization in a fleet is determined by considering number of EVs and their energy requirements. SOC is the ratio of available energy to maximum storable energy in the battery. The available energy in the PEV battery is calculated by multiplying the given SOC by the maximum storable energy in the battery. The driving habits in each fleet determine the charging/discharging patterns of aggregated EVs [Kh012].

---

[18] CPLEX optimizers are designed to solve large-scale, challenging problems quickly and with minimal user intervention. CPLEX solves LP problems employing several alternative algorithms. The majority of LP problems resolve best using CPLEX's dual simplex algorithm.

As discussed in Chapter 2, the Monte Carlo simulation method is employed in the proposed stochastic model. Random outages in power systems are denoted by incorporating probability distribution functions and forced outage rates. Load projection errors, EV energy utilization patterns, and the number of EVs in a fleet are represented by truncated normal distribution functions [Chapter 2]. Wind speed disparities are simulated by the Weibull distribution function, auto correlation factor and diurnal pattern. Wind forecast errors are considered and the wind unit generation is based on the wind speed data and typical wind power curve. The mean daily wind speed is 10 meter per second (m/s), which follows a Weibull distribution function with Weibull coefficient equal to 2.1. The wind turbine is assumed to have zero operation cost. Further, as explained in chapter 2 forward and backward algorithms are established to cut the number of scenarios with an acceptable precision. The convex operation cost of aggregated PEVs would be subject to the number of vehicles and charging/discharging cycles [Tom07].

The objective function (6.1) minimize the operation cost, in which the projected quantities of load, wind, and EV batteries are included, subject to system and generating unit constraints and uncertainties. The objective function consists of the base case operation cost, including generation cost of thermal units, startup and shutdown costs of thermal units, and the operation cost of EV fleets; in which outages of generators and transmission lines are not included. Moreover, the availability costs for facilitating spinning reserve in Monte Carlo scenarios are taken into consideration in the objective function. The payment to the generators that facilitate spinning reserve refers to as the availability cost. One third of the marginal cost of a generating unit is considered as availability cost [Gan03].

In response to the existence of uncertainties, the provision of reserve is exercised as a remedial action by generators. Generators capability to provide remedial actions are bounded by their ramp up/down limitations. The objective function also considers the expected cost of remedial actions in scenarios for accommodating uncertainties. Thermal units are assumed to be non-quick start units; as such their scenario commitment status is the same as that in the base case. So no extra startup/shutdown costs are introduced in scenarios.

Further, since wind farms usually have trivial operation costs, we consider a no cost operation for wind energy units in the objective function. The system and generating unit constraints in the base case are demonstrated in (6.2)-(6.21).

$$\left\{ \min \begin{bmatrix} \sum_t \sum_i \left(p^b F_{c,i}\left(P_{i,t}\right) + SU_{i,t} + SD_{i,t} \right) + \\ \sum_t \sum_v p^b . C_{v,t} \end{bmatrix} + \left[\sum_t \sum_i (F^r_{c,i}(\Delta^{\max}_{i,t})) \right] + \sum_s P^s . \left[\sum_t \sum_i F_{c,i}\left(P^s_{i,t}\right) + \sum_t \sum_v C^s_{v,t} \right] \right.$$

(6.1)

$$F_{c,i}\left(p_{it}\right) = a_i + b_{ci} p_{it} + c_{ci} p_{it}^2$$

Where a, b, and c are the cost coefficients. The nonlinear production cost function can be approximated by a set of piecewise linear blocks as described in the previous chapters. The second term in (5.1) denotes the startup cost (SU), which is a function of the length of time that the thermal unit has been off. The startup cost is given as:

$$SU_{it} = I_{it}\left[1 - I_{i(t-1)}\right]\left[\alpha_i + \beta_i (1 - e^{-x_{it}^{off}/\lambda_i})\right]$$

Where α is the integrated cost of for startup and equipment maintenance, β is the startup cost of unit when initiating from cold conditions, X^{off} is the number of hours that the unit has been Off, and λ_i is the thermal time constant that characterizes the cooling speed of the unit. Similarly, the shutdown cost (SD), which is formulated as $SD_{it} = kP_{it}$, here k is the incremental shutdown cost. The operation cost of EVs, $C_{v,t}$, depends on the number of vehicles and charging/discharging depth and frequency [Kho12]. Further, $F^{r}_{c,i}(\Delta^{\max}_{i,t})$ represents the hourly cost of corrective action.

The wind curtailment happens when there is an inadequate ramping down capability of thermal units or major transmission congestion for utilizing the available wind power in power systems. The wind curtailment constraint is given in (6.2) in which the sum of dispatched and curtailed wind power is the same as the wind power forecast.

$$P_{w,t} + P_{d,w,t} = P_{f,w,t} \tag{6.2}$$

When there is an inadequate ramping down capability of thermal units or major transmission congestion for utilizing the available wind power in power systems the wind curtailment takes place [Lew11].

The thermal unit generation range (6.3) implies that once committed (I=1), the generation unit must operate between its min and max generating capacity. If I=0, the unit is de-committed.

$$P_{i,\min} I_{i,t} \le P_{i,t} \le P_{i,\max} I_{i,t} \quad \forall i, \forall t \tag{6.3}$$

Equation (6.4) denotes min off time indicating that a unit must be off for a certain period before it can be turned on again. Equation (6.5) denotes that a unit must be on for a certain period before it can be turned off, representing min on time constraint.

$$\left[X^{off}_{i(t-1)} - T^{off}_{i}\right] * \left[I_{it} - I_{i(t-1)}\right] \ge 0 \quad \forall i, \forall \mathrm{t} \tag{6.4}$$

$$\left[X^{on}_{i(t-1)} - T^{on}_{i}\right] * \left[I_{i(t-1)} - I_{it}\right] \ge 0 \quad \forall i, \forall \mathrm{t} \tag{6.5}$$

System ramp up/down limits between adjacent hours are demonstrated by (6.6)-(6.7). Equation (6.6) conveys that when unit i starts up at time t, its generating output (P_{it}) is equal to the minimum generating capacity of unit (p_{min}), while (6.7) conveys when unit i is shutting down at time t, its generating output ($P_{i(t-1)}$) is equal to the minimum generating capacity of unit (p_{min}) [Sha05].

$$P_{it} - P_{i(t-1)} \leq \left[1 - I_{it}(1 - I_{i(t-1)})\right] UR_i + I_{it}\left(1 - I_{i(t-1)}\right) P_{i,\min} \qquad \forall i, \forall t \tag{6.6}$$

$$P_{i(t-1)} - P_{it} \leq \left[1 - I_{i(t-1)}\left(1 - I_{it}\right)\right] DR_i + I_{i(t-1)}\left(1 - I_{it}\right) P_{i,\min} \qquad \forall i, \forall t \tag{6.7}$$

Equation (6.8) indicates that the daily emission is capped. For the purpose of this study, the primary concerns are carbon dioxide (CO_2) and carbon dioxide equivalent (CO_{2e}). The emission function, as a convex quadratic function of power generation, is modeled as[19]: $F_{e,i}\left(p_{it}\right) = a_{ei} + b_{ei} p_{it} + c_{ei} p_{it}^2$

Where a_{ei}, b_{ei}, c_{ei} represent emission coefficients[20] of unit i.

$$\sum_i \sum_{t=1}^{24} \left[F_{e,i}^{ET}(p_{it}) + SU_{e,it}^{ET} + SD_{e,it}^{ET} \right] \leq EMS_{\max,i}^{ET} \qquad \forall i, ET = \{CO_2 \,\&\, CO_{2e}\} \tag{6.8}$$

Emission constraints are coupling constraints over a group of generating units and period of study. The startup/shutdown emissions denoted by SU_e and SD_e The nonlinear emission function is piecewise linearized and incorporated into the proposed MILP formulation.

The system power balance and dc power flow constraints are expressed by (6.9)-

[19] Emission functions are computed using historical generator data. For each thermal units, heat curve (MBTU/MW) and (MBTU/Metric Tons of emissions) are considered with their interactions computed as emission curve (MW/metric tons); the curves are piecewise linearized. Slope of segments indicate the incremental emission for each unit.

(6.11), respectively. The power flow (6.10) indicates that the transmission flow is dependent on the voltage angle difference between the corresponding buses and the line impendence. The power flow is limited by (6.11).

$$\sum_i P_{i,t} + \sum_v P_{v,t} + \sum_w P_{w,t} = \sum_{d \in D_b} P^d_{D,t} + \sum_{l \in L_{f,b}} PL_{l,t} - \sum_{l \in L_{t,b}} PL_{l,t} \quad \forall i, \forall t \tag{6.9}$$

$$PL_{l,t} = \left(\frac{\theta_{j,t} - \theta_{o,t}}{X_{jo}} \right) \quad \text{line l is from bus j to bus o} \tag{6.10}$$

$$\left| PL_{l,t} \right| \leq PL_l^{\max} \tag{6.11}$$

The EV fleet constraints are expressed by (6.12) - (6.19) where (6.12) conveys the net hourly absorbed/injected energy and the dispatched power of EV fleet. Here, the difference between the energy stored in the aggregated EV battery and the EV energy injected back to the grid is measured by the charging cycle efficiency of the aggregated EV.

$$\begin{cases} E_{v,t}^{net} = \eta_v . P_{c,v,t} - P_{dc,v,t} \\ P_{v,t} = P_{c,v,t} - P_{dc,v,t} \end{cases} \tag{6.12}$$

Once an EV fleet is connected to the power system ($N_{v,t}=1$), the aggregated battery will be charged, discharged, or remain in the idle mode (6.13).

$$I_{dc,v,t} + I_{c,v,t} + I_{i,v,t} = N_{v,t} \tag{6.13}$$

Charging and discharging constraints for preserving the battery life are given as (6.14) and (6.15) equations :

$$I_{c,v,t} . P_{c,v}^{\min} \leq P_{c,v,t} \leq I_{c,v,t} . P_{c,v}^{\max} \tag{6.14}$$

$$I_{dc,v,t} . P_{dc,v}^{\min} \leq P_{dc,v,t} \leq I_{dc,v,t} . P_{dc,v}^{\max} \tag{6.15}$$

Energy balance per hour is ensured by equation (6.16).

$$E_{v,t} = E_{v,t-1} + E_{v,t}^{net} \tag{6.16}$$

Energy range of each aggregated unit is addressed in (6.17)-(6.18) representing the capacity limit in each fleet.

$$E_v^{\min} \le E_{v,t} \le E_v^{\max} \tag{6.17}$$

$$E_v^{\min} \le E_{v,t} \le E_v^{\max}$$

$$E_{v,0} = E_{v,NT} \tag{6.18}$$

The piecewise linear function of convex charge/discharge cost curve of EV batteries is expressed by (6.19) which shows a direct correlation with the number of vehicles and the depth of charging/discharging cycles. A higher depth in battery charging/discharging causes the number of cycles to failure decrease dramatically, which corresponds to an increase in the cost of EV charging/discharging [Tom07]; as for a fixed battery price, the total energy stored by/drawn from the battery during its lifetime will deteriorate [Kem05b].

The nonlinear battery charging/discharging cost curves which are convex quadratic functions are piecewise linearized in the MILP formulation. A tighter piecewise linear estimation is presented in [Kho12]. The assumption that the aggregated state of charge (SOC) of batteries is set to be fixed at specific operation periods is addressed by (6.20).

$$\begin{cases} C_{v,t} = N_{v,t} \cdot \left[\sum_m b_{m,v} . P_{m,v,t} \right] & 0 \le P_{m,v,t} \le P_{m,v}^{\max} \\ N_{v,t} \cdot \left| E_{v,t} - E_{v,t-1} \right| = \sum_m P_{m,v,t} & \end{cases} \tag{6.19}$$

$$E_{v,T} = E_v^{\max} \tag{6.20}$$

It is assumed that the SOC is at 100% when a PEV fleet is departing the station.

The system and generating unit constraints in the Monte Carlo scenarios comprise those that are similar to base case constraints, except the base case variables are replaced by scenario variables. The scenario constraints for EV fleets are demonstrated in (6.21)-(6.32).

$$\begin{cases} C_{v,t}^{s} = N_{v,t} \cdot \left[\sum_{m} b_{m,v} \cdot P_{m,v,t}^{s} \right] & 0 \le P_{m,v,t}^{s} \le P_{m,v}^{\max} \cdot NE_{v}^{s} \\ N_{v,t} \cdot \left| E_{v,t}^{s} - E_{v,t-1}^{s} \right| = \sum_{m} P_{m,v,t}^{s} & \end{cases} \tag{6.21}$$

$$\begin{cases} E_{v,t}^{net,s} = \eta_{v} \cdot P_{c,v,t}^{s} - P_{dc,v,t}^{s} \\ P_{v,t}^{s} = P_{c,v,t}^{s} - P_{dc,v,t}^{s} \end{cases} \tag{6.22}$$

$$I_{dc,v,t}^{s} + I_{c,v,t}^{s} + I_{i,v,t}^{s} = N_{v,t} \tag{6.23}$$

$$\mathrm{N}_{v,t} \cdot I_{c,v,t}^{s} \cdot P_{c,v}^{\min} \cdot NE_{v}^{s} \le P_{c,v,t}^{s} \le \mathrm{N}_{v,t} \cdot I_{c,v,t}^{s} \cdot P_{c,v}^{\max} \cdot NE_{v}^{s} \tag{6.24}$$

$$\mathrm{N}_{v,t} \cdot I_{dc,v,t}^{s} \cdot P_{dc,v}^{\min} \cdot NE_{v}^{s} \le P_{dc,v,t}^{s} \le \mathrm{N}_{v,t} \cdot I_{dc,v,t}^{s} \cdot P_{dc,v}^{\max} \cdot NE_{v}^{s} \tag{6.25}$$

$$E_{v,t}^{s} = E_{v,t-1}^{s} - E_{v,t}^{net,s} \tag{6.26}$$

$$E_{v}^{\min} \cdot NE_{v}^{s} \le E_{v,t}^{s} \le E_{v}^{\max} \cdot NE_{v}^{s} \tag{6.27}$$

$$E_{v,0}^{s} = E_{v,NT}^{s} = E_{v0} \cdot NE_{v}^{s} \tag{6.28}$$

Equation (5.30) addresses the scenario corrective action;

$$\begin{cases} -\Delta_{i,t}^{\max} \le P_{i,t}^{s} - UX_{i,t}^{s} \cdot \mathrm{P}_{i,t} \le \Delta_{i,t}^{\max} \\ \mathrm{P}_{i}^{\min} \cdot UX_{i,t}^{s} \cdot I_{t}^{i} \le P_{i,t}^{s} \le \mathrm{P}_{i}^{\max} \cdot UX_{i,t}^{s} \cdot I_{t}^{i} \end{cases} \tag{6.29}$$

The DC power flow constraints for each Monte Carlo scenario are denoted by Equations (6.30)–(6.32). The grid connection of PEV fleet at time t is illustrated by $B_{b,t}^{v}$ in equation (5.30).

$$\sum_{i\in B_b^i} P_{i,t}^s + \sum_{v\in B_{b,t}^v} P_{v,t}^s + \sum_{w\in B_b^W} P_{w,t}^s = \sum_{d\in D_b} P_{D,t}^{d,s} + \sum_{l\in L_{f,b}} PL_{l,t}^s - \sum_{l\in L_{t,b}} PL_{l,t}^s \tag{6.30}$$

$$-M.(1-UY_{l,t}^s) \le PL_{l,t}^s - \left(\frac{\theta_{j,t}^s - \theta_{o,t}^s}{X_{jo}}\right) \le M.(1-UY_{l,t}^s) \tag{6.31}$$

$$-PL_l^{\max} UY_{l,t}^s \le PL_{l,t}^s \le PL_l^{\max} UY_{l,t}^s \tag{6.32}$$

An expected emission limit is considered for scenario emission constraint (6.33).

$$\sum_i \sum_{t=1}^{24} p^b.\left[F_{e,i}^{ET}(p_{it}) + SU_{e,it}^{ET} + SD_{e,it}^{ET}\right] + \sum_s p^s.\left[F_{e,i}^{ETS}(p_{it}) + SU_{e,it}^{ETS} + SD_{e,it}^{ETS}\right] \le Expected(EMS_{\max,i}^{ET}) \tag{6.33}$$

The two-level hierarchical structure of the MILP problem makes it a suitable candidate for BD. The flowchart of the proposed stochastic SCUC formulation is demonstrated in Figure 5.1.

6.2 Numerical Results

In this section, the IEEE[21] 30-bus power system is utilized to demonstrate the effectiveness of the proposed stochastic day-ahead solution. The examples investigate the coordination among thermal units, wind, and mobile-EV fleets at bus-level and system-level and its impact on the hourly commitment and dispatch of generation units. Furthermore, total expected operation cost, base cost, capacity cost, total diurnal expected emission, base and expected wind energy curtailment are taken into consideration.

[21] IEEE stands for Institute of Electrical and Electronics Engineers

6.2.1 IEEE 30-Bus System. The 30-bus system incorporates 6 thermal units, and a wind turbine. The installed wind capacity is 150 MW, which is about 30% of the system peak load with an hourly average wind generation of 11.7%. Furthermore, the system includes 41 transmission lines. The data are given in http://www.ee.washington.edu/research/pstca/pf30/pg_tca30bus.htm. Forced outage rates of thermal generators and transmission lines are 4% and 1%, respectively.

Using the Monte Carlo simulation, 3000 scenarios are generated and scenario reduction techniques are used to obtain 12 scenarios. The parameters of generating units and emission function coefficients are depicted in Tables 6.1 and 6.2.

Table 6.1. Thermal Unit Characteristics

Unit	a ($/MW^2)	b ($/MW)	c ($/h)	P_{min} (MW)	P_{max} (MW)	SU ($)	SD ($)	Min. Up(h)	Min Dn.(h)
G1	0.099	6.589	211.4	100	320	200	50	4	3
G2	0.203	7.629	217.4	10	160	150	40	3	2
G3	0.089	6.58	210.4	10	100	50	10	1	1
G4	0.494	10.07	102.8	10	320	200	50	1	1
G5	0.494	10.07	102.8	10	320	200	50	1	1
G6	0.494	10.07	102.8	10	320	200	50	1	1

Table 6.2. Emission Function Coefficients

Unit	a ($/lb^2)	b ($/lb)	c ($/h)
G1	0.000304	19.943	0.0
G2	0.000312	18.933	0.0
G3	0.000316	16.745	0.0
G4	0.000320	15.842	0.0
G5	0.000340	12.432	0.0
G6	0.000351	10.032	0.0

EV fleet characteristics include max/min capacities, SOC, and charge/discharge capacities of aggregated vehicles. Table 6.3 illustrates characteristics of five EV fleets consist of 3,400, 2000, 1,000, 1,600, and 2,000 vehicles, respectively. The charging efficiency of a fleet, is assumed 85%. Table 6.4 shows the EV fleet travel characteristics in the power system under investigation. The required energy for driving in one direction is assumed the same as that of returning to the origin location. Energy requirements for the EV fleets are different. The driving distance by an EV fleet is 12,000 miles annually with a 32.88 miles diurnal average [Sab], [Roe08]. The required energy by an EV is 9 kWh/day with an average of 3.65 miles/kWh [Tom07]. Accordingly, the energy required by the fleets is 7.65, 9.00, 2.25, 7.20, and 4.50 MWh respectively.

Table 6.3. Electric Vehicle Fleet Features

EV Fleet No.	Min Cap. (MWh)	Max Cap. (MWh)	Min Charge/Discharge (kW)	Max Charge/Discharge (kW)	a ($\$/MW^2$)	b (\$/MW)	c (\$/h)
1	13.152	65.76	7.3/6.2	24.8/21.08	0.17	8.21	0
2	10.96	54.8	7.3/6.2	14.58/12.4	0.20	8.21	0
3	5.48	27.4	7.3/6.2	7.29/6.2	0.41	8.21	0
4	8.768	43.84	7.3/6.2	11.67/9.92	0.25	8.21	0
5	10.96	54.8	7.3/6.2	14.58/12.4	0.20	8.21	0

Table 6.4. Electric Vehicle Travel Characteristics

EV Fleet No.	Number of EVs	First Trip				Second Trip			
		Departure		Arrival		Departure		Arrival	
		Time	Bus	Time	Bus	Time	Bus	Time	Bus
1	3,400	6:00	21	8:00	2	17:00	2	19:00	21
2	2,000	7:00	30	8:00	4	16:00	4	17:00	30
3	1,000	5:00	24	7:00	12	16:00	12	18:00	24
4	1,600	5:00	17	6:00	15	17:00	15	18:00	17
5	2,000	7:00	19	9:00	8	18:00	8	20:00	19

6.2.2 Case Studies. The following 4 cases are tested in which the diurnal emission cap of 86,500 pounds and diurnal expected emission cap of 192,000 pounds is imposed in all cases.[22]

Case 1: Stochastic SCUC with thermal generation units, and a wind unit, considering environmental externalities

Case 2: Stochastic SCUC with thermal generation units, a wind unit, and EV fleets as intelligent stationary storage facilities, considering environmental externalities

Case 3: Stochastic SCUC with thermal generation units, a wind unit, and EV fleets as intelligent mobile storage facilities, considering environmental externalities (Intelligent-V2G)

Table 6.5 depicts the optimal expected operation cost in each of the above three cases. In which introduction of EVs, in case 2, has dramatically reduced the expected operation cost by 15.12%. As EVs can be synchronized with our wind turbine, store the excess capacity during off-peak hours, and inject the stored power back to the system during

[22] Daily emissions are computed using historical generator data. Daily emission cap is also imposed based on the historical data.

peak hours in which LMPs are higher. Accordingly, reduce the expected operation cost of the power system. Moreover, inclusion of mobility to the EV fleets (case 3), has even further shrunk the expected operation cost as EV mobility provides EVs the option to charge/discharge in different locations, and allows EVs to relocate the energy. As such facilitate a smoother integration of EVs into the power system.

Table 6.5. Expected Operation Cost ($)

	Case 1	Case 2	Case 3
Expected Operation Cost ($)	465,979.23	393,174.31	**391, 954.73**

Table 6.6 demonstrates the optimal base case cost, wind curtailment, and emission in each of the three cases.

Table 6.6. Summary of Results – Base Case

Case	Cost ($)	Wind Curtailment (MWh)	Emission (Pounds)
1	440,799.98	160.25	80,586.15
2	422,330.91	154.85	79,146.08
3	**421,686.162**	**144.74**	**79,001.13**

Table 6.7 displays the availability cost, expected wind curtailment, and expected emission in each of the three cases.

Table 6.7. Expected Scenario Results

Case	Avail.Cost ($)	Exp.Wind Curtailment (MWh)	Exp.Emission (Pounds)
1	51,253.15	93.86	78,468.380
2	29,632.46	80.26	77,961.113
3	**29,380.29**	**69.84**	**77,201.80**

Tables 6.6 and 6.7 both indicate that intelligent integration of EVs as distributed storage facilities to the power system minimize the hourly curtailments, and cut the diurnal emissions. As V2G not only allows a smoother integration of renewable sources witch have less carbon footprint compare to conventional units, but also reduce deployment of more pollutant thermal units. Additionally, tables 6.6 and 6.7 show when mobility has taken into consideration (case 3), base case cost, availability cot, base and expected wind curtailment, and emission are even lower. Consequently, use of EVs as mobile energy storage units provides the grid with additional reliability, cost- effectiveness, and efficiency.

Table 6.8 illustrates the operation costs in scenarios. In which the operation costs are lowest in the intelligent V2G case (case 3) due to a wider usage of wind energy and the EV storage at peak hours. Accordingly, the mobility of EVs could improve the optimal generation while addressing the fleet requirements.

Table 6.8. Scenario Costs ($)

Scenario	Case 1	Case 2	**Case 3**
1	386,869.120	335,366.279	**334,019.01**
2	449,349.419	383,241.12	**382,453.38**
3	417,342.94	350,443.81	**349,120.80**
4	395,713.48	339,912.49	**341,510.38**
5	394,098.24	338,338.37	**337,306.15**
6	348,717.08	301,081.72	**299,171.32**
7	433,384.48	374,285.04	**373,972.34**
8	436,571.89	379,315.19	**375,414.96**
9	417732.24	363,691.38	**362,640.40**
10	416,889.74	362939.18	**360,921.77**
11	415,077.25	367434.78	**365,974.331**
12	412,249.288	357892.71	**355,004.423**

Case 4: Stochastic SCUC with thermal generation units, a wind unit, and Rule-Based-EV fleets as mobile storage facilities, considering environmental externalities (Rule-Based-V2G)

In this case (the rule-based mode), SOCs are tuned at certain hours to showcase consumer charging/discharging adjustments. While in the intelligent-controlled mode (Case 3), electric power system operators control the EV fleets charge/discharge decisions based on the system operation requirements.

Table 6.9 compares the results between cases 3 and 4. As Table 6.9 demonstrates, base case operation cost, availability cost, expected cost, emission, and wind curtailment all are increased in comparison with case 3 in which EV fleets are controlled intelligently. Accordingly, simulation results imply that enforcement of additional constraints on charge/discharge of EVs by consumers, results in less efficient use of EV fleets.

Table 6.9. Summary of Results in Cases 3&4

Case	Expected OperationCost ($)	Base Cost ($)	Availability Cost ($)	Exp. Wind Curtailment (MWh)	Exp. Emission (Pounds)
3	**391,954.72**	**421,689.16**	**29,380.29**	**69.84**	**77,201.8**
4	400,286.06	431,922.15	34420.99	82.92	78,255.55

Figure 6.1 illustrates the diurnal EV fleets charge/discharge pattern for case 3. In which negative numbers indicate EVs are charging during off peak hours, while positive numbers indicate EVs are discharging or injecting power back to the system during peak hours.

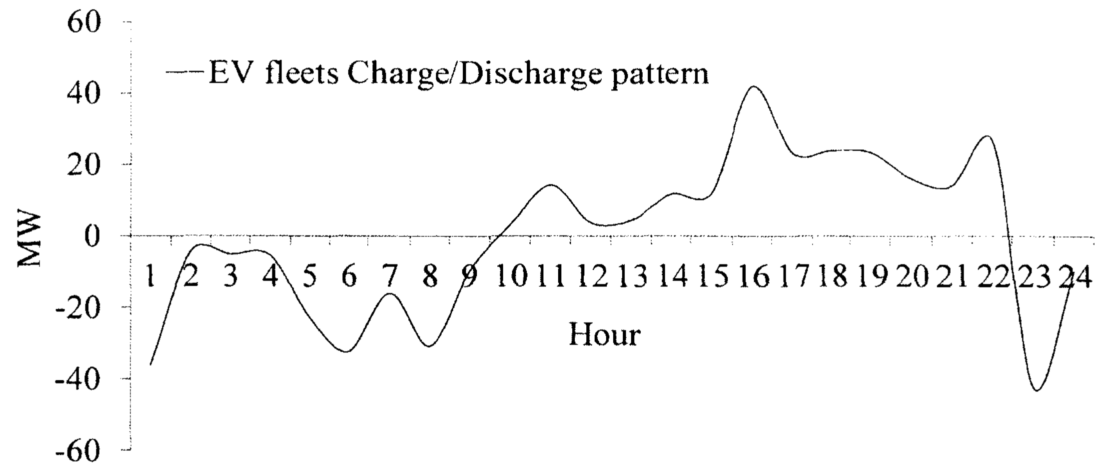

Figure 6.1. EV Fleets Charge/Discharge Pattern – Case 3 (Base Case)

The aggregated hourly load dispatch with and without the V2G deployment, is sketched in Figure 6.2. This figure demonstrates that at off-peak hours, in which LMPs are lower the EV fleets are charged as such demand is higher. At hour 10 when the LMP increases at peak-hours, EV fleets would inject power back to the system which would lower the aggregated demand. As such, intelligent deployment of EVs as mobile energy storage units could offer ancillary services and reduce operation costs in power systems.

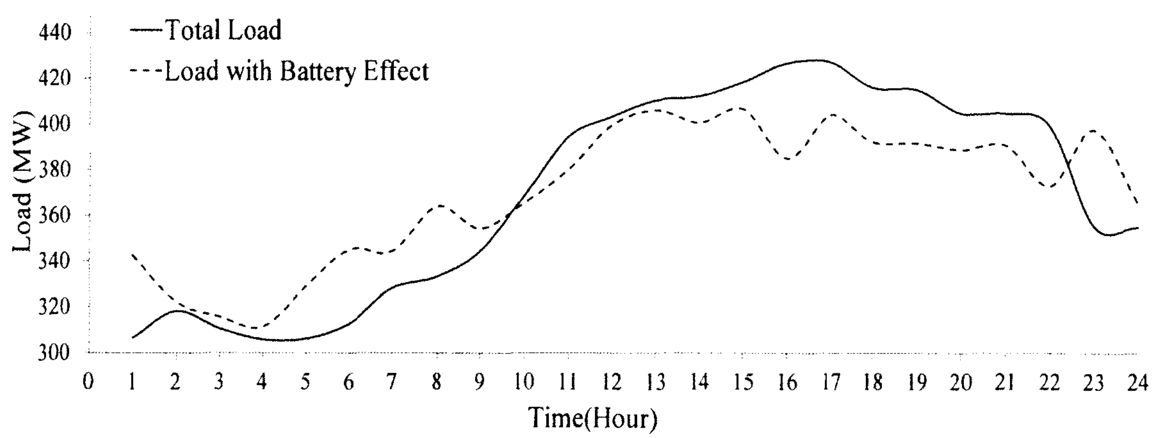

Figure 6.2 Hourly Aggregated Load with and without Storage – Case 3 (Base Case)

6.3 Conclusion

Future energy mix will be made of multitude of sources to fulfill the growing energy demand. Coal, crude oil and natural gas will continue to lead the energy mix in the short-term, as they have the most well-established infrastructures and are currently in many locations and applications. Further in order to remain within the boundaries of sustainable development, future energy mix should be Harnested in a cost-effective, environmentally responsible and socially acceptable way. Renewable energy, mainly wind and solar, can shrink emission from the electricity industry. Additionally, EVs can be synchronized with distributed renewable sources to minimize the hourly curtailments, and store the excess energy in their batteries. This stored energy can be used for driving needs or can be injected in the distribution grid at a later time. Deployment of EVs as mobile energy storage units provides the grid with additional stability, reliability, cost-effectiveness, and efficiency. Moreover, with the higher fuel efficiency of EVs, the transportation and power generation sectors can collectively cut their ecologically harmful emissions and strengthen their reliance on environmentally friendly energy sources.

The intelligent V2G implementation is an especially promising method for ensuring that the renewable energy supply would match the hourly demand, smoothening out the variability of resources, and providing a long-term, decentralized form of electricity storage in electric power systems.

Accordingly, intelligent V2G, unlocks numerous potential benefits of large-scale penetration of renewable sources, optimize the grid operation cost, and significantly curbs the carbon foot print of the conventional thermal units. Further, EV mobility offers a significant potential for load management and additional grid support.

This study opens ways to new research: One question is how could possibility of speed-charging stations, which allow fast charging of EVs, impact our findings. This would help both to optimally plan such infrastructure and to investigate its impact on traffic demand and the electric grid. In addition, the robustness of the proposed model with regard to daily and seasonal fluctuations should be examined. Finally, the model can be used to analyze the impact of different charging infrastructures. In connection with this, monetary aspects can also be considered such as the impact of dual tariff charging.

CHAPTER 7

SUMMARY, INSIGHTS, AND RECOMMENDATIONS

The vibrancy and sustainability of the entire economy is extensively influenced by the energy industry. Embraced as a key solution to the trilateral challenges of economic supply, security, and climate change, renewable energy continues to play a pivotal role in today's energy stock; providing a sustainable basis for greening and growing the economy. However, the high penetration of variable renewable generation assets (such as wind and solar) in the electricity grid has introduced major reliability challenges in sustainable operation of electric power systems. Coordination between thermal units, renewable sources, and distributed storage can address these challenges.

The study in this dissertation is the application of MILP to large-scale systems; as an example optimal operation of electric power systems is investigated. This dissertation proposes an efficient and practical methodology that has the potential to advance energy sector strategies regarding sustainability, keep the sector on track to address the 2DC climate goals by 2050 while addressing natural security issues. The study investigates the integration of aggregated EV fleets as distributed load and energy storage facilities, known as V2G, for high penetration of wind energy, while limiting emissions from fossil fuels.

Chapter 1 discusses importance of sustainable, secure, and low emission electric power systems operation. Further, it provides a concrete background about electric power systems operation, and discusses risks that are involved. Goal and objectives of this dissertation is presented in Chapter 1 as well.

Chapter 2 provides a big picture regarding the mathematical modeling employed in this dissertation.

In Chapter 3 the sustainable day-ahead scheduling of electric power systems with the integration of distributed energy storage devices is investigated. The main objective is to minimize the hourly electric power system operation cost with a cleaner, socially responsible, and sustainable generation of electricity. Emission constraints are enforced to reduce the carbon footprint of conventional thermal generating units. The stationary electric vehicles (EV) are considered as an example of distributed storage and V2G concept is considered to demonstrate the bilateral role of EV as supplier and consumer of energy. Distributed battery storage can ease the impact of variability of renewable energy sources on electric power system operations and reduce the impact of thermal energy emission at peak hours. The day-ahead scheduling of electric power systems is modeled as a mixed-integer linear programing (MILP) problem for solving the hourly deterministic SCUC. In order to expedite the real-time solution for large-scale electric power systems, we consider a two-stage model of the hourly SCUC by applying BD. Numerical simulations illustrate the effectiveness of the proposed MILP approach and its potentials as an optimization tool for sustainable operations of electric power grids.

Chapter 4 focuses on the integration of distributed storage with high penetration of variable renewable sources in electric power systems. This chapter analyzes the impact of such integrations on the security, emission reduction, and the economic operation of electric power systems. Strategies for a larger penetration of variable generation resources without compromising the electric power system security are identified. MILP is applied for the optimization of the day-ahead hourly SCUC. The assimilation of EVs (both as a provider and a utilizer of energy), renewable energy sources, and smart grid is regarded as a low-cost, and low-emission solution to the existing challenges of electric power systems including the means of storing large quantities of energy considering variable renewable energy sources and large carbon footprints of conventional thermal units. Numerical studies in this chapter to showcase the potential impacts of EV fleets as battery storage for peak load shaving, minimizing power grid operation costs and hourly wind curtailments, and optimizing the environmental impacts based on hourly commitment and dispatch of thermal generating units.

Chapter 5 evaluates the potential for utilizing stationary fleets of electric vehicles (EVs) as distributed storage, in an uncertain environment, for mitigating energy imbalances caused by the integration of variable renewable sources in electric power systems. This chapter shows the effectiveness of such integrations on the three pillars of sustainability including environmental sustainability, social sustainability, and the economic operation of electric power systems; while spearheads the push to keep the energy sector on track to address the 2 degree Celsius (2DC) target per Copenhagen climate agreement. Chapter 5 identified strategies for a larger integration of variable generation resources without compromising the electric power system security in a scenario based approach. Hourly load, wind energy uncertainties, and random outages of generation and transmission components in the coordination between wind EV fleets are also taken into consideration in this chapter. The efficiency and usefulness of the developed optimization models are shown using four numerical case studies.

Chapter 6 focuses on the mobility of electric vehicles and their impact as mobile distributed load and storage facilities on the optimal operation of network-constrained power systems, and their carbon footprint in an uncertain environment. Unlike conventional storage capabilities, the grid-connection storage topography of EVs may vary during the daily operation of power systems. Hourly load and wind energy forecast errors, random outages of generation and transmission components, random driving patterns of EVs are taken into consideration in this study. The synchronized integration of aggregated electric vehicle fleets and intermittent energy sources, specifically wind energy, in power systems is examined by stochastic security constrained unit commitment model. Numerical results depict that intelligent integration of aggregated fleets of mobile EVs in the power system unlocks numerous potential benefits of large-scale penetration of renewable sources, optimize the grid operation cost, and significantly curbs the carbon foot print of the conventional thermal units. Accordingly, EV mobility offers a significant potential for load management and additional grid support.

Findings from all the above studies indicate that EV fleets as an alternate energy storage system for electric power dispatch are a viable and marketable option for alleviating some of the challenges plaguing the current United States power grid. Applications of renewable energy sources and the intelligent assimilation of EV fleets (as mobile distributed load and storage facilities) in power systems offer potentials for alleviating peak demands, mitigating variability and intermittency of wind generation, minimizing power grid operation costs and hourly wind curtailments, removing transmission flow congestions as such improving the system security, and limiting the environmental impacts of fossil fuel-based thermal generating units in the operation of electric power systems. The proposed model is designed to establish a sustainable, low-carbon energy complex beyond fossil fuels and nuclear energy in an efficient, cost-effective manner.

Overall, V2G technologies have the potential to make a paradigm shift in a number of fundamental ways including: diminishing the installation of conventional peak generation capacity, encouraging the installation of renewable electricity sources, and accelerating the adaptation of new transport technologies. The implementation of such models worldwide could reduce the global warming, eliminate energy insecurity, and pave the road towards a greener growth. Moreover, decoupling electricity and transportation industries, which represent main sources of greenhouse gas emission, from their reliance on oil would enable positive changes for global prosperity. In addition, understanding and gauging the impacts associated with the introduction of EV fleets as virtual power plants is essential to guide a society's energy policy; hence, this study was instigated to support decision-makers to facilitate a more effective transition to new energy architectures.

The proposed modeling approach opens ways to new research for instance:

- One critical question is what are the implications of this study for policy change, and how should the presented results translate to policy design? What are the challenges involved?
- Further, assessing the geopolitical implications of the proposed model introduce several challenges that necessitate further investigations. For example this model might perfectly work for smaller countries, like Denmark, but be more challenging to implement for China.

- In addition, the robustness of the proposed model with regard to seasonal fluctuations should be examined.
- Moreover, the model can be used to analyze the impact of different charging infrastructures. In connection with this, monetary aspects can also be considered such as the impact of dual tariff charging.
- Another question is how could possibility of speed-charging stations, which allow fast charging of EVs, impact the presented results? This would help both to optimally plan such infrastructure and to investigate its impact on traffic demand and the electric grid.
- Last but not least, an expansion of the proposed model in a larger scope, considering the emission reductions from the transportation sector, would demonstrate much lower emission when conventional vehicles are replaced gradually with EV fleets.

BIBLIOGRAPHY

[Ack05] Ackermann, T., & Söder, L. (2005). *Wind Power In Power Systems: An Introduction.* New York: Wiley, 25-52.

[Adi01] Aditya, S.K., & Das, D. (2011). Battery energy storage for load frequency control of an interconnected power system. *Electric Power Systems Research*, *58*, 179-185.

[And10] Andersson, L., Elofsson, K., Galus, D., Goransson, L., Karlsson, S., Johnsson, F., & Andersson, G. (2010). Plug-in hybrid electric vehicles as regulating power providers: case studies of Sweden and Germany. *Energy Policy*, *38*, 2751–2762.

[Bal11] Balijepalli, M., Pradhan ,V. & Khaparde, S. (Dec 2011). Review of demand response under smart grid paradigm. *IEEE PES Innovative Smart Grid Technologies Conferenc-India*, pp. 236 – 243.

[Bat12] Battistelli, C., Baringo, L., & Conejo, A.J. (2012). Optimal energy management of small electric energy systems including V2G facilities and renewable energy sources. *Electric Power Systems Research, 92*, 50–59.

[Bil96] Billinton, R., & Allan, R. (1996), *Reliability Evaluation of Power Systems, Second Edition*, London: Plenum Publishing Corporation, New York .

[Bir11] Birol F. (Nov 2011). World Energy Outlook 2011. *International Energy Agency (IEA).* Retrieved March 16, 2013, from http://www.worldenergyoutlook.org/publications/weo-2011/

[Bir13] Birol, F. (June 2013). Redrawing the energy climate map, world energy outlook 2013 special report. *International Energy Agency (IEA)*. Retrieved Jun 18, 2013, from http://www.iea.org/publications/freepublications/publication/name,38764,en.html

[Boo05] Boone, A. (2005). *Simulation of Short-Term Wind Speed Forecast Errors Using a Multi-Variate ARMA (1,1) Time-Series Model* (Master's Thesis). Retrieved from ProQuest Dissertations and Theses Database. (X-ETS/EES-0513).

[Bor12] Borba, B., Szklo, A., & Schaeffer, R. (2012). Plug-in hybrid electric vehicles as a way to maximize the integration of variable renewable energy in power systems: The case of wind generation in northeastern Brazil. *Energy, 37*, 469-481.

[Cle11] Clement-Nyns, K., Haesen, E., & Driesen, J. (2011) The impact of vehicle-to-grid on the distribution grid. *Electric Power Systems Research, 81*, 185-192.

[Del12] De Los Ríos, A., Goentzel, J., Nordstrom, K., & Siegert, C. (January 2012). Economic analysis of vehicle-to-grid (V2G)-enabled fleets participating in the regulation service market. *IEEE PES Innovative Smart Grid Technologies (ISGT) Conference, Washington, DC,* 1-8.

[Den11] Denholm, P., & Hand, M. (2011). Grid flexibility and storage required to achieve very high penetration of variable renewable electricity." *Energy Policy, 39* (3),1817–1830.

[Dow11] Downing, N., Wrigley, S., Greenwood, D., Smith, B., & Hyde, J. (2011). Bucks for balancing: Can plug-in vehicles of the future extract cash – and Carbon - from the power grid?. *Ricardo and National Grid joint Report,* Retrieved March 16, 2013, from http://www.ricardo.com/en-GB/News--Media/Press-releases/News-releases1/2011/Report-shows-how-future-electric-vehicles-can-make-money-from-the-power-grid/Personal-Details/vehicles-of-the-future/

[Dup03] Dupactová, J., Gröwe-Kuska, N., & Römisch, W. (2003). Scenario reduction in stochastic programming: An approach using probability metrics. *Math. Program., ser. A 95*, 493-511.

[Ekm11] Ekman, C.K. (2011). On the synergy between large electric vehicle fleet and high wind penetration an analysis of the Danish case. *Renewable Energy, 36*, 546-553.

[EPA13] *Environmental Protection Agency.* (n.d.). Retrieved January 8, 2013, from http://www.epa.gov/climatechange/basics

[Fer11a] Fernandes, C., et al. (2011). Economic impact of plug-in hybrid electric vehicles on power systems operation. Retrieved June 18, 2013, from http://www.iit.upcomillas.es/aramos/papers/Economic Impact of Plug-In Hybrid Electric Vehicles on Power Systems Operation_.pdf

[Fer11b] Fernández, P., Gómez San Román, L., Cossent, T., Domingo, R., & Frías C. (2011). Assessment of the impact of plug-in electric vehicles on distribution networks. *IEEE Transactions on Power Systems, 26*(1), 206 – 213.

[Gam02] GAMS/SCENRED Documentation. (May 2002). Retrieved February 10, 2013, from http://www. gams.com/docs/document.htm.

[Gan03] Gan, D., & Litvinov, E. (Feb 2003). Energy and reserve market design with explicit consideration to lost opportunity costs. *IEEE Transactions Power*

Systems, *18*(1), 53–59.

[Gla03] Glasserman, P. (2003). *Monte Carlo Method in Financial Engineering*. New York: Springer.

[Glo08] Global Wind Energy Council (GWE). (2008). Global Wind 2008 Report, Retrieved August 25, 2013, from http://www.gwec.net/fileadmin/documents/Global%20Wind%202008%20 Report.pdf

[Har10] Harvey, D. (2010). *Energy And the New Reality 2-Carbon-Free Energy Supply*. London: Earthscan.

[Hea11] Head, C. (2011). How cheap and abundant natural gas affects renewables. *Americans for Energy Leadership,* Retrieved June 18, 2013, from http://leadenergy.org/2011/01/how-cheap-and-abundant-natural-gas-effects-renewables/

[Hed12] Hedegaard, K., Ravn, H., Juul, N., & Meibom, P. (2012). Effects of electric vehicles on power systems in Northern Europe. *Energy, 48*(1), 356–368.

[Jen08] Jenkins, S., Rossmaier, J., Ferdowsi, M. (September 2008). Utilization and effect of plug-in hybrid electric vehicles in the united states power grid. *IEEE Vehicle and Propulsion Conference (VPPC), Harbin*, 1-8.

[Kem05a] Kempton, W., & Tomic, J. (April 2005). Vehicle to gird power implementation: from stabilizing the grid to supporting large-scale renewable energy. *Journal of Power Sources, 144*(1), 280-294.

[Kem05b] Kempton, W., & Tomic, J. (June 2005). Vehicle-to-grid power fundamentals: calculating capacity and net revenue. *Journal of Power Sources*, *144* (1), 268-279.

[Kha10] Khalid, M., & Savkin, A.V. (2010). A model predictive control approach to the problem of wind power smoothing with controlled battery storage. *Renewable Energy*, *35*, 1520-1526.

[Kho12] Khodayar, M., Wu, L., & Shahidehpour, M. (2012). Hourly coordination of electric vehicle operation and volatile wind power generation in SCUC. *IEEE Transactions on smart grid*, *3*(3), 1271-1279.

[Lee09] Lee, Y., Khaligh, A., & Emadi, A. (October 2009). Advanced integrated bi-directional AC/DC and DC/DC converter for plug-in hybrid electric vehicles. *IEEE Trans. on Vehicular Technology*, *58*(8), 3970-3980.

[Let06] Letendre, S., Denholm, P., & Lilienthal, P. (2006). Electric & Hybrid Cars:

New Load, or New Resource?. *Public Utilities Fortnightly*, Retrieved August 25, 2013, from http://www.ferc.gov/about/com-mem/5-24-07-electric-hybrid-wellinghoff.pdf

[Lew11] Lew, D., Milligan, M., Jordan, G., & Piwko, R. (January 2011). The value of wind power forecasting. *Proc. 91st American Meteorological Society Annual Meeting, the Second Conference on Weather, Climate and New EnergyEconomy.*

[Li05] Li, T., Shahidehpour, M. (2005). Price-based unit commitment: A case of Lagrangian relaxation versus mixed integer programming. *IEEE Transactions on Power Systems*, *20*(4), 2015–2025.

[Lu09] Lu, M., Chang, C., Lee, W., & Wang, L. (November 2009). Combining the wind power generation system with energy storage equipment. *IEEE Trans. on Industry Applications*, *45*(6), 2109-2115.

[Luk08] Lukic, S.M., Cao, J., Bansal, R.C., Rodriguez, R., & Emadi, A. (June 2008). Energy storage systems for automotive applications. *IEEE Trans. Ind. Electron, 55*(6), 2258-2267.

[Man06] Manwell, J. F., et al. (June 2006). Hybrid2- a hybrid system simulation model theory manual. *Renewable Energy Research Labo*ratory, Department of Mechanical Engineering, University of Massachusetts.

[Man09] Manwell, J., McGowan, J., & Rogers, A. (2009). *Wind energy explained.* New York: Wiley.

[Man02] Manwell, J.F., McGowan, J.G., & Rogers, A.L. (2002). *Wind Energy Explained*, New York:Wiley.

[Mas04] Masters, G. (2004). *Renewable and Efficient Electric Power Systems*. New York: Wiley.

[Met11] Mets, K., Verschueren, T., De Turck, F., & Develder C. (2011). Exploiting V2G to optimize residential energy consumption with electrical vehicle (dis)charging. *IEEE first international workshop on Smart Grid Modeling and Simulation (SGMS)*, pp. 7-12.

[Met12] Metz, M., & Doetsch, C. (April 2012), Electric vehicles as flexible loads e A simulation approach using empirical mobility data, *Energy*, 48, 369-374.

[Mul12] Mullan, J., Harries, D., Braunl, T., &Whitely, S. (2012). The technical, economic and commercial viability of the vehicle-to-grid concept. *Energy Policy, 48*, 394-406.

[Pil12] Pillai, J., Bak-Jensen, B., & ThogersenP. (2012). Electric vehicles to support large wind power penetration in future Danish power systems. *IEEE Vehicle Power and Propulsion Conference, Seoul, Korea,* 1475-1479.

[Rag12] Raghavan, S., & Khaligh, A. (March 2012). Electrification potential factor: energy- based value proposition analysis of plug-in hybrid electric vehicles. *IEEE Trans. on Vehicular Tech, 61*(3), 1052-1059.

[Rag10] Raghavan, S.S., Onar, O.C., & Khaligh, A. (July 2010). Power electronic interfaces for future plug-in transportation systems. *IEEE Power Electronics Society Newsletter, 24*(3), 23-26.

[Ric13] Richardson, D. (2013). Encouraging vehicle-to-grid (V2G) participation through premium tariff rates. *Journal of Power Sources, 243,* 219–224.

[Roe08] Roe C., Meliopoulos, A., Meisel, J., & Overbye T. (2008). Power system level impacts of plug-in hybrid electric vehicles using simulation data. *Proc. IEEE Energy 2030, Atlanta, GA,* 1-6.

[Rol13] Rolink, J., & Rehtanz, C. (2013). Large-Scale Modeling of Grid-Connected Electric Vehicles, *IEEE Transactions On Power Delivery, 28*(2), 894-901.

[Sab] Saber, A., & Venayagamoorthy G. (unpublished). Plug-in vehicles and renewable energy sources for cost and emission reduction. *IEEE Trans. Ind. Electron.*

[Sab11] Saber, A., &Venayagamoorthy, G. (April 2011). Plug-in vehicles and renewable energy sources for cost and emission reduction. *IEEE Trans. Ind. Electron, 58*(4), 1229-1238.

[Sha05] Shahidehpour, M. & Fu, Y. (March 2005). Benders decomposition: applying benders decomposition to power systems. *IEEE Power and Energy Magazine, 3*(2), 20-21.

[Sha02] Shahidehpour, M., Yamin, H., & Li, Z. (2002). *Market Operations in Electric Power Systems.* New York: Wiley.

[Sha09] Shao, S., Pipattanasomporn, M., & Rahman, S. (July 2009). Challenges of PHEV Penetration to the Residential Distribution Network. *Power & Energy Society General Meeting, PES . IEEE. Calgary, AB,* pp. 1-8.

[Sod04] Söder, L. (September 2004). Simulation of wind speed forecast errors for operation planning of multiarea power systems. *International Conference on Probabilistic Methods Applied to Power Systems, Ames, IA,* 723-728.

[Str07] Strbac, G., Shakoor, A., Black, M., Pudjianto, D., & Bopp, T. (2007).

Impact of wind generation on the operation and development of the UK electricity systems. *Electric Power Systems Research, 77*, 1214-1227.

[Str11] Stroehle, P., Becher, S., Lamparter, S., Schuller, A., & Weinhardt, C. (2011). The impact of charging strategies for electric vehicles on power distribution networks. *8th International Conference on the European Energy Market (EEM)*, 51-56.

[Tom0] Tomić, J., & Kempton, W. (2007). Using fleets of electric-drive vehicles for grid support. *Journal of Power Sources, 168* (2), 459-468.

[Tom07] Tomic, J., & Kempton, W. (2007). Using fleets of electric-drive vehicles for grid support. *Journal of Power Sources, 168.2*, 459–468.

[Val13] Valentine, K., Temple W., & Zhang, k. (2013). Electric vehicle charging and wind power integration: coupled or decoupled electricity market resources? Retrieved March 16, 2013, from http://energy.mae.cornell.edu/PDF/2012PESGeneralMeetingConferencePaper_formatted.pdf

[Wan12] Wang, S., Li, Z., Shahidehpour, M., & Zhang, N. (2012). Modeling and impact analysis of large scale V2G electric vehicles on the power grid. *IEEE Innovative Smart Grid Technologies – Asia,* 1-6.

[Whi11] White, C., & Zhang, K. (2011). Using vehicle-to-grid technology for frequency regulation and peak-load reduction. *Journal of Power Sources, 196*, 3972–3980.

[Wir08] Wirasingha, S., Schofield, N., & Emadi, A. (September 2008). Plug-in hybrid electric vehicle developments in the US: trends, barriers, and economic feasibility. *IEEE Vehicle Power and Propulsion Conference (VPPC), Harbin,*

[WWE13] *World Wind Energy Association.* (n.d.). Retrieved January 8, 2013, from http://www.wwindea.org/

[Wu11] Wu, L. (2011). A tighter piecewise linear approximation of quadratic cost curves for unit commitment problems. *IEEE Trans. Power Systems, 26*(4), 2581–2583.

[Wu07] Wu, L., Shahidehpour, M., & Li, T. (May 2007). Stochastic security-constrained unit commitment. *IEEE Trans. on Power Syst, 22*(2), 800-811.

[Wu08] Wu, L., Shahidehpour, M., & Li, Z. (November 2008). GENCO's risk-constrained hydrothermal scheduling. *IEEE Trans. on Power Systems, 23*(4), 1847-1858.

[Yan12] Yang, H., Jin, L., Cheng, F., Zhou. Y., & Zhao, R. (2012) A Novel approach for the Unit Commitment with Vehicle-to-grid. *Electrical Machines and Systems (ICEMS), 2012 15th International Conference, Sapporo,* 1-6.

[Yer12] Yergin, D. & Gross, S. (Jan 2012). Energy for economic growth energy vision update 2012. *World Economic Forum in partnership with IHS Cambridge Energy Research Associates (CERA).* Retrieved January 8, 2013, from http://www.weforum.org/reports/energy-economic-growth-energy-vision-update-2012

[Yer13] Yergin, D., Gross, S., Meyer, N., & Tillemann, L. (Jan 2013). The energy vision 2013, energy transitions: past and future report. *World Economic Forum in partnership with IHS Cambridge Energy Research Associates (CERA)*. Retrieved May 23, 2013, from http://www.weforum.org/reports/energy-vision-2013-energy-transitions-past-and-future. Retrieved on: March 2013.

[Zah12] Zahedi, A. (2012). Electric vehicle as distributed energy storage resource for future smart grid. *Australasian Universities Power Engineering Conference (AUPEC),* 1-4.

[Zho09] Zhong, X., Cruden, A., Infield, D., Holik, P., & Sikai H. (September 2009). Assessment of vehicle to grid power as power system support. *Universities Power Engineering Conference (UPEC), Glasgow,* 1-5.